ASSESING THE IMPACT OF LAND USE / LAND COVER CHANGE ON STREAM FLOW (THE CASE OF UPPER AWASH RIVER BASIN, ETHIOPIA)

MSC THESIS

WORKU NIGUSSIE YOSEF

HAWASSA UNIVERSITY, HAWASSA, ETHIOPIA
SEPTEMBER_2020

ASSESING THE IMPACT OF LAND USE / LAND COVER CHANGE ON STREAM FLOW (THE CASE OF UPPER AWASH RIVER BASIN, ETHIOPIA)

WORKU NIGUSSIE YOSEF

A THESIS SUBMITTED TO THE

DEPARTMENT OF WATER RESOURCES AND HYDRAULIC ENGINEERING,

INSTITUTE OF TECHNOLOGY, SCHOOL OF

GRADUATE STUDIES

HAWASSA UNIVERSITY

HAWASSA, ETHIOPIA

IN PARTIAL FULFILLMENT OF THE

REQUIREMENTS FOR THE

DEGREE OF

MASTER OF SCIENCE IN HYDRAULIC ENGINEERING

ADVISOR: SHIMELIES ASSEFFA (Ph.D.)

CO-ADVISOR: SIRAK TEKLEAB (Ph.D.)

SCHOOL OF GRADUATE STUDIES

HAWASSA UNIVERSITY

ADVISORS' APPROVAL SHEET

This is to certify that the thesis entitled " **ASSESING THE IMPACT OF LAND USE / LAND COVER CHANGE ON STREAM FLOW (THE CASE OF UPPER AWASH RIVER BASIN, ETHIOPIA)**" submitted in partial fulfillment of the requirements for degree of Masters with specialization in Hydraulic Engineering, the Graduate program of the school of Hydraulic Engineering, and has been carried out by **WORKU NIGUSSIE**, **Id No PGHY /016 /10** under our supervision. Therefore, we recommend that the student has fulfilled the requirements and hence hereby can submit the thesis to the school.

SHIMELIES ASSEFFA (Ph.D.)	----------	----------
Name of Major Advisor	Signature	Date

SIRAK TEKLEAB (Ph.D.)		----------
Name of Co- Advisor	Signature	Date

EXAMINERS' APPROVAL SHEET

SCHOOL OF GRADUATE STUDIES

HAWASSA UNIVERSITY EXAMINERS' APPROVAL SHEET

We, the undersigned, members of the Board of Examiners of final open defense by "WORKU NIGUSSIE YOSEF'' have read and evaluated his/her thesis entitled" **ASSESING THE IMPACT OF LAND USE / LAND COVER CHANGE ON STREAM FLOW (THE CASE OF UPPER AWASH RIVER BASIN, ETHIOPIA)**" and examined the candidate. This is, therefore, to certify that the thesis has been accepted in partial fulfillment of the requirements for the degree.

_____	_____	_____
Name of the Major Advisor	Signature	Date
_____	_____	_____
Name of Internal Examiner – I	Signature	Date
_____	_____	_____
Name of Internal Examiner – II	Signature	Date
Michael Mehari Mogas (Ph.D. P.E)	_____	_____
Name of External Examiner	Signature	Date
_____	_____	_____
SGS Approval	Signature	Date

Final approval and acceptance of the thesis is contingent upon the submission of the final copy of the thesis to the School of Graduate Studies (SGS) through the Department/School Graduate

Committee (DGC/SGC) of candidate's department

Stamp of SGS Date: _____

Remark

- Use this form to submit the thesis **with or without minor correction** suggested by examining board.
- 3 copies

DECLARATION

I, **WORKU NIGUSSIE YOSEF**, hereby declare that this thesis submitted for the partial fulfillment of the requirements for the Master of Science in Hydraulic engineering, in the original work done by me under the supervision of Shimelis Assefa (Ph.D.) and Sirak Tekleab (Ph.D.) and it has not been published or submitted elsewhere for the requirement of a degree program to the best of my knowledge and belief. Materials or ideas of other authors used in this thesis have been accordingly acknowledged.

Signature: - ---------- Date: ----------

Workunigussie8@gmail.com

ACKNOWLEDGEMENT

First of all, thanks to the Almighty God for granting me his limitless care, love and blessings all along the way. Next, to that, my sincere gratitude goes to my research advisors, Dr. Shimelies Aseffa (Ph.D) and Dr. Sirak Tekleab (Ph.D), for their unreserved advice, guidance and continuous encouragement. The careful comments I have received from them throughout my thesis work helped me to complete it successfully. It was their skillful contribution and continuous encouragement that made me strong to face every up and down with confidence during the research study.

I am indeed grateful to my family, for their persistent love, patience, support, continuous moral and encouragement during my postgraduate study. I wish if I could list all individuals who stood by my side, but I simply forward my heartfelt thanks and appreciation.

I am also thankful to the Ministry of Water, Irrigation and Energy of Ethiopia and the National Meteorological Agency of Ethiopia for providing me all the relevant data used as input for my research findings.

ABBREVIATION AND ACRONYMS

CAD	Computer Aided Design
CN	Curve number
CRV	Central Rift Valley
DEM	Digital Elevation Model
EEPCo	Ethiopia electric power corporation
ERDAS	Earth Resource Data Analysis System
ETM+	Enhanced thematic mapper
FAO	Food Agricultural Organization
GIS	geographical information system
HRU	Hydrological Response Unit
LULC	Land Use Land Cover
MoWIE	Ministry of Water Irrigation and Energy
MSS	Multiple Spectral Scanners
NMA	National metrological agency
NSE	Nash Sutcliff efficiency
PET	Potential evapotranspiration
R^2	Coefficient of determination
SCS	Soil (conservation) service
SUFI2	Sequential uncertainty fitting
SWAT	Soil and water assessment tool
SWAT-CUP	Soil and water assessment tool- calibration and uncertainty program
USGS	United State Geological Survey
TM	Thematic mapper

Table of Contents

LIST OF TABLES

LIST OF FIGURES

LIST OF APPENDICES

ABSTRACT

The population growth for the last 33 years caused changes in land cover of the upper Awash River basin of Ethiopia. The effect of the land cover changes has impact on the stream flow of the watershed by altering the magnitude of surface runoff and ground water flow. This study aimed at investigating the impacts of the land use/land cover change (LU/LCC) on the stream flow of the upper Awash River basin. Both meteorological and hydrological dataset was gathered and analyzed for a period of 1986 to 2018. Land use change detection was done using remote sensing techniques and the maps were processed using ERDAS Imagine 2014 in conjunction with ArcGIS10.1 software. The land use land cover maps were classified using the Maximum Likelihood Algorithm of Supervised Classification. The accuracy of the classified maps was assessed using Confusion Metrics. The result of this analysis showed that the cultivated land, water body and settlement area has expanded but forest and, grass lands has shown a substantial decline during the study period of 1986-2018. The Soil and Water Assessment Tool (SWAT) model was used to simulate the stream flow under different LU maps. The model was calibrated during a periods of (1986 to 1991), (1996 to 2001), (2006 to 2011) and validated during a periods of (1992 to 1995), (2002 to 2005), (2012 to 2015) for land use/land caver of 1986, 2002 and 2018 respectively. The results of sensitivity analysis show that fifteen flow parameters were identified to be sensitive for the stream flow. Calibration and validation on monthly stream flow is performed by dividing stream flow from (1986_1995) first class for1986 land use and land cover, (1996_2005) second class, for 2002 land use and land cover and (2006_2015) 3rd class for 2018 land use and land cover respectively. For 1986 LULC class of Calibration period, Nash-Sutcliffe simulation efficiency (ENS) of 0.78 and coefficient of determination (R^2) of 0.84 and validation ENS value of 0.60 and R^2 of 0.76 respectively. For 2002 LULC class of Calibration period, Nash-Sutcliffe simulation efficiency (ENS) of 0.81 and coefficient of determination (R^2) of 0.86 and validation with the ENS value of 0.62 and R^2 of 0.82 respectively. For the 2018 LULC class of Calibration period, Nash-Sutcliffe simulation efficiency (ENS) of 0.85 and coefficient of determination (R^2) of 0.89 and validation with the ENS value of 0.64 and R^2 of 0.84 respectively. The trend analysis indicated that flow during the wet months has increased by 34.4% and 10.7% between 1986 to 2002, and 2002 to 2018 respectively. While the flow during the dry months decreased by 4.6% and 6.9% between 1986 to 2002, and 2002 to 2018 respectively. Generally, the analysis indicated that flow during the wet months has increased, while the flow during the dry months decreased. The SURQ increased, while GWQ decreased from 1986 to 2018 due to the increment of cultivated land and expansion of urbanization. The model results showed that the stream flow characteristics changed due to the land cover changes during the study period.

Key word: *Land use/land cover change (LULC), stream flow, calibration and validation, Remote Sensing (RS) and Geographic Information System (GIS).*

1. INTRODUCTION

1.1 Background

Water is a valuable substance and essential for all living things. It is a limited resource and must be managed in sustainable way to meet human as well as environmental needs. Land use land cover change has an effect for alteration of watershed hydrology. The land use planning and management are highly related to the sustainability of water resources as changes of land use are linked with amount of water through relevant hydrological processes (Guo, 2008). Real methods and mechanism should be used to maintain water sustainability. Nowadays, the hydrological models are good to represent the hydrological characteristics (Surur, 2010).

Water resource management and hydrological modeling are highly connected to the processes of the hydrologic cycle. Hydrologic cycle can be affected by land use and land cover variation. Land use land cover is in a dynamic condition especially in developing countries like Ethiopia. The land use and land cover variations can be caused by human and natural factors (Meyer and Turner, 1994). The impact of land use land cover change on hydrology allows water resource planners to formulate policies to decrease the effects of future land cover changes on hydrology. The Ethiopian Water Resource Policy is to increase and encourage all national hard work toward the effective, equitable and optimum utilization of the available water resources of the country for significant socio- economic development on sustainable basis. The impact of land use land cover changes due to population growth that affect water resource, are expansion of agricultural activities and urbanization. Clearing of forests and tillage of the land can change infiltration and runoff characteristics, which disturb ground water recharge, water yield and Evapotranspiration. Water resources degradation and land use land cover change are the main problems in the Ethiopian Central Rift Valley Basin. The area is one of the most important from its water resources development point of view. The Central Rift Valley Basin lakes are undergoing degradation due to upstream land use land cover change impacts like agricultural expansion which affects streams feeding the lakes. The lakes surface water levels have dropped across the Central Rift Valley because of water extraction for irrigation (Legesse and Ayenew, 2006). Agricultural expansion (irrigation system), urbanization, poor land use practices and improper management systems have a significant impact on basin hydrology. Farm lands and settlements expanded which is mostly associated with the decrease in forest land (Kassa, 2007).

1.2 Statement of the problem

Even though Ethiopia also known as a tower of East Africa, today many rivers and lakes become reduction in size due to the decrease in river flow and some small streams dry up completely and finally the magnitude of flow of the medium to large rivers will decline expressively (Melese, 2016). Stream flow is one of the most vulnerable components undergoes variability that poses alarming significances for water demand by different sectors. Land use change variability is important factors impacting watershed hydrology, which is strongly related to the availability of water resources and the sustainability of native ecosystems. Land use fluctuations, which are mostly induced by human activities, affect hydrological progressions such as evapotranspiration, interception and infiltration, resulting in alterations of surface and subsurface flows. It is possibly the most prominent form of global environmental change phenomenon happening at spatial and temporal scales. It is the single most important factor affecting water resource availability both in terms of their quantity, quality and increased variability of hydrological components. Awash River basin is the most developed and exploited of all Ethiopian River Basins. This implies that it has substantial economic significance for the development of the country. Upper Awash (UA), part of Awash River Basin, is densely populated and large population growth as well as the expansion of development activities and large farms such as flower farms in the region is expected to put further pressure on the water and associated resources of the area. Land use and land cover change is the core characteristic in the runoff process that affects infiltration, interception, erosion and evapotranspiration. These variations have produced severe stress on forest and water resources in Upper Awash river basin. Deforestation, expansion of cultivation and other land use actions can considerably change the maximum and minimum flows of the river. Even if LU/LC changes in the area are a present phenomenon, the severity of their effects on hydrology of Awash River watershed might pose serious concern on the future functioning of this fragile resource if serious action is not taken into attention. Overgrazing of the forest lands, deforestation, and expansion of the agricultural area is action of the people living in the watershed. The watershed is similarly facing high erosion by the special effects of intense rainfall of the watershed which aggravates the land cover alteration of the watershed. Poor land use practices, uncontrolled soil erosion, improper mitigation management systems and land degradation resulting in heavy sediment transport in streams and rivers causes' significant reduction of the capacity of Koka reservoirs.

This continuous conversion in land cover has impacted the water balance of the watershed (inflow) by changing the magnitude of the components of stream flow which are surface runoff and ground water flow, which results increasing the extent of the water management problem.

The previous studies in the entire Awash River Basin mainly focus on; past land use changes and their impacts on stream flow, and the impact of land use land cover change in the future on stream flow. Even if the previous research is necessary, it were not include the objective illustrated in this research and land use land cover research is a dynamic change; it need further investigations. Some studies were not analyze and detect the change in land use/land cover on stream flow by dividing in decades in the basin. But in this research stream flow for calibration and validation is divided based on land use/land cover change at three decades; that is the model was calibrated during a periods of (1986 to 1991), (1996 to 2001), (2006 to 2011) and validated during a periods of (1992 to 1995), (2002 to 2005), (2012 to 2015) for land use/land caver of 1986, 2002 and 2018 respectively. There are also identified the trend exist in rainfall and stream flow at given periods and explored land use/land cover change on stream flow on annual and seasonal time scales. Therefore, the necessity for a scientific research is unquestionable. Specially, this research is address estimating the effect of land use land cover changes on the stream flow of Awash River basin to contribute a lot on the way toward deal with the above problems.

1.3 Objectives

1.3.1 General objective

The main objective for this study is to investigate the impact of land use / land cover change on stream flow in the Upper Awash river basin, Ethiopia.

1.3.2 Specific objectives

- ✓ To analyze and detect the change in LU/LC over three decades in the basin
- ✓ To identify the trends exist in rainfall and stream flow over a period 1986 to 2018
- ✓ To examine the stream flow response due to the LU/LC change on annual time scale and at sub-basin scale.
- ✓ To explore the LU/LC change impacts on stream flow on seasonal time scale.

1.4 Research questions

- What are the trends of land use land cover change in the study area over the last three decades?
- Could we detect the LU/LC change impacts on stream flow?
- Which runoff components (surface runoff and base flow) significantly change due to the LU/LC change spatially on a sub-basin scale?
- What are the trends of rainfall and stream flow over a period 1986 to 2018?

1.5 Scope of study

The studies assess the impact of land use land cover change on stream flow and drivers of the change, then it predict the future land use land cover change impact on stream flow. Methodologically the study used different methods and approaches (remote sensing, swat model for data analysis, field observation, and focus group discussion, and use of secondary data). For predicting future land use land cover impact on stream flow the study was used Swat Model.

1.6 Limitation of the study

The most significant constraint of this work was the inadequacy of the daily stream flow data, and the recorded stream flow data have missing values that does not suitable for calibration and validations at the given periods.

This research did not study the combined factors of: Climate change, soil erosion, sedimentation and land use land cover change with stream flow due to limitation of data, budget and time.

1.7 Significance of the Study

The land use and land cover change has significantly impacts on natural resource, socio economic and environmental system. understanding the types and impacts of land use land cover is essential indicator for resource base analysis and development of effective and appropriate response strategies for sustainable management of natural resources in the country in general and at the study area in particular. Moreover, the study presents a method to quantify land use and land cover change and their impact on stream flow. This will achieved through a method that combines the hydrological model (SWAT) to simulate the hydrological processes, GIS and remote sensing techniques to analysis the land use land cover change.

2. LITERATURE REVIEW

2.1 Land Use /land cover change

Land cover refers to the biophysical and physical appearance of Earth's surface and immediate, captured in the distribution of vegetation, water, desert, ice and other physical features of the land, including those created solely by human activities e.g., settlements. Land use refers to the intended use or management of the land cover type by human beings. Hence, land use involves both the manner in which the biophysical features of land are manipulated and intent underlining that manipulation (the purpose for which the land is used e.g., agriculture, grazing, etc.), which are more subtle alterations that affect the character of the land cover without changing its overall classification. Definition of land use in this way establishes a direct link between land cover and the actions of people in their environment (FAO, 1998).

Cultivation of land exerts a major influence on the relationship between surface and subsurface flow. According to use data from long term observations done in paired watersheds, in the forest zone of Central Russia (Golosov, and Panin, 2006). Surface runoff is extremely limited under grass or forest vegetation compared with agricultural land.

Land use/land cover change effects on hydrological is manifested in many ways and at different spatial and temporal scales. Furthermost understandable is the immediate and direct effects on the quantity and quality of watershed's runoff. For example, land cover change is the most significant factor driving hydrologic changes such as runoff volume, timing and variability (Fohrer, 2001). The simplest technique to assess these effects on hydrologic response of watershed is by comparing stream flow and runoff generated from the watershed areas with the contrasting land use types (Barkhordari, 2003). The main causes for land use change are due to manmade and natural causes, where the manmade causes are mainly attributed to the reach for resources to meet human needs. For instance, deforestation is a result of the need for timber for construction, fuel wood and clearing for agricultural development and for settling the ever increasing population (Chemelil,1995) and increase in foreign direct investments or land grabbing (Getnet and Svondo,2010), increased deforestation in the investment area (Gobena,2010).

2.2 Application of Remote Sensing on Land use Land cover Change

Remote Sensing (RS) is defined as the science of obtaining information about an object, area, or phenomenon through the analysis of data acquiring by a device that is not contact with the object, area, or phenomenon under investigation (Bawahidi,2005). It provides a large amount of data about the earth surface for detailed analysis and change detection with the help of sensors.

Land use and land cover is changing rapidly in most parts of the world. In this situation, accurate, meaningful and availability of data is highly essential for planning and decision making. Remote sensing is particularly attractive for the land cover data among the different sources. (Stefanov,2001) reported that in 1970's satellite remote sensing techniques have started to be used as a modern tool to detect and monitor land cover change at various scales with useful results.

The importance of land cover mapping is to show the land cover changes in the watershed area and to divide the land use and land cover in different classes of land use and land cover. For this purpose, remotely sensed imagery play a great role to obtaining information on both temporal trends and spatial distribution of watershed areas and changes over the time dimension for projecting land cover changes but also to support changes impact assessment (Atasoy, 2006).

2.3 Land Use /Land Cover Change Studies in Ethiopia

In Ethiopia, land is used for agricultural purposes, for construction of buildings and roads and extra purposes. In the country most of the land is used for subsistence farming. With the population growing and slow technological adoption which can increase production, there is deforestation for more production which means conversion of forest to agricultural land and expansion of urban settlements.

The other research specified that the growth and intensification of agricultural land is due to population growth (Efrem, 2010) in the semiarid of Central Rift Valley of Ethiopia and (Molla, 2014) Concluded that land use land cover dynamics in the Central Rift Valley Region of Ethiopia was due to population pressure which caused agricultural expansion in to marginal land and more sever land degradation. The researches that have been conducted in different parts of Ethiopia have shown that there were considerable land use and land cover changes in the country.

Most of these studies indicated that croplands have expanded at the expanse of natural vegetation including forests and shrub lands; for example Kassa (2003) in his study, in southern Wello, reported the decline of natural forests and grazing lands due to conversions to croplands. Bewket (2003) have reported an increase in wood lots (eucalyptus tree plantations) and cultivated land at the expense of grazing land in both Chemoga watershed in north-western Ethiopia, and Sebat-bet Gurage land in south-central Ethiopian. The changes of land use / land cover that have occurred from 1971/72 to 2000 in Yerer Mountain and its surrounding results an expansion of cultivated land at the expense of the grasslands (Gebrehiwet, 2004). Hadgu (2008) identified that decrease of natural vegetation and expansion of agricultural land over a period of 41 years in Tigray, northern part of Ethiopia. He concluded that population pressure was an important deriver for expansion and intensification of agricultural land in recent periods. Garedew, (2010) in the semi-arid areas of the central Rift Valley of Ethiopia, during the period 1973-2000 cropland coverage has increased and woodland cover lost. According to many literatures, population growth has a paramount impact on the environment. For instance, population pressure has been found to have negative effect on Riverine vegetation, scrublands and forests in Kalu district (Tekle and Hedlund, 2000), Riverine trees in Chemoga watershed (Bewket, 2003), and natural forest cover in Dembecha Woreda north-western Ethiopia (Zeleke and Hurni, 2001). Similarly, Pender *et al.*, (2001) reported that the population growth has significant effect on land degradation, poverty and food insecurity in the northern Ethiopian highlands. However, most of the empirical evidences indicated that land use and land cover changes and socioeconomic dynamics have a strong relationship; as population increases the need for cultivated land, grazing land, fuel wood; settlement areas also increases to meet the growing demand for food and energy, and livestock population. Thus, population pressure, lack of awareness and weak of management are considered as the major causes for the deforestation and degradation of natural resources in Ethiopia. (Geremew, 2013)

2.4 Land Use /Land Cover change impacts on stream flow

Water on earth occurs in a space called the hydrosphere and lithosphere, circulates and forming hydrologic cycle. The cycle has no beginning and no ending and can be affected by different factors. Among those factors, manmade activities, land use and land cover change can affect hydrological processes such as infiltration, runoff and groundwater recharge.

Land cover can affect both the degree of infiltration and runoff following rainfall events, while the degree of land cover can affect rates of evaporation. Land cover has various properties that help to regulate water flows both above and below ground. For example, tree canopy and leaf litter can help decrease the impact of raindrops on the ground, hence reduce soil erosion, while roots hold the soil in place and also absorb water. In the absence of vegetative cover, soil erosion will result and the effects of this phenomenon have been detailed previously. Ethiopia is the water tower of north eastern Africa. However, land cover change can affect the amount of runoff to the downstream countries of the Awash River basin, where every main rainy season big floods are reported. The effects of land cover are not only contained within the country, but also on the low-lying of countries of Africa as well. That is why agreements are being signed between Ethiopia and these countries so that Ethiopia takes care of its soil erosion. Land cover change does not only affect the neighboring countries but also the basin itself, with in the country, where flooding is a common phenomenon. As a result of this, millions worth of resources are lost nearly every main rainy season. Low level vegetative cover could also affect infiltration and could lead to reduced groundwater levels and therefore the base flow of streams (Dagnachew, 2003). Mach of the present understanding Of land use effects on hydrology is derived from controlled experiments and manipulations of the land surface coupled with observations of hydrological processes, commonly precipitation inputs and stream discharge outputs (De Fries and Eshleman,2004).

2.4.1 Evaporation and transpiration

Land use land cover plays an important role in influencing the water cycle through changes in evapotranspiration, soil water holding capacity and the vegetation's ability to intercept precipitation (Zhang *et al*., 2014). Evapotranspiration is one of the most significant components of the hydrologic budget, which is a combination of two sub-processes: evaporation and transpiration. Evaporation is water loss from open water bodies, wetlands, bare soil, snow cover, etc. while transpiration is water loss from living plant surfaces. Thus, land surface characteristics influence the process of evapotranspiration (Hanson, 1988). Evaporation from an open water surface is influenced by two main factors first the supply of energy to provide the latent heat of vaporization and second the ability to transport the vapor away from the evaporative surface. Solar radiation is the main source of heat energy.

The ability to transport vapor away from the evaporative surface depends on the wind velocity over the surface and the specific humidity gradient in the air above it. Evaporation from the land surface comprises evaporation directly from the soil and vegetation surface, and transpiration through plant leaves, in which water is extracted by the plant's roots, transported upwards through its stem, and diffused into the atmosphere through tiny openings in the leaves called stomata. The process of evaporation from the land surface and transpiration from vegetation are collectively termed evapotranspiration (ET). Wohlrab et. al., (1992) defined that ET is the turbulent mass transfer of water vapor and heat energy to the atmosphere. Net transfer of water molecules occurs only if there is a vapor pressure gradient between the evaporating surface and the air, i.e, evaporation is nil when the relative humidity of the air is hundred percent (Chorley, 1977).

2.4.2 Surface Runoff and Groundwater

Land use land cover changes alter vegetation cover and surface roughness that affect the timing and magnitude of surface runoff and groundwater discharge, leading to changes in stream flow and magnitude and frequency of floods (Schilling *et al*., 2014). Land use changes, such as urbanization and agricultural activities cause greater surface runoff (Pai and Saraswat, 2011).
Deforestation may also cause greater surface runoff. In East Africa, (Baker and Miller, 2013) reported that due to land conversion from forest to agricultural land increased surface runoff. Ghaffari *et al*. (2010) showed that decreasing grassland and increasing agricultural land decreased groundwater recharge and base flow in the semi-arid Zanjan rood Basin in Iran.

2.4.3 Stream flow and Flood

Increasing land use conversion (especially for urbanization, deforestation, grassland depletion) can potentially lead to an increase in stream flow and flood frequency (Schilling *et al*., 2014). During storm events, greater surface runoff can exceed the flow carrying capacity of the stream within the watershed, which may increase the risk of potential flooding. In addition, grassland expansion can reduce flood potential due to a decrease in stream flow. Grassland has higher evapotranspiration compared to agricultural land and may promote higher infiltration, leading to a reduction of flood potential in the watershed. Stream flow is the total flow of water, or stream discharge, past a specified point in a stream channel, and for a specified period of time. It is the component of the hydrologic cycle which transfers water, originally falling as a rain or snow onto a watershed, from the land surface to the oceans.

Hence stream flow at a particular point on a channel system is contributed by runoff from the watershed upstream of that point, and return flow from the groundwater aquifer (Maidment. 1993). Stream flow is the main form of surface water flow and all the other surface and subsurface flow processes contribute to it and it is generated by a combination of; base flow (return flow from groundwater), interflow (rapid subsurface flow through pipes, macro pores, and seepage zones in the soil), and saturated overland flow from the surface of poorly permeable or temporarily saturated soil, or from permanently saturated zones near the channel system. A stream flow rate integrates all the hydrologic processes and storages upstream of a particular point on a drainage system at a particular time.

2.5 Hydrologic Models

Hydrologic modeling were proved to be very important tool that can be applied to understand and explain the effects of land use land cover change on hydrologic response of a watershed (Baldyga, 2005). Hydrological models are mathematical descriptions of components of the hydrologic cycle. They were developed for many different reasons and therefore have many different forms. However, hydrological models are in general designed to get a better understanding of the hydrologic processes in a watershed and of how changes in the watershed may these phenomena and for hydrologic prediction (Tadele, 2007). They are also providing valuable information for studying potential impacts of changes in land use and land cover or climate change. There are many classification of hydrologic models, deterministic versus stochastic, lumped versus distributed and etc. On the basis of process description, the hydrological models can be classified in to three main categories (Cunderlik, 2003).

2.5.1 Lumped models

Parameters of lumped hydrologic models do not vary spatially within the basin and thus, basin response is evaluated only at the outlet, without explicitly accounting for the response of individual sub basins. The parameters often do not represent physical features of hydrologic processes and usually involve certain degree of empiricism. These models are not usually applicable to event scale processes. If the interest is primary in the discharge prediction only, then these models can provide just as good simulations as complex physically based models (Beven, 2000).

2.5.2 Distributed models

Parameters of distributed models are fully allowed to vary in space at resolution chosen by the user. Distributed modeling approach attempts to incorporate data concerning the spatial distribution of parameters together with computational algorithms to evaluate the influence of this distribution on simulated precipitation runoff behavior. Distributed models generally require large amount of data.

2.5.3 Semi distributed models

Parameters of semi distributed models are partially allowed to vary in space by dividing the basin in to a number of smaller sub basins. The main advantage of these models is that their structure is more physically based than the structure of lumped models and need less input data than fully distributed models. SWAT, HEC-HMS and HBV are Considered as semi distributed models.

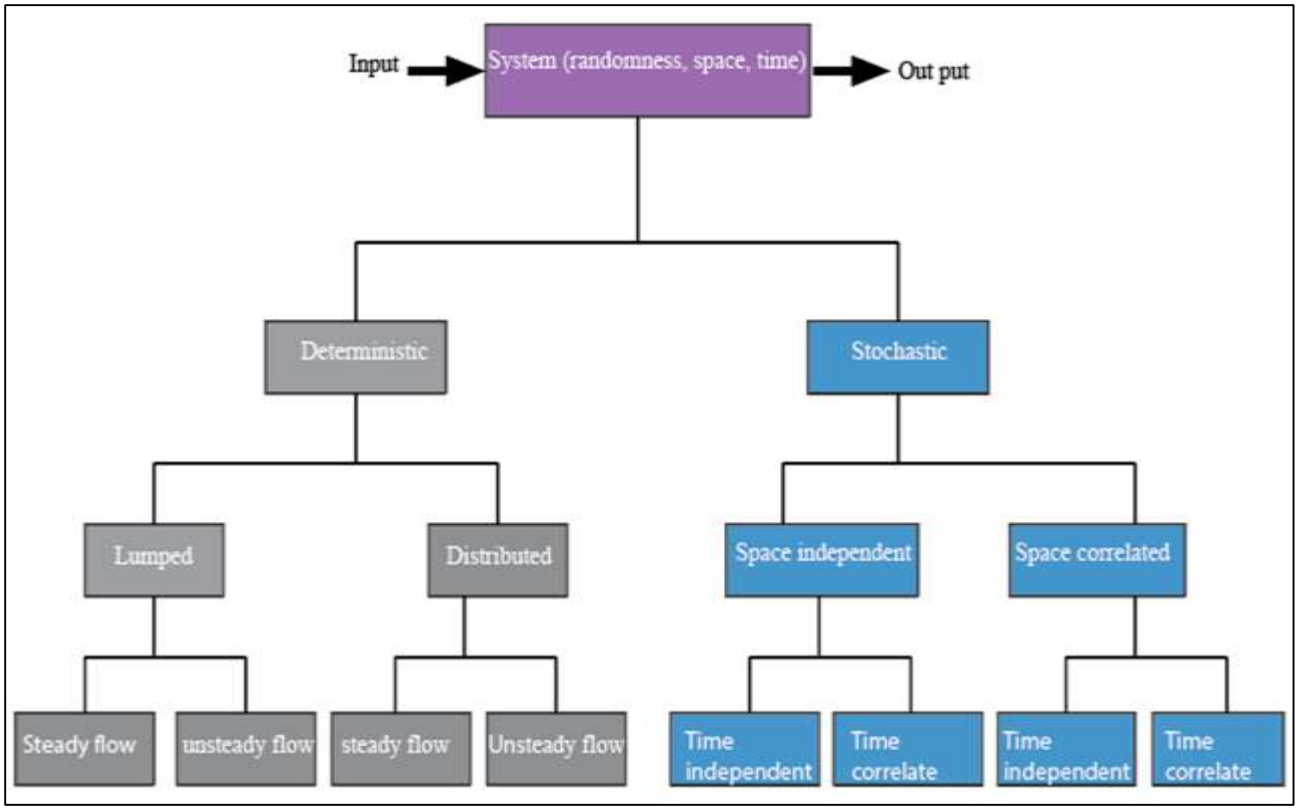

Figure 2.1: Classification of Hydrologic model (Nigussie, 2012)

2.5.4 Hydrological Model Selection Criteria

There are many criteria which can be used for choosing the right hydrologic model. These criteria always project dependent, since every project has its own specific requirements and needs. Further, some criteria are user dependent, such as the personal preference for graphical user interface (GUI), computer operating system, input out management system and structure. The four fundamental criteria that must be considered for model selections are:

Predict the impact of land management practices on water, sediment, and agricultural yields in large complex watersheds with varying soils, land use and management conditions over long periods of time. It requires specific information about weather, soil properties, topography, vegetation, and land management practices in watershed areas. Hydrological processes that need to be modeled to estimate the desired outputs adequately (Is the model capable of simulating single event or continuous processes?)

Available of input data (Can all the inputs required by the model be provided within the time and cost constraints of the project?

In addition, the model must be readily and freely available within available documentation and should be applied over a range of watershed sizes from large to global. For this study SWAT (semi distributed model) is selected because its structure is more physically based than the structure of the lumped model, freely available and meets the objective of this study.

2.6 SWAT Development and Interface

SWAT model is a semi distributed; time continuous watershed simulator operating on daily time step (Arnold., Srinivasan., Muttiah, and Williams et al., 1998). It is developed for assessing the impact of management and climate on water supplies, sediment and agricultural chemical yields in watersheds and larger river basins. The model is physically based and allows simulation of a high level of spatial detail by dividing the watershed into a large number of sub watersheds. The major components of SWAT include hydrology, weather, erosion, plant growth, nutrients, pesticides, land management and stream routing. The program is provided with an interface in Arc GIS (Arnold, 2012) for the definition of watershed hydrologic features and storage as well as the organization and manipulation of the related spatial and tabular data.

2.7 Application of Hydrological Model (SWAT)

2.7.1 Application of SWAT Model in the worldwide

SWAT model has been applied in agricultural watersheds and have been successfully Calibrated and validated in many areas of the world. The studies indicated that the SWAT model is capable of simulating hydrologic process from complex and data poor watershed with reasonable model performance statistical values. Ndomba (2002), was applied the SWAT model in modeling of Pangari River (Tanzania) to evaluate the applicability of the model in complex and data poor watershed. Adeogun and Adeniyi (2014), was used SWAT models to predict water balance and water yield of a watershed area in Nigeria. It has been suggested that, SWAT model could be a promising tool to predict water balance and water yield in sustainable management of water resource. Shrestha *et al*. (2015) used the SWAT model to analyze the impact of land use changes on runoff and sediment yield in Da River Basin of Hoa Binh province, northwest Vietnam. The results showed that SWAT was adequately capable of simulation of runoff and sediment yield as depicted from Nash-Sutcliffe Efficiency, percentage bias and Observation's Standard Deviation Ratio values. Vegetation significantly affects the runoff and sediment yield of the area. The study by Shimaa (2015) in this study the Arc SWAT interface implemented in the Arc GIS software was used in order to model the hydrology of Simlydam watershed area. SWAT model was successfully calibrated. Manual calibration has been performed first on annual basis followed by monthly basis. The calibration and validation of the model produced good simulation results. The efficiency of the model has been tested by a coefficient of determination, Nash-Sutcliffe Efficiency (NSE) in addition to another two recommended static coefficients: Percent Bias and RMSE observation standard deviation ratio. The study by Golmar *et al*. (2017) they concluded that a good agreement was also found between the simulated and recorded hydrographs. Temporal variation in the flow generating areas for individual events using the SWAT model and in a modified precipitation index method was performed. A good agreement between the two methods demonstrates the suitability of the SWAT model for estimating time-varying runoff generating areas across a watershed.

Donizete *et al*. (2016) they concluded that the SWAT model showed the potential to simulate the hydrological variables analyzed: maximum and minimum annual daily stream flows and minimum reference stream flows for water use rights.

The hydrological variables simulated by the SWAT model did not statistically differ from those observed at a 5% probability level, which qualifies the model for simulations of maximum stream flows associated with different return times, important for hydraulic projects, and to simulate reference stream flows, important to assess the water availability and for irrigation projects.

2.7.2 Application of SWAT Model in Ethiopia

SWAT model has been applied in watersheds and have been successfully Calibrated and validated in many areas in Ethiopia. (Tegegne, 2013), was applied SWAT model on Lake Tana Reservoir Water Balance and reported that, the overall model performance was satisfactory. Similarly, (Tibebe and Bewket., 2010) also applied SWAT model to evaluate surface runoff generation and soil erosion rates for a small watershed (Melka hombole Watershed) in the Awash River basin, Ethiopia, and recommended that, the SWAT model provides a useful tool for soil erosion assessment from watersheds and facilitates planning for a sustainable land management. Fufa (2015), was applied SWAT model for hydrological modeling of Katar watershed, Lake Ziway watershed and recommended the use of SWAT model for further future research. The above literature review indicated that the SWAT model is capable of simulating hydrological process with reasonable accuracy and can be applied to large and complex watersheds.

2.7.3 Application of SWAT Model in Awash River basin

A number of hydrological models have been used to simulate; stream flow, soil loss and flood forecasting in a wash River Basin for protection of Koka Reservoirs.

Study by Assefa and Sileshi (2015) 'charcterization of runoff generation mechanisms for modeling of flow , soil erosion and sedimentation of upper awash river basin. Performance of the model for both the calibration and validation watershed was found to be reasonably very good with Nash-Sutcliffe coefficient (NSE) is 0.68 and coefficient determination (R^2) is 0.57 for calibration and Nash-Sutcliffe coefficient (NSE) is 0.73 and coefficient determination (R^2) is 0.52 for validation respectively. Therefore, this indicated that the SWAT model performed well for the simulation of the hydrology of the watershed.

The study by Behailu (2004) applied the Famine Early Warning System Stream Flow Model (FEWS-SFM) that was designed to produce a three days forecast for a forecasted rainfall and potential evapotranspiration.

The model overestimated the stream flow for the first rain season (April to July) which has low amount of rainfall while the peak flow during heavy rainfall season (July to September) and was underestimated.

For this study Soil and Water Assessment Tool (SWAT) model was selected because it has the ability to characterize complex watershed representations and to explicitly account for spatial variability of soils, rainfall distribution, and vegetation heterogeneity. And it has the ability to characterize surface runoff there by sediment yield producing mechanisms, in addition it also show the effects of land use and land cover on surface runoff and sediment yield.

As a physically-based model, SWAT uses hydrologic response units (HRUs) to describe spatial heterogeneity in terms of land cover and soil type within a watershed. The model estimates relevant hydrologic components such as stream flow, evapotranspiration, surface runoff, and groundwater flow and sediment yield at as much details at each of hydrologic response units HRUs.

2.8 SWAT Calibration and Uncertainty Procedures (SWAT-CUP)

SWAT-CUP is a public domain and any calibration, uncertainty or sensitivity can be linked to SWAT. The program links Generalized Likelihood Uncertainty Estimation (GLUE), Parameter Solution (ParaSol), Sequential Uncertainty Fitting (SUFI2) and Markov Chain Monte Carlo (MCMC) procedures to SWAT (Abbaspour, 2015). It enables sensitivity analysis, calibration, validation and uncertainty analysis of SWAT models. SUFI method determines uncertainty though the sequential and fitting process in which iteration and unknown parameter estimates are achieved before the final estimates.

2.9 Trend Detection and Analysis in Hydro-climatic Variables

Trend analysis in hydro-climatic variables is one way to evaluate how the climate has changed over time. Trend detection refers to methods used to extract an underlying behavioral pattern in a time series otherwise that would be partly or fully hidden by noise. The detection of abrupt and gradual changes in hydrological and meteorological records has been explored in considerable detail by researchers. Information about Spatio-temporal variability in hydro-climatic time series is of great importance from both scientific and practical viewpoints. For example, the interpretation of the significance of trends existing in the annual maximum (flood), mean, and low flows in rivers

is very valuable for flow regulation (Tharme, 2003). This is because they are considered when designing flood mitigation structures, flood protection systems, and water storage reservoirs.

Trend detection and forecasting of low flow are of importance due to the quantity of water to be released downstream of a dam, in order to protect ecological integrity and sustainability (Smakhtin, 2001).

2.10 Application of Mann-Kendall Statistics Test for Climate Trend Analysis

According to the study by Anzhou *et al*. (2016) in the Weihe River Basin of northwest China, concluded that, during 1980-2000, the farmland in the Weihe River Basin decreased by 1.4%, and the woodland, grassland and construction land increased by 0.6%, 0.2%, and 0.6%, respectively, due to land use change. The Mann-Kendall test indicates a statistically insignificant decreasing trend in rainfall, but a statistically significant decreasing trend in temperature.

The study by Belihu *et al*. (2018) in Gidabo River Catchment; to detect trends the analysis was done by using Mann-Kendal (MK), Sen's graphical method and to detect change point using the Pettit test. The comparison of trend analysis between MK trend test and Sen graphical method results showed the most similar pattern. The annual rainfall trends exhibited a significant decrease by about 12 mm per year in the upstream, which is largely driven by the significant decrease in the peak season rainfall. The Pettit test revealed that the years 1997 and 2007 were the change points.

The study by Belete (2013) in Lake Hawassa, by using the Mann-Kendall test Results of the Mann-Kendall trend analyses revealed the significant increasing trend of the lake level and stream flow. On the contrary, a decreasing trend of evaporation was observed while rainfall exhibits no trend over the study period.

3. MATERIALS AND METHODS

3.1 Descriptions of the Study Area

3.1.1. Location

The geographical location of the Awash River Basin is between 7°53'N and 12°N latitudes and 37°57'E and 43°25'E of longitudes. Awash River Basin is one of the twelve major river basins in Ethiopia. Unlike many Trans-boundary Ethiopian rivers it rises and terminates in the country. Awash rises in the central high plateau of altitude 3000 (m. a. s. l) west of Addis Ababa and flow east wards through the Becho plain and joins several small tributaries before entering Koka reservoir ,built in 1960 for the production of hydropower. The river then descends into the Rift Valley and flow north east wards to the Afar triangle where it terminates in Lake Abe at an elevation 250 (m.a.s.l). The Awash Basin is narrow in the upper part and widens towards the north of the watershed. The total length of the main course is 1200 km. The total mean annual water resource of the basin is 4.9 billion meter cube.

3.1.2. Upper Awash Sub Basin

The Upper Awash river basin lies in the Ethiopian highland plateau in elevation ranging from 1500 to 3000 above sea level. It is located upstream of Koka dam (Figure 3.1). The Upper Awash watershed is found in the highlands of central Ethiopia with all lands above 1500 m a.s.l. The land use condition in the Upper Awash watershed includes mainly of cultivated agricultural land, water body, forest land, rural and towns. The Upper Awash River covers the river section from its source up to Koka Reservoir. The Upper Awash River drains a watershed area close to 11,300 km^2 and the length of the river up to Koka is around 220 km (Halcrow, 1989). The major tributaries to the upper awash basin are Akaki and Mojo rivers. Akaki River starts from the mountainous areas of the northern part of Addis Ababa and join the main Awash River between Melka-Kunture and Hombole gauging stations. Mojo River, the other main tributary to Awash, originates from the high lands northeast of Addis Ababa.

It drains a watershed area close to 1,900 km2 and travels a total length of about 105 km before joining Awash. According to currently available Ethio-GIS five sub watersheds are located within the Upper Awash River Basin. Source (Gobena, 2010).

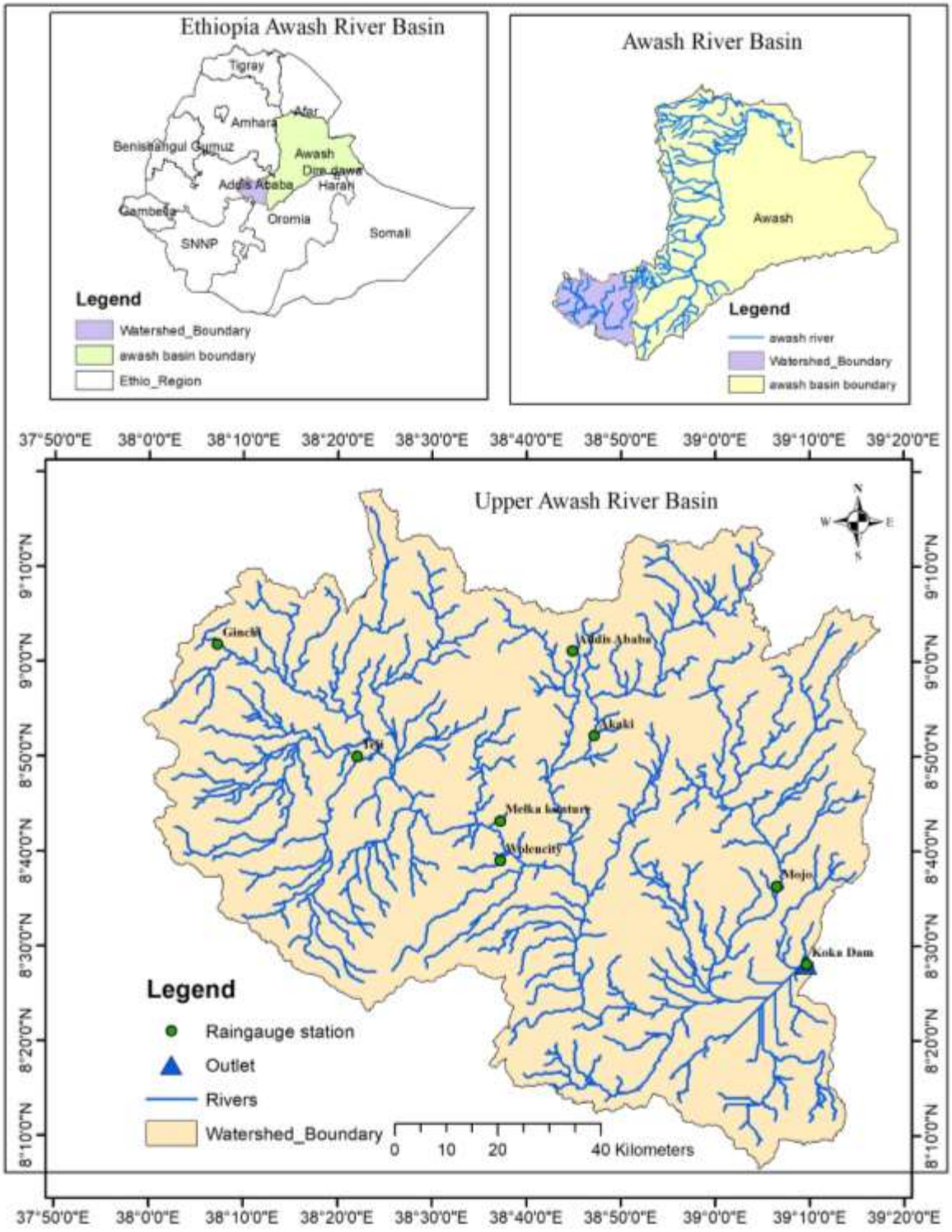

Figure 3.1: Location map of upper Awash Sub Basin

Table 3.1: Sub-watersheds in the upper Awash Sub Basin

S. No	Sub-Watersheds	Area (km^2)	Perimeter (Km)	River gauging stations in the sub watersheds	Mean Slop of sub-watersheds (%)
1	Sub-watersheds-1	4530.38	412.35	Ginchi Berga A.Bello Teji M.kunture	64
2	Sub-watersheds-2	474.11	108.85	Holeta	68
3	Sub-watersheds-3	1608.8	196.21	Akaki	83
4	Sub-watersheds-4	2176.57	216.99	Hombole	38
5	Sub-watersheds-5	1901.70	235.38	Mojo	81

Table 3.2: River Gauging Stations and Sub Watersheds in the Upper Awash Sub- Basin

S. No	Name of Station	River Length (km)	Watershed Slope (%)	Watersheds (km^2)	Latitude (N) in UTM	Long.(E) in UTM
1	Berga Nr. Addis Alem	13.485	17	249	996668	428556
2	Holeta Nr. Holeta	14.97	76	119	1004010	446886
3	Teji @Asgori	24.142	61	663	970876	426678
4	Awash @ Belo	32.383	35	2568	978231	435855

S. No	Name of Station	River Length (km)	Watershed Slope (%)	Watersheds (km^2)	Latitude (N) in UTM	Long.(E) in UTM
5	Akaki at Akaki Village	44.799	68	884	981872	476159
6	Mojo @ Mojo Village	42.526	96	2175	950545	509170
7	Awash @ Melka Hombole	106.151	33	7656	950551	476159
8	Awash @ Melka Kunture	57.353	30	4456	961622	455998
9	Litle Akaki	21.34	56	131	466795	999047
10	Awash @ Ginchi	58.36	24	76	404697	997173

3.1.3. Land Use and Soil Type

Upper Awash land use condition in the watersheds consists of mainly cultivated agricultural land, grassland, and forestland, rural and urban settlements. It is estimated that 67% is intensively cultivated, 25.5% is moderately cultivated, 4.5% is bush land or shrub land or wooded grassland, and 3% is urban area and alpine vegetation. Strictly speaking, even the land use within the upper Awash is diverse.

The soil type in the upper awash sub-basin is diverse. The most common soil types are Clay, Sand, Clay-Loam, Silt-Clay -Loam, Sand-Clay, Silt-Clay (Paulos 1989). Land use and soil type have a direct impact on the flood amount, speed and potential to form damage that the study should give attention for land use and land cover of the sub basin.

3.1.4 Climate

The World Meteorological Organization (WMO), define Climate as the synthesis of weather condition in a given area characterized by long-term statistics (mean, variance, probabilities of extremes, etc.) of the meteorological elements in an area (NEDECO, 1998). The WMO usually accepts 30 years of statistical data series to define climate.

In January, when the ITCZ is in its most southerly position, most of Ethiopia comes under the influence of North East trade winds, resulting in a pronounced dry season. In March, when the ITCZ crosses the basin from the south, the small spring rain occurs. In, June and July the ITCZ reaches its most northerly location. This is associated with relatively humid south west monsoon air, which is responsible for the main rainy season in July and August with heavy rains. The climate of the Upper Awash Basin, in general, comes under the influence of the Inter Tropical Convergence Zone (ITCZ). This zone of low pressure makes the convergence of dry tropical easterlies and moist equatorial westerly. The explanation of the seasonal rainfall distribution within the basin lies in the annual migration of the ITCZ across the basin. The ITCZ starts its advance across the basin from the south in March, bringing the small or spring rains. In June and July the ITCZ reach its most northerly location beyond the basin which then experiences the heavy or summer rains throughout. The ITCZ returns southwards during August, September and October, restoring drier, easterly airstreams that prevail until the ITCZ resumes its northward migration in March (Halcrow, 1989).

3.1.5 Temperature

Temperature varies considerably over the basin and range from a mean annual temperature of 16.7^0C to 29^0C. The mean annual temperature range in the basin is around 15^0C. The temperature at Addis Ababa ranges from a mean monthly maximum of 22.5^0C to a mean monthly minimum of 9.6^0 C (Halcrow, 1989).

3.2 Data collection and analysis

Climatic inputs and HRU hydrological balance inputs used in SWAT include daily precipitation, maximum and minimum temperature, solar radiation data, relative humidity, and wind speed data, which can be input from measured records and generated.

Daily precipitation, maximum and minimum temperature data will obtain from National Meteorological Service Agency (NMSA) for the nearby weather stations (Taye, 2009). Engineering studies of water resources development and management be determined by heavily on hydro-meteorological data. These data would be stationary, consistent, and homogeneous when they are used to simulate a hydrological system. If it does not fulfill one of the above criteria's, it will result in a big problem that contradicts the actual situation.

3.2.1 Meteorological Data

The most prerequisite parameter of SWAT model is climate data. This data is collected from Ethiopian National Metrological Agency. The data is collected based on their homogeneity of the pattern, which can be representative to the Upper Awash River basin. The meteorological data such as, Precipitation, maximum and minimum temperature is collected. SWAT weather generator model (WGEN) is used to fill missing values in weather data of relative humidity, sunshine hour and solar radiation. The Penman–Montheith method which utilizes the solar radiation, relative humidity and wind speed data records is employed for estimation of potential evapo-transpiration (PET) for this specific study. Meteorological stations also geo-referenced using latitude, longitude, and elevation data.

Table 3.3: Meteorological stations around the watershed

Station name	Latitude(degree)	Longitude(degree)	Total period(year)
Addis Ababa	9.0	38.7	33
Akaki	8.9	38.8	33
Mojo	8.6	39.1	33
U/S Koka	8.4	39.3	33
Adama	39.3	8.6	33
Teji	8.8	38.4	33
Wolencity	8.7	38.6	33

A. Checking consistency of selected stations

Numerous factors could affect the consistency of rainfall record at a given station. A time series observational data is relatively consistent and homogeneous if the periodic data are proportional to an appropriate simultaneous period. This proportionality is tested by double mass analysis in which accumulated rainfall/hydrological data is plotted against the mean value of all neighborhood stations (Nigussie, 2007). Double mass curve method helps in determining the best realistic correlation of stations located near or within watershed. This technique is based on the principle that when each recorded data comes from the same parent population, they are consistent. The double mass curve technique is used to check whether the collected rainfall data from Ethiopian meteorological station is consistent through the selected period of study and reveals if correction will be needed. The recording rain gauge station may have undergone change during the period of record as a result of shifting of rain gauge to new location, change due to change in ecosystem such as forest and occurrence of observational error from a certain date.

A group of certain numbers of neighboring stations is chosen as base stations from the vicinity of a doubtful, all stations said as doubt stations unless they are checked. The data of the annual rainfall of the doubtful station and the average rainfall of the group of base stations covering a long period is arranged in the reverse chronological order (i.e. the latest record as first entry and the old record as the last entry in the list.

The precipitation of station x (doubtful station) can be corrected using the following formula (Nigussie, 2012)

$$Pcx = \frac{Mc}{Ma} \qquad \text{Equn (3.1)}$$

Where,

P_{CX}= corrected precipitation at any time period t at station X

P_X=original recorded precipitation at time period t at station X,

M_C= Corrected slope of double mass curve

M_a= original slope of the double mass curve

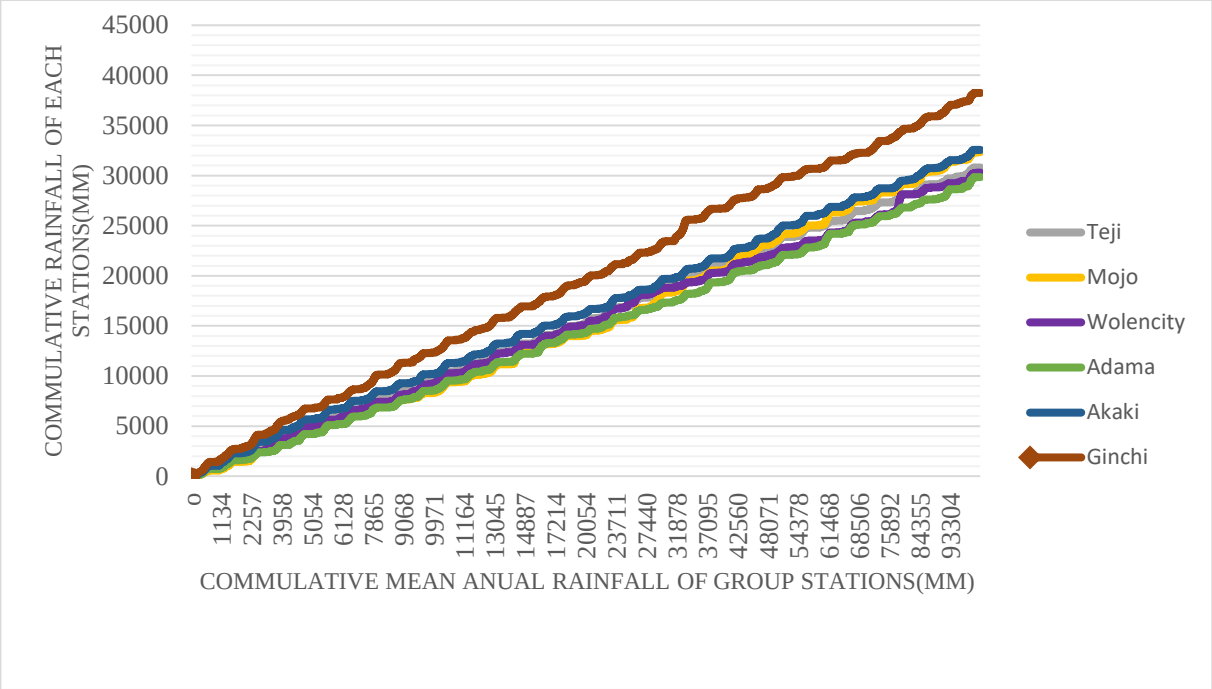

Figure 3.2: Consistency test for rainfall stations

B. Checking homogeneity of stations

Homogeneity analysis is used to recognize a change in the statistical properties of the time series. The reasons can be either natural or manmade. These include alterations to land use and relocation of the observation station. Therefore, in order to select the representative meteorological station for the analysis of areal rainfall estimation, checking homogeneity of group stations is essential. The Standard Normal Homogeneity Test (SNHT) was used for the determination of the inhomogeneous metrological time series for the annual total values of the stations. SNHT test assume the series consisted of break in the mean considered as inhomogeneous. To evaluate the performance of the methods used, three different testing variables were used, which are annual mean, annual maximum and annual median. As stated above, the homogeneity of the annual mean precipitation series of the stations throughout Awash Hombole watershed were tested for the whole 1986–2018 periods. The homogeneity test for Awash Hombole station is shown as a typical example (See figure 3.3).

Given Yi (i, is the year from 1to n) is the testing variable with $\bar{Y}$ the mean and s is the standard deviation.

A statistic T(y) is used to compare the mean of the first y years with the last of (n- y) years and can be written as below: The maximum value of T, denoted Ty

$$Ty = yZ_1^2 + (n-y)Z_2^2, \qquad Y = 1,2,\ldots..n \qquad \text{Equn (3.2)}$$

$$\text{Where, } \acute{Z}_1 = \frac{1}{y}\sum_{i=1}^{n}\left(\frac{Y_i - \bar{Y}}{s}\right) \quad \text{and} \quad \acute{Z}_2 = \frac{1}{n-y}\sum_{i=y+1}^{n}\left(\frac{Y_i - \bar{Y}}{s}\right) \qquad \text{Equn (3.3)}$$

Where Z_1 and $\acute{Z}_2$ are the mean values before and after the shift. The year y consisted of break if value T is maximum. The corresponding value of y is the most probable break point, i.e. the last year at the old level. The null hypothesis can be rejected, if the test statistic (To) is above the selected significance level, which depends on the sample size. (Nigussie, 2012)

$$T_o = \max T_y, \quad 1 \leq y \leq n-1 \qquad \text{Equn (3.4)}$$

WhereZ1and$\acute{Z}$2 are the mean values before and after the shift.

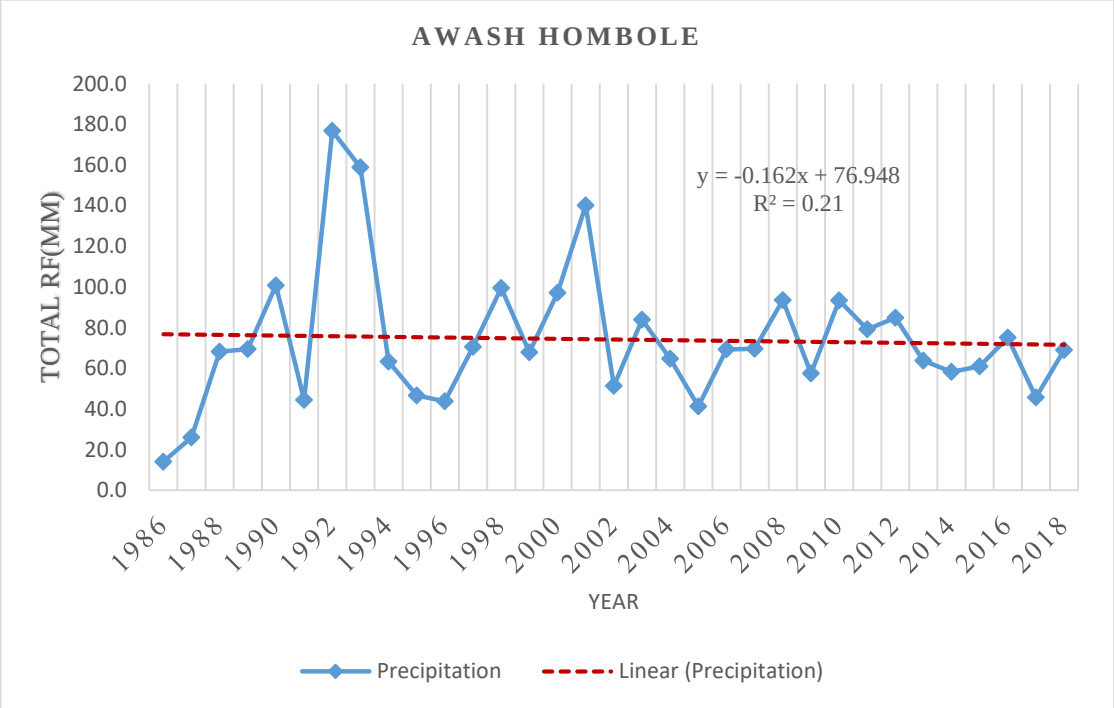

Figure 3.3: Homogeneity test of yearly precipitation

C. Missing data analysis

Even though complete hydro-meteorological data is a pre-requisite for successful water resource planning and management, important data sets are usually missing due to disturbance of measurements caused by natural and human-induced factors Elshorbagy, (2000) as cited in Habtom (2009).

Some techniques of filling missed rainfall data is simple linear interpolation, arithmetic mean method, inverse distance and normal ratio method. If data gaps are big, incomplete time series may hide the pattern of the data, and they may considerably distort the results of any statistical analysis. Filling the gaps in daily climate data is therefore a crucial issue. A way to amends the issue in existing time series data is filling the gaps using one of the many available techniques. For this study, the missing values of daily rainfall recorded were completed by using the normal ratio method whereas air temperature, relative humidity, sunshine hours, wind velocity and hydrological data were corrected with arithmetic mean methods. Filling method gives poor results when the climate variable under analysis has a high spatial variability. Hence, in order to reduce this effect, those stations that are less important due to their distant location from the border of the watershed were used for filling purpose with their corresponding nearby stations.

Normal ratio method: This method is used if any surrounding gauges have the normal annual precipitation exceeding 10% of the considered gauge. But, if all (not some) value of normal annual precipitation of surrounding gauges lies within 10% range the arithmetic mean method would be used. First, we were determined that weather arithmetic mean or normal ratio method is to be applied. Therefore, since some value of normal annual precipitation of neighboring stations is beyond 10% range normal ratio method was applied.

The missing data are estimated by;

$$Pm = \frac{1}{n} * \sum_{i=1}^{n} \left(\left(\frac{Nm}{Ni}\right) Pi\right) \qquad \text{Equn. (3.5)}$$

Where; Pm is precipitation at the missing location, Pi is precipitation at index station, Ni is over year's average annual precipitation at index stations, Nm is over years average annual precipitation at missing data gauge and n is number of rain gauges.

3.2.2 Hydrological Data

In hydrological data collection and analysis, Stream flow measurement is used for evaluations against the modeled stream flow in model calibration and validation. Daily stream flow data for Awash Watershed is collected from Ministry of Water, Irrigation and Energy (MoWIE) for long periods for SWAT simulation result of calibration and validation. Water resource studies highly depend on stream flow data. These data was checked for consistent, stationary and homogenous.

3.2.3 Spatial data

The Digital Elevation Model (DEM) which is the main parts of spatial data was collected from Ministry of Water, Irrigation and Energy (MoWIE) with resolution of (30mx30m). Land use map was produced from satellite images (USGS GLOVIS).

3.2.3.1 Digital Elevation Model (DEM)

Digital Elevation Model (DEM) is defined topography that refers to the elevation of any point in a given area at a specific spatial resolution. The DEM is any digital representation of a topographic surface and specifically to a raster or regular grid of spot heights. It is the basic input of the Arc GIS integrated SWAT hydrologic model to delineate the watershed, to extract information about the topography/elevation of the watershed and to analyze the drainage patterns of the land surface terrain. Sub-basin parameters such as slope gradient, slope length of the terrain, and the stream network characteristics were also derived from the DEM. The digital elevation model used in this study was obtained from the Ministry of Water Resource with a resolution of 30m*30m.

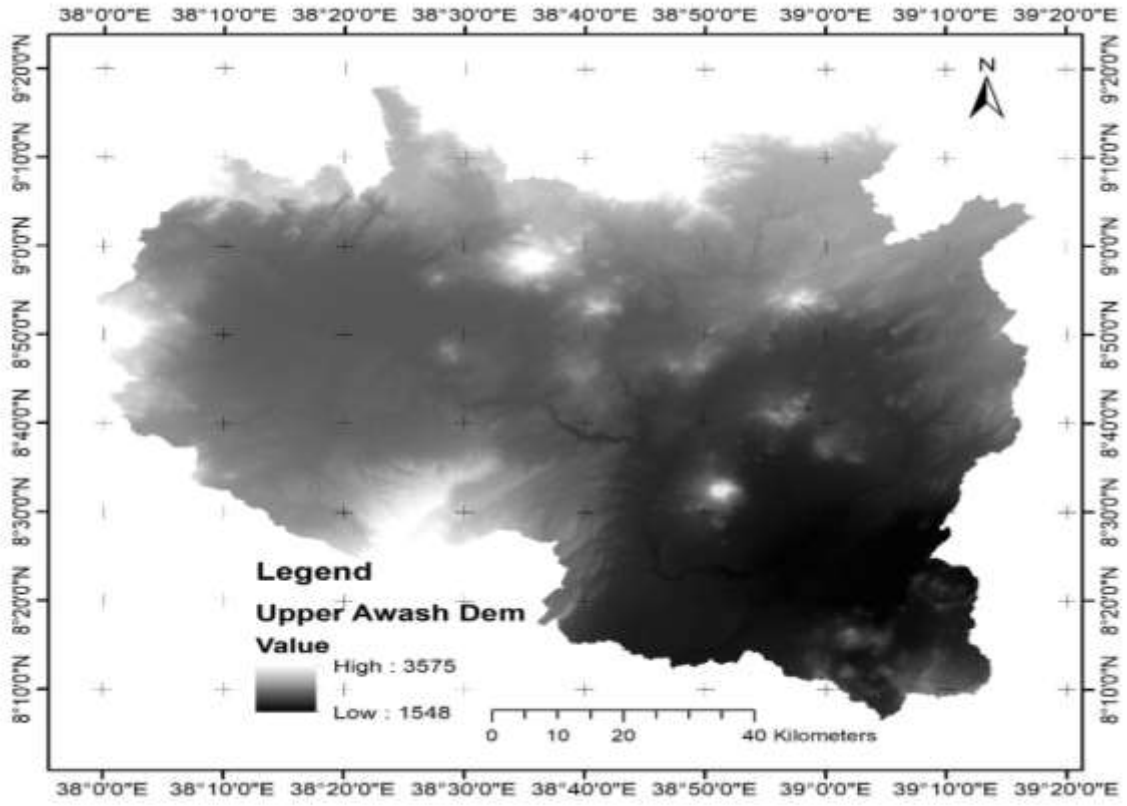

Figure 3.4: Map of the digital elevation model

3.2.3.2 Land use/ Land cover data

The main input data of the SWAT model is Land use land cover that describe the Hydrological Response Units (HRUs) of the watersheds which affect runoff, evapotranspiration and surface erosion in a watershed. It is furthermore used for comparison of impacts on stream flow of the watershed with in time (Briley, 2010).

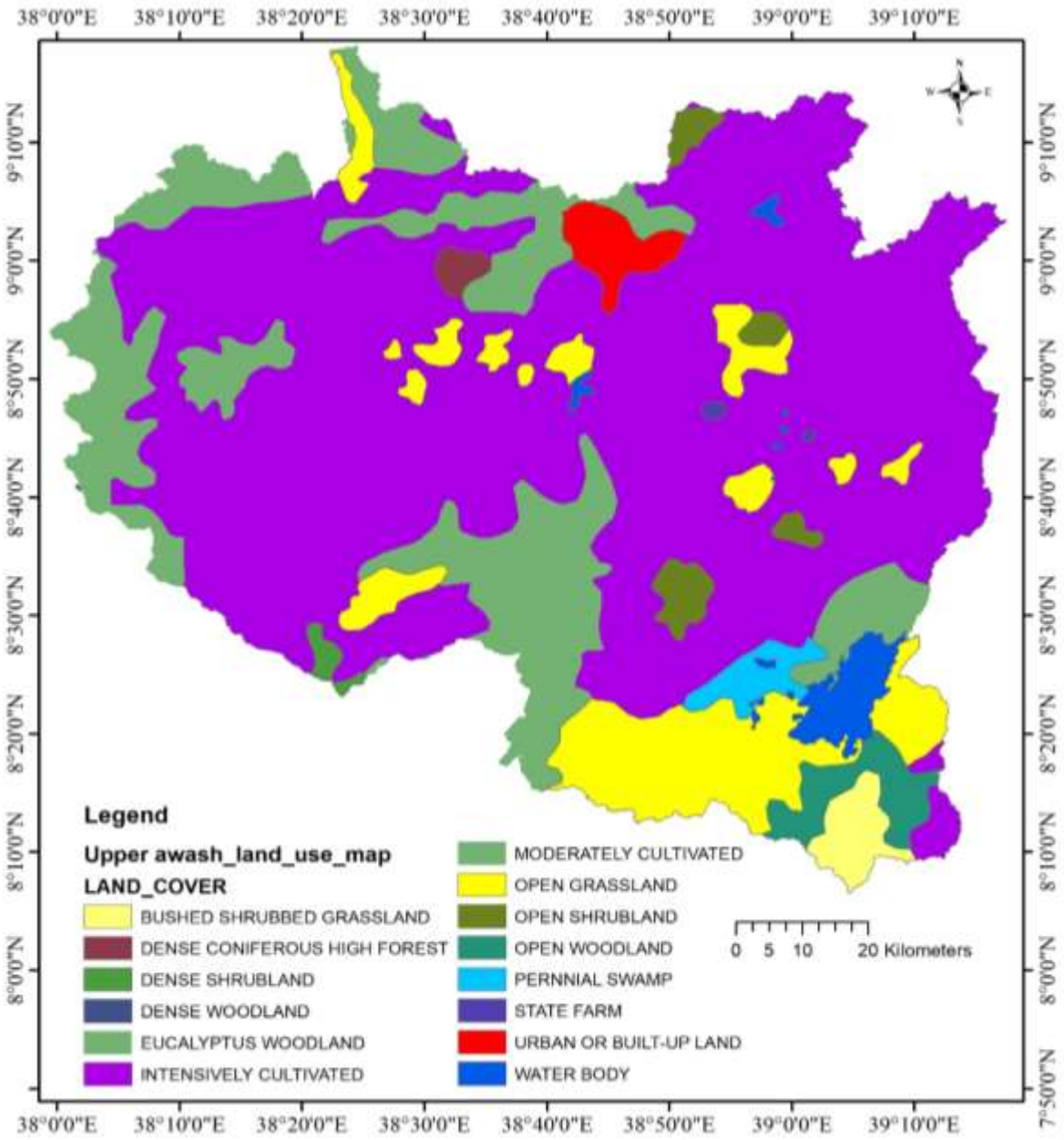

Figure 3.5: Upper Awash land cover Map

3.2.3.3 Soil Data

The soil data of the upper awash is required for the SWAT model inputs concerning watershed's soil physical and chemical properties, first the shape file format of soil type distribution through the watershed was collected from Ethiopian MoWR GIS department. Using this shape file, soil texture, available water content, hydraulic conductivity, bulk density and organic carbon content for different layers of each soil type were extracted from Major Soils of the world database FAO (1995) and Digital soil map of the world data base and derived soil properties from FAO (1998).

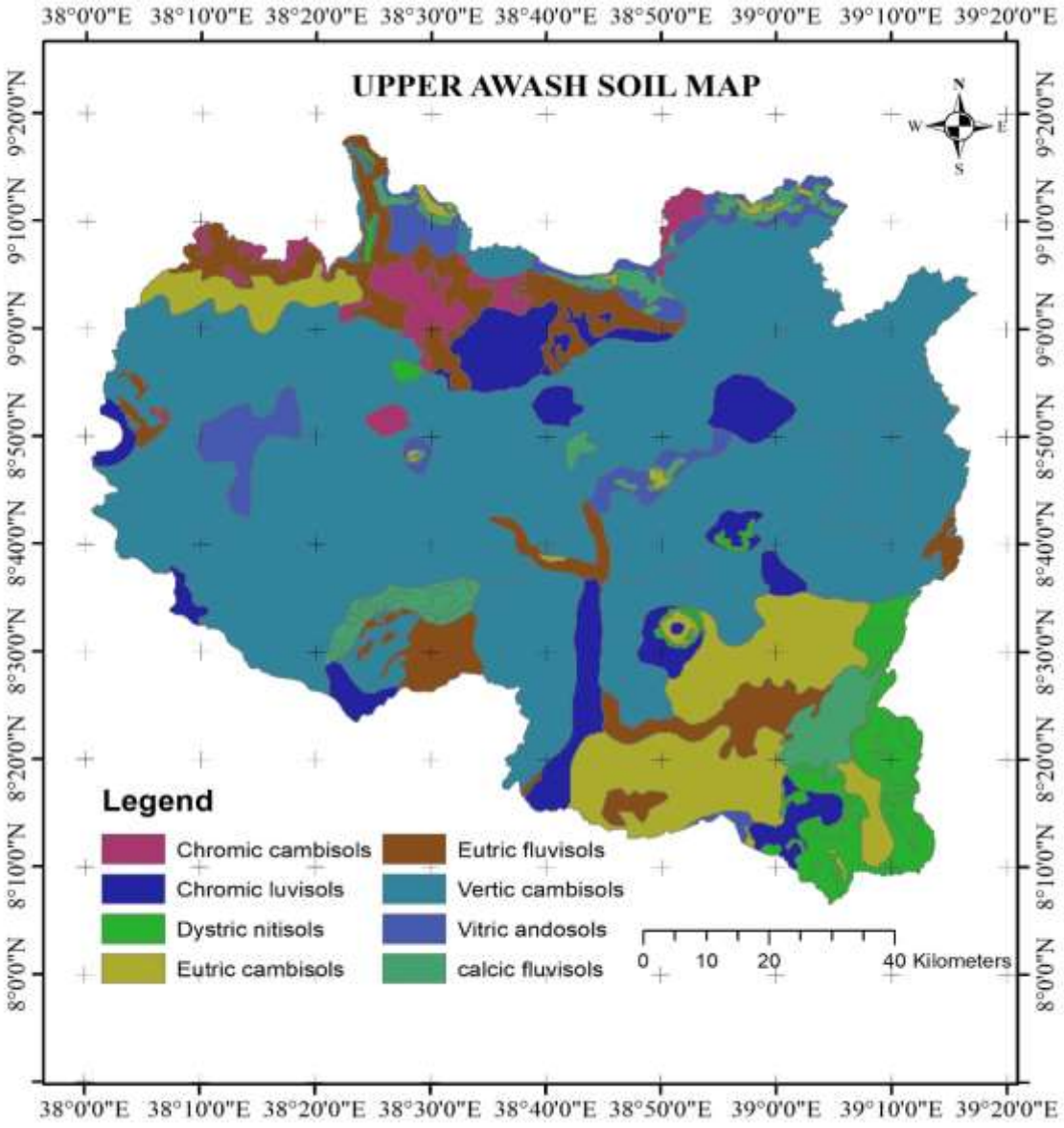

Figure 3.6: Soil Map of upper awash watershed

Table 3.4: Major soil type of upper awash watershed

		Area coverage	
No	Soil type	Area km^2	Area%
1	Calcic fluvisols	480.28	21.1
2	Chromic camisoles	257.04	11.3
3	Chromic luvisols	315.92	13.9
4	Dystric nitisols	289.44	12.7
5	Eutric cambisols	157.4	6.9
6	Eutric fluvisols	216.44	9.5
7	Vertic cambisols	266.76	11.7
8	Vitric andosols	288.92	12.7
	Total	2272.2	100.0

3.2.3.4. Stream flow Data

The stream flow data of the upper awash watershed is required for the calibration and validation of the model. The daily stream flow data (1986-2015) were collected from the Ministry of Water, Irrigation and Energy of Ethiopia at Awash Hombole river gauging station.

3.3. The SWAT Model

3.3.1 The SWAT Model selection

The reasons behind for selecting the SWAT model for study of land use land cover are; the model was applied for land use, land cover and climate change impact assessment on stream flow in different parts of the world (Setyorini *et al*., 2017; Yang *et al*., 2017; Yin *et al*., 2017; Zhang *et al*., 2017). The SWAT model simulates the major hydrological process in the watershed and capable of yearly, monthly, daily or sub-daily data over long periods; it is ready and freely available. The SWAT model combines studies of water quantity (river discharge, surface flow, sub-surface flow, lateral flow, base flow, drains, irrigation, reservoirs, and lakes).

SWAT is a recent model used to assess the watershed hydrology (Jha, 2011). According to Kannan *et al*. (2007), it is the best among the different hydrological models due to its capability for application to large-scale watersheds (>100km^2), interface with a Geographic Information science (GIS), continuous time simulations performance and generation of the maximum number of sub-basins and ability to characterize the watershed in enough spatial detail.

3.3.2 Description of the SWAT model

The SWAT model was developed to evaluate the impact of land management practices on the water in large, climate and complex watersheds with varying soils, land use and management conditions over long periods of time (Arnold *et al*., 1998). The SWAT model is a watershed scale hydrological model based on the principles of the water balance equation:

$$SW_t = SW_O + \sum_{i=0}^{t}(R_{day} - Q_{surf} - E_a - W_{seep} - Q_{gw}) \qquad Eqn.(3.6)$$

Where, SW_t is the final soil water content (mm), SW_0 is the initial soil water content on day i (mm), t is the time (days), R_{day} is the daily precipitation on a day i(mm), Q_{surf} is the amount of surface runoff on a day i(mm), E_a is the evapotranspiration on a day i(mm), W_{seep} is the amount of water entering the unsaturated zone on a day i(mm) and consists of the infiltration rate minus the capillary rise, and Q_{gw} is the amount of return flow on a day i (mm).

3.4 Stream flow Components

3.4.1 Surface runoff

The portion of rainwater that is not lost to interception, infiltration, and evapotranspiration is surface runoff (Solomon, 2005). It occurs when the rate of precipitation exceeds the rate of infiltration. SWAT compromises two methods for estimating the surface runoff: the Soil Conservation Service (SCS) curve number method and the Green and Ampt infiltration method. The Green and Ampt method needs sub-daily time step rainfall, which made it difficult to be used for this study due to unavailability of sub-daily rainfall data. Therefore, the SCS curve number method was adopted for this study.

The general equation for the SCS curve number is:

$$Q_{surf} = \frac{(R_{day} - I_a)^2}{(R_{day} - I_a + S)} \qquad Eqn.(3.7)$$

Where, Q_{surf} is the accumulated runoff or rainfall excess (mm), R_{day} is the rainfall depth for the day (mmH_2O), I_a is initial abstraction which includes surface storage, interception and infiltration prior to runoff (mmH_2O) and S is retention parameter (mmH_2O).

The retention parameter varies spatially due to changes in land surface features such as soils, land use, slope and management practices. These parameters also can be affected temporally due to changes in soil water content. It is mathematically expressed as:

$$\mathrm{S} = 25.4\left(\frac{1000}{\mathrm{CN}} - 10\right) \qquad Eqn.\ (3.8)$$

Where, CN is the curve number for the day and its value is the function of land use practice, soil permeability and soil hydrologic group.

The initial abstraction I_a, is commonly approximated as $0.2S$ and equation 3.7 becomes:

$$\mathrm{Q_{surf}} = \frac{(R_{day} - I_a)^2}{(\mathrm{R}_{day} - 0.8\mathrm{S})} \qquad Eqn.(3.9)$$

Runoff will only occur when $R_{day} > I_a$

3.4.2 Lateral and Interflow

As soon as the surface runoff is calculated from rainfall, the remaining amount of water is permitted to infiltrate in soil layers. The infiltrated water is then routed through soil layers by the storage routing methodology (Han *et al*., 2012; Neitsch *et al*., 2011). The storage routing method first fulfils the field capacity requirement of the upper soil layer and calculates if there is excess soil water available:

$$SW_{ly.excess} = Q_{perc,ly-1} - FC_{ly} \qquad Eqn.(3.10)$$

Where, $SW_{ly.excess}$ is the water content in a soil layer above the field capacity (mm), $Q_{perc,ly}$ is the amount of water percolating into lower soil layer (mm) and FC_{ly} is the depth of water in soil layer when it is at field capacity (mm).

If there is excess soil water available then the lateral flow from an HRU is calculated as:

$$Q_{lat} = 0.024\left(\frac{2 * SW_{ly.excess} * K_{sat.ly} * slp}{\emptyset_d * L_{hill}}\right) \qquad Eqn.(3.11)$$

Where, $K_{sat.ly}$ is saturated hydraulic conductivity (mm/hr), slp is the steepness of a slope (m/m), $\emptyset_d$ is the drainable porosity of soil layer (mm/mm), and L_{hill} is the hill slope length(m).

3.4.3 Base flow

To simulate the groundwater SWAT partitions groundwater into two aquifer systems: a shallow, unconfined aquifer which contributes return flow to streams within the watershed and deep, confined aquifer which contributes return flow to streams outside the watershed (Neitsch *et al*., 2011). In SWAT the water balance for a shallow aquifer is:

$$aq_{sh,i} = aq_{sh,i-1} + W_{rchg} - Q_{gw} - W_{revap} - W_{deep} - W_{pump,sh} \quad Eqn.(3.12)$$

Where, $aq_{sh,i}$ is the amount of water stored in the shallow aquifer on day i (mm), $aq_{sh,i-1}$ is the amount of water stored in the shallow aquifer on day $i-1$ (mm), W_{rchg} is the amount of recharge entering the aquifer on day i(mm), Q_{gw} is the groundwater flow, or base flow, or return flow, into the main channel on day i (mm), W_{revap} is the amount of water moving into the soil zone in response to water deficiencies on day i (mm), W_{deep} is the amount of water percolating from the shallow aquifer into the deep aquifer on day i (mm), and $W_{pump,sh}$ is the amount of water removed from the shallow aquifer by pumping on day i (mm). The shallow aquifer contributes base flow to the main channel or reaches within the sub-basin.

3.4.4 Flow Routing

Two possibilities are available to route the flow in the channel network: the variable storage and Muskingum methods. The variable storage method uses a simple continuity equation in routing the storage volume, whereas the Muskingum routing method models the storage volume in a channel length as a combination of wedge and prism storages (Arnold *et al*., 1995).

For a given reach segment, storage routing is based on the continuity equation:

$$V_{in} - V_{out} = \Delta V_{stored} \qquad Eqn.\ (3.13)$$

Where, V_{in} is the volume of inflow during the time step (m^3H_2O), V_{out} is the volume of outflow during the time step (m^3H_2O) and ΔV_{stored} is the change in the volume of storage during the time step (m^3H_2O).

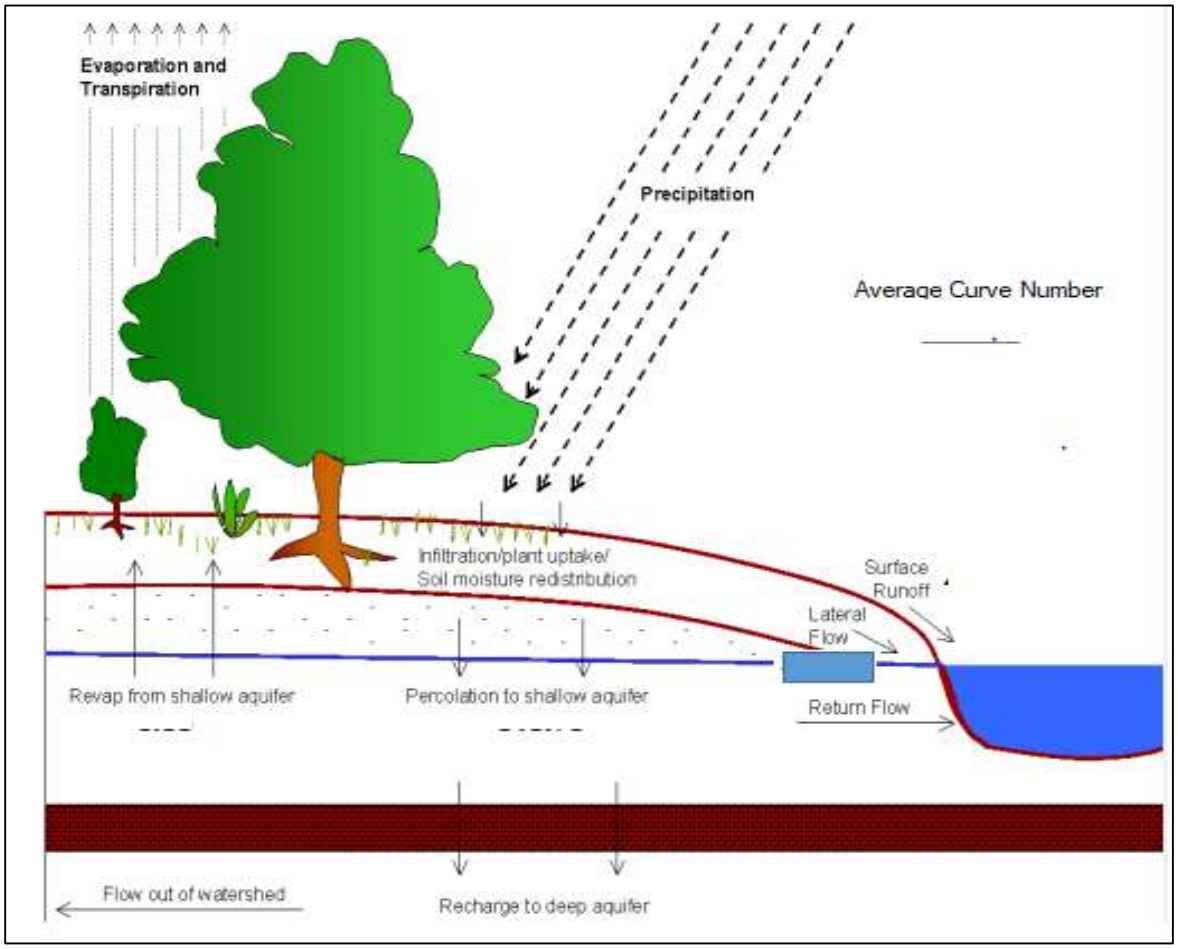

Figure 3.7: Schematic representation of the hydrological cycle

3.5. General framework of the study

The technique to assess the impact of land use and land cover change, on hydrological regimes can be accomplished through integrating GIS, remote sensing, and hydrological models. Satellite image have great impact for preparation of land use land cover of the area.

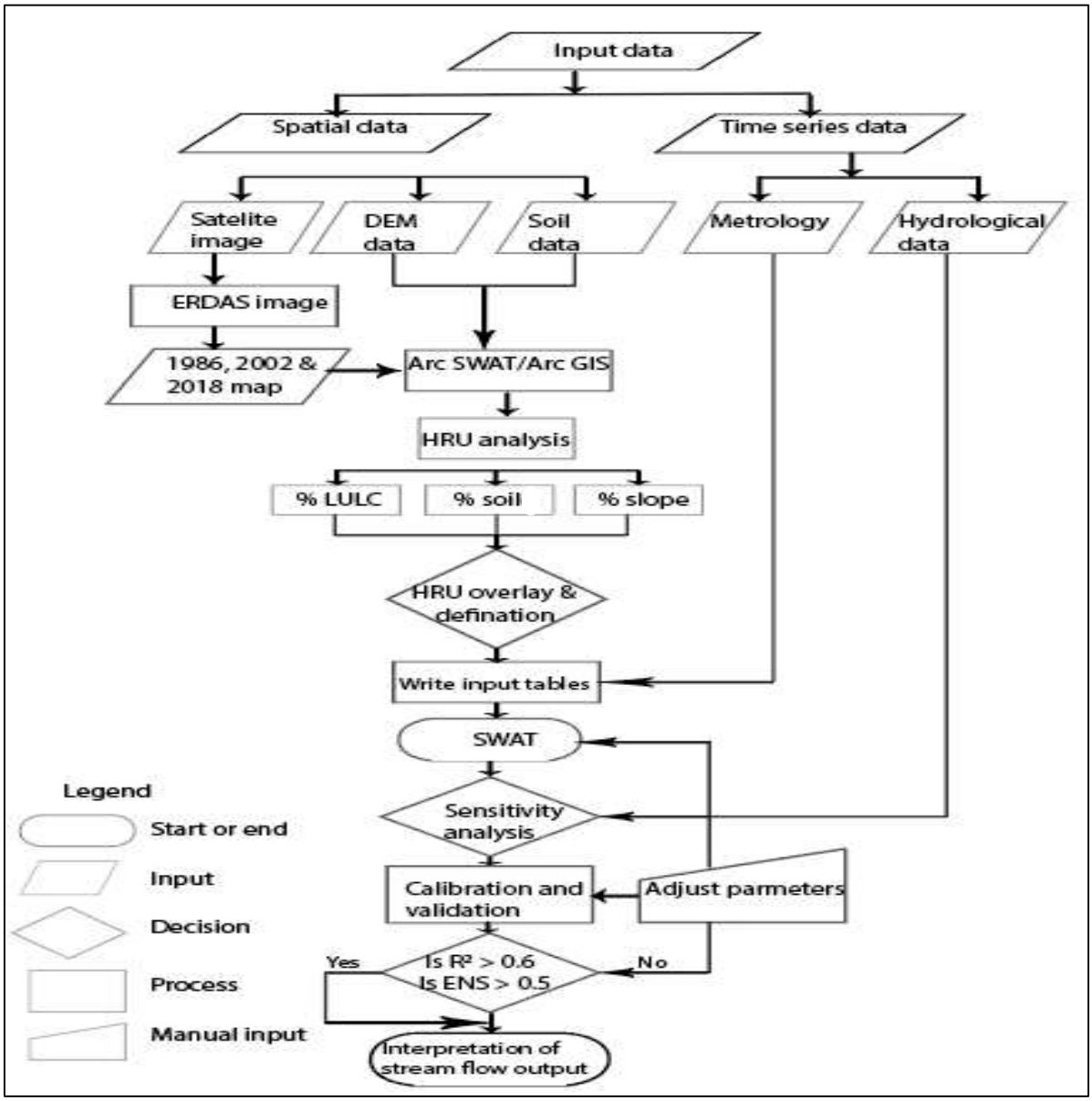

Figure 3.8: Conceptual frame work of the study

Table 3.5: Software and tools used for this research

No	Software and Tools	Purpose
1	Arc GIS 10.3.1	Spatial data processing and to run arc SWAT software
2	Arc SWAT 2012_10.3.19	Hydrologic modeling purpose
3	ERDAS imagine 2014	LU/LC map classification and interpretation
4	Google earth	Classified image accuracy assessment
5	GPS Garmin 78	Collecting accuracy assessment points
6	SWAT-CUP 5.1.6.2	Model Calibration and validation

3.6 Types and Sources of Data

Land use land cover study required several data that includes topographic data (DEM), Land use and land cover data, soil data, stream flow data, daily data of climatic variables (daily data of precipitation, maximum and minimum temperature, relative humidity, wind speed and solar radiation). The DEM, land cover satellite data, Soil and hydrological data were collected from the Ministry of Water, Irrigation and Energy of Ethiopia. The climatic data were obtained from the National Meteorological Agency of Ethiopia.

3.6.1 Landsat Data

Land use and land cover distribution of the upper awash watershed was prepared by using Landsat imageries to classify changes in land use and land cover distribution over 33 years period from 1986 to 2018. Landsat images; Landsat-5 TM, Landsat-7 ETM+ and Landsat-8 were selected for the period of 1986, 2002 and 2018 respectively. In order to avoid a seasonal difference in vegetation pattern and distribution throughout a year, the selection of dates of the developed data were made as much as possible in the same annual season of the attained years.

Table 3.6: Characteristics of satellite imagery used

Year	Sensors	Spatial resolution	Acquisition date	Path/row
1986	Landsat-5 TM	30×30m	January 26, 1986	168/85
2002	Landsat-7 ETM+	30×30m	January 21, 2002	168/85
2018	Landsat-8OLI/TIRS	30×30m	January 24, 2018	168/85

The images were gained from the United States Geological Survey (USGS) Earth Resources Observation Systems (EROS) data Centre under the Landsat Archive. The years were carefully chosen by taking into consideration availability and quality of Landsat images. The images were picked up as much as possible in the same season to avoid the effect of seasonal variations. Other data were also collected for the analyses, including GPS points for major Land use and land cover classes, high-resolution Google earth images for accuracy assessment.

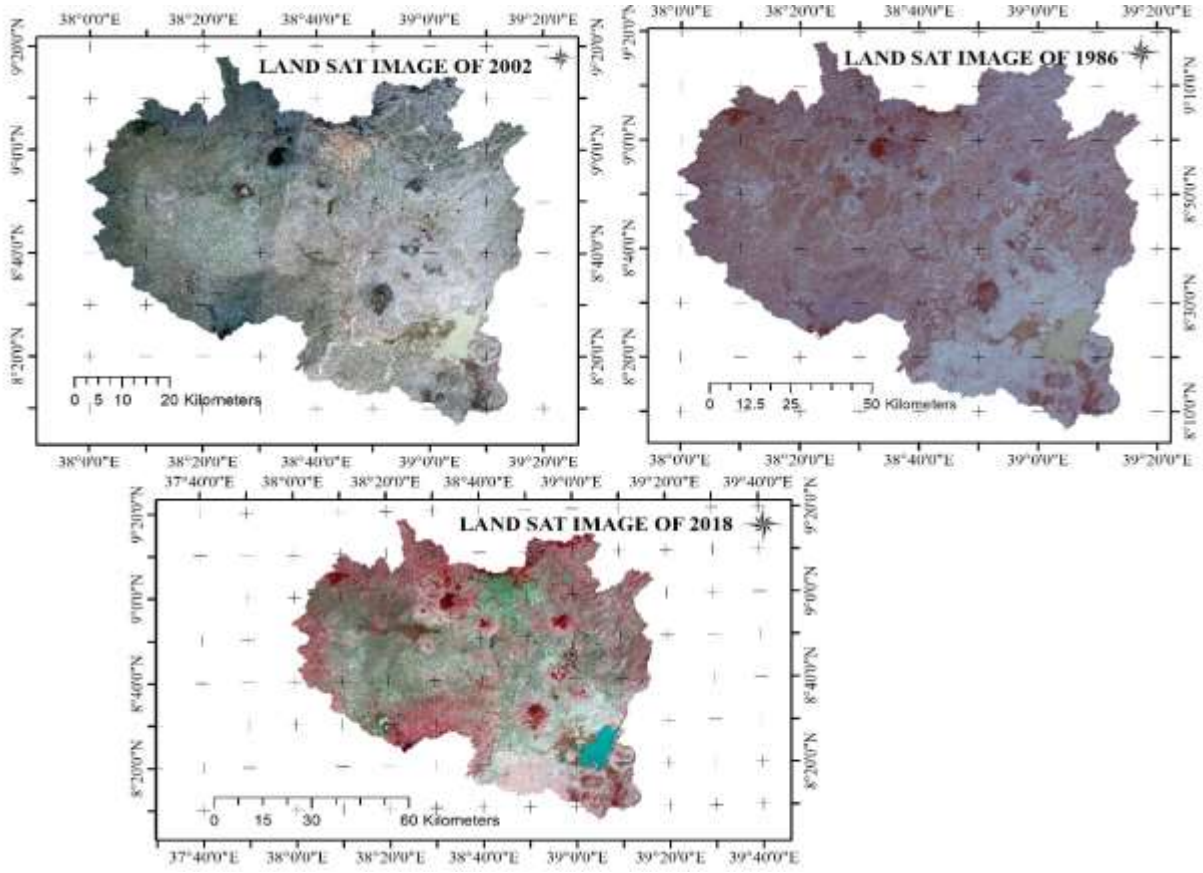

Figure3.9: Raw Landsat satellite imageries in the study area

3.7 Image Classification

Based on the satellite images and training points the land use land cover classes studied for changes were; Forest land, Grass land, cultivated land, Settlement (urban) and Water body.. Classifying the above-listed land use and land cover classes were done based on visual interpretation of the satellite images and field observation.

Forest Land: Area with high concentration of trees which contain deciduous forest land, evergreen forest land, mixed forest land and plantation forests that mostly are eucalyptus, junipers and conifers.

Grass land: Area enclosed with grass that is used for grazing and that covered for a considerable period of the year.

Water body: Area which remains water logged throughout the year, in this study refer to manmade reservoirs.

Cultivated Land: Areas which can be used for both annual and perennial crop cultivation

Settlement (Urban): areas that are a permanent concentration of people, building, and other man-made structures and other activities. (Berga, 2011)

3.7.1 Supervised Classification

This method is used to cluster pixels in a data set into classes corresponding to user-defined area of interest (AOIs) or training classes which are carefully chosen as representative areas to be mapped in the output. Supervised classification done using Maximum Likelihood algorithm.

3.8 Accuracy Assessment

The most essential process in the image classification is Accuracy assessment. It is a procedure used to estimate the accuracy of image classification by comparing the classified map with a reference map (Caetano *et al*., 2005). The most commonly used classification accuracy is in the form of error matrix, which can be used to derive a series of descriptive and analytical statistics (Manandhar *et al*., 2009). The rows show the number of pixels per class, and the columns of the matrix display the number of pixels per class for the reference data for the classified image. From this error matrix, the number of accuracy methods such as overall accuracy, user's and producer's accuracy determined. The overall accuracy is used to indicate the accuracy of the whole classification (i.e. number of correctly classified pixels divided by the total number of pixels in the error matrix), whereas the other two measures indicate the accuracy of individual classes.

Product's accuracy represents the probability that a pixel on reference data has been correctly classified, whereas User's accuracy is regarded as the probability that a pixel classified on the map actually represents that class on the ground or reference data. Accuracy assessment of the classified map is the evaluation of the classified image and the sampling points from the Google Earth Imageries and present land cover maps (Yesserie, 2009). In this study, the assessment was carried out using 1986 maps and 2002 maps together with the historic Google Earth Image and previous knowledge of the area was used as reference data to generate testing data set, and for 2018 image, GPS points were collected for each land use/land cover classes. According to (Anderson *et al*, 1976), the minimum accuracy value for consistent land cover classification is 85 %. The other authors (Bedru, 2006), explains that the expected accuracy is determined by the users themselves depending on the type of application the map product will be used later. Accuracy levels are accepted by users may not acceptable by other users for certain task (Bedru, 2006).

3.8.1 Producer's Accuracy

This accuracy expresses us it is how well attained by dividing the number of correctly classified pixels in the category by the total number of pixels of the category in the reference data. The producer's accuracy is also recognized as an Omission Error, which is the possibility of a reference pixels being classified correctly. It gives only the proportion of appropriately classified pixels. The overall result of the producer's accuracy ranges from 82.5 % to 95%. The lowest values were misclassified due to the similar spectral value of different land cover classes

3.8.2 User's Accuracy

It is the ratio between the total number of pixels properly belonging to a class (diagonal elements) and the total number of pixels allocated to the same class by the classification procedure (row total). This quantity describes the probability that a pixel of the classified image truly corresponds to the class to which it has been allocated.

According to the formula given by Foody (2002) overall accuracy and Kappa coefficient is calculated as follows;

$$\text{Overall accuracy} = \sum_{k=1}^{q} \frac{nkk}{N} * 100 \qquad Eqn.\ (3.14)$$

$$\text{Kappa coefficient} = \frac{N\sum_{k=1}^{q} nkk - \sum_{k=1}^{q} nk+n+k}{N^2 - \sum_{k=1}^{q} nk+n+k} * 100 \qquad Eqn.\ (3.15)$$

Where; N is total number of reference points, q is number of rows in the matrix, nkk is sum of correctly classified cells, n+k is the total for row i and nk+ is the total for column i

Studies suggested that >80% overall classification accuracy is required to guarantee the quality of the LULC classification (Li & Wang, 2009).

3.8.3 Ground truth

Ground truth is important in the initial supervised classification of image. More specifically, ground truth may refer to a process in which a pixel on a satellite image is compared to what is there in reality (at the present time) in order to verify the contents of the pixel on the image. In the case of a classified image, it allows supervised classification to help determine the accuracy of the classification performed by the remote sensing software. The spectral characteristics of these areas area are used to train the remote sensing software using decision rules for classifying the rest of the image. Additional ground truth sites allow the remote sensor to establish an error matrix which validates the accuracy of the classification method used. It is important that the remote sensor chooses classification method that works best with the number of classifications used while providing the least amount of error. The accuracy assessment of the classified map is the comparison of the classified image and the sampling points from the orthophotos, Google Earth Imageries and existing land cover maps (Yesserie, 2009). In this study a total of 182 testing sample points were selected randomly for each year of 1986, 2002 and 2018 map respectively.

Land Use / land Cover Code According to SWAT model

Land use land cover is one of the most influencing the hydrological properties of the watersheds. It is one of the core input data of the SWAT model to describe the Hydrological Response Units (HRUs) of the watersheds. The SWAT model has pre-defined four-letter codes for everyone land use category.

These codes were used to linkage to the land use map of the study area to SWAT land use databases. Therefore, while formulating the lookup-table, the land use types were made compatible with the input needs of the model.

Table 3.7: LULC classification of the watershed as per SWAT model

LULC classes	LULC class for SWAT	SWAT code
Cultivated land	Agricultural land close to grown	AGRC
Mixed forest	Forest-Mixed	FRST
Grazing land	Pasture	PAST
Water & marshy land	Water	WATR
Settlements/Built-up area	Residential	URBN

3.9 SWAT Model Setup

3.9.1 Watershed Delineation

The major stage in generating SWAT model input is delineation of the watershed from a DEM. Data's that entered as inputs into the SWAT model were prepared to have spatial characteristics. Before going in hand with spatial input data i.e. the soil map, LULC map and the DEM will project into the similar projection called UTM Zone 37N, which is projection parameter for Ethiopia. Watershed delineation method include five major steps, DEM setup, stream definition, outlet and inlet definition, watershed outlets selection and definition and calculation of sub-basin parameters.

3.9.2 Hydrological Response Units (HRU)

For purpose of simulation, a watershed is divided into a number of similar sub-basins (hydrologic response units or HRUs) having unique soil, slope and land use properties. The input data for each sub-basin is grouped into categories of weather; unique areas of land cover, soil, and management within the sub-basin; reservoirs; groundwater; and the main channel or reach, draining the sub-basin. (Nigussie, 2012)

The HRU analysis tool in Arc SWAT helps in order to load land use, soil layers and slope map to the projected area. The delineated watershed by Arc SWAT and the organized land use and soil layers were overlapped. HRU analysis in SWAT contains divisions of HRUs by slope classes in addition to Land use and soils. The multiple slope choice which considers different slope classes for HRU definition is selected.

The land use land cover, soil and slope map is reclassified in order to match up with the parameters in the SWAT database. Next to reclassifying the land use, soil and slope in SWAT database, all these physical properties made to be overlaid for HRU definition. The final step in the HRU analysis was the HRU distribution.

The HRU distribution in this study will determine by assigning multiple HRU to each sub-watershed. In multiple HRU importance, a threshold level is used to remove minor land uses, soils or slope classes in each sub-basin. Subdividing the sub watershed into areas having unique land use, soil and slope mixtures makes it possible to study the differences in Evapo-transpiration and other hydrologic conditions for different land covers, soils and slopes (Abdrhman,2011). The slope, land use, and soil datasets were imported, overlaid and linked with the SWAT 2012 databases.

3.10 The Trend Analysis for Stream flow

For this study, the trend analysis was done based on stream flow at awash Hombole river gauging station. The mean annual stream flow computed over the period 1986 to 2015 for past 30 years. The non-parametric Mann-Kendall's test (Mann, 1945; Kendall, 1975) is used to detect trends of annual stream flow, precipitation, and mean temperature in the upper awash watershed.

The Mann-Kendall (MK) is a rank-based non-parametric method for randomness against a time series trend. It is a strong method to avoid the influence of extreme values and is widely used for trend analysis in hydrology and climatology (Belihu *et al*., 2018; Hamed, 2008; Tao *et al*., 2016; Tesemma *et al*., 2010; Yang *et al*., 2017).

The Mann-Kendal trend test was used in this study to examine trends in the climatic and stream flow variables deliberated. The test was based on S statistics and each paired observed values x_j (j > k) of the random variable were inspected to find out whether $x_j > x_k$ or $x_j < x_k$.

The Mann-Kendall S Statistic is computed as follows: equn (3.16_3.21) (Rientjes *et al.,* 2011)

$$S = \sum_{k=1}^{n-1} \sum_{j=k+1}^{n} sgn(x_j - x_k) \qquad Eqn.(3.16)$$

Where, x_j and x_k are the annual values in years *j* and *k*, *j* >*k*, respectively, and n is the length of the data set. If the value of S is positive, there is upward trend and vice versa.

$$sgn(x_j - x_k) = \begin{cases} 1\ if\ x_j - x_k > 0 \\ 0\ if\ x_j - x_k = 0 \\ -1\ if\ x_j - x_k < 0 \end{cases} \qquad Eqn.(3.17)$$

The mean of S is E(S) = 0 and the variance σ^2 is

$$\sigma^2 = \frac{\left[n(n-1)(2n+5) - \sum_{j=1}^{p} t_j(2t_j+5)\right]}{18} \qquad Eqn.(3.18)$$

Where, p is the number of the tied groups in the data set and t_j is the number of data points in the j^{th} tied group.

In the case where there are no ties in either ranking, the distribution of S may be well approximated by a normal distribution with mean zero and variance,

$$\sigma^2 = \frac{n(n-1)(2n+5)}{18} \qquad Eqn.(3.19)$$

The statistic S is approximately normal distributed provided that the following z transformation is employed:

$$Z = \begin{cases} \frac{S-1}{\sqrt{\sigma}} if\ S > 0 \\ \frac{S-1}{\sqrt{\sigma}} if\ S = 0 \\ \frac{S+1}{\sqrt{\sigma}} if\ S < 0 \end{cases} \qquad Eqn.(3.20)$$

The Mann-Kendal trend test was used in this study to investigate trends in the climatic and stream flow variables considered. The test was based on S statistics and each paired observed values. The presence of a statistically significant trend is evaluated using the Z value. A positive and Negative value of Z indicates an upward and (downward) trend. The statistic Z has a normal distribution. To test for either an upward or downward monotonic trend (a two-tailed test) at α level of significance, H_o is rejected if the absolute value of Z is greater than $Z_{1-\alpha/2}$, where $Z_{1-\alpha/2}$ is obtained from the standard normal cumulative distribution tables. For this study, confidence level of 95% was determined by the test statistics.

For significant trends the magnitude of changes were analyzed by estimating slope (β); thus β can be defined as:

$$\beta = \frac{x_j - x_k}{j - k} \qquad Eqn.(3.21)$$

Where, j>k and β is a robust estimate of the slope.

3.11 Model Sensitivity analysis, Calibration and Validation

3.11.1 Sensitivity Analysis

Arc SWAT sensitivity analysis tool has performing two types of analyses. The first type of analysis uses only modeled data to identify the effect of adjusting a parameter value on some measure of simulated output, such as average stream flow. The second type of analysis uses measured data to provide overall "goodness of fit" estimation between the modeled and the measured time series. The first analysis assist to recognize parameters that improve a particular process or characteristic of the model, while the second analysis identifies the parameters that are affected by the physical characteristics of the study watershed and those to which the given project is best sensitive (Veith and Michael, 2009). After an initial SWAT simulation was accompanied, a sensitivity analysis was implemented to highlight basin particular parameters that drive model simulations and make sensitivities to model outputs (Arnold *et al*., 2012). SWAT-CUP 5.1.6.2 is an interface developed for SWAT that can do sensitivity analysis, calibration, validation, uncertainty analysis as well as easily be linked to SWAT.

It was aimed as an interface for SWAT to link the inputs and outputs of a calibration program to the model through text file formats. Srinivasan (2015) recommended that by a trial and error method of parameter range adjustment was used for calibration using SWAT-CUP. In SUFI-2, the assessment of the sensitive parameters is measured using the t-stat values where the values are further sensitive for a larger in absolute t-stat values. P-values are used to define the significance of the sensitivity where the parameter becomes significance if the P-values are close to zero (Khalid *et al*., 2016).

3.11.2 Model Calibration

Model calibration is a means of correcting or fine tuning model parameters to match with the observed data as much as possible, with limited range of deviation established. It is also the adjustment of parameter values and evaluation of predicted output of interest to measured data until a defined objective function is attained.

In this research model was calibrated during a periods of (1986 to 1991), (1996 to 2001), (2006 to 2011) for land use/land caver of 1986, 2002 and 2018 respectively. Parameters for adjustment are selected from those identified by sensitivity analysis. Other parameter further than those recognized during sensitivity analysis was used primarily for calibration due to the hydrological processes naturally occurring in the watershed. Sometimes it is necessary to change parameters in the calibration process other than those recognized during sensitivity analysis because of the type of miss match of the observed variables and predicted variables (White and Chaubey, 2005).

3.11.3 Model Validation

Hydrological model Validation is the comparison of the model outputs with in independent data set without making any adjustment. The main purpose of model validation is to check whether the model can predict flow for another range of period. In this research model was validated during a periods of (1992 to 1995), (2002 to 2005), (2012 to 2015) for land use/land caver of 1986, 2002 and 2018 respectively. Model calibration is utilized for estimating the effectiveness of future potential management practices, the model will be tested against free set of measured data. For instance the model predictive capability will demonstrated as being reasonable in the calibration and validation phases, the model will be used for future predictions under different land use scenarios (Berga, 2011).

3.11.4 Uncertainty analysis

SUFI-2 parameter uncertainty accounts for all bases of uncertainties in driving variables (e.g. rainfall), parameters, the conceptual model, and measured data (e.g., observed flow, sediment). The parameter uncertainty was termed by a multivariate uniform distribution in a parameter hypercube, while the output uncertainty was quantified by the 95% prediction uncertainty band (95PPU) calculated at the 2.5% and 97.5%levels of the cumulative distribution function of the output variables. The 95PPU stands for the 95percent prediction uncertainty or P-factor. The 95PPU measured how well the observed data fit into a 95 per cent confidence range of uncertainty from the simulated output. R-factor measures the range of output uncertainty represented by the visual band. A well-calibrated model will have a small R-factor, represented as a thin 95PPU band that houses the observed measurements (Jemberye, 2016).

Table3.8: Model parameters and permissible ranges. (Tekleab and Kassew, 2019)

No	Parameters	Allowable range
1	CN2	±25%
2	ESCO	±25%
3	Gwqmn	0-5000
4	Canmx	0-10
5	SOL_Z	±25%
6	SOL_K	±25%
7	SOL_AWC	+25%
8	Slope	+25%
9	Cn	35-98

The average thickness of the 95PPU band ($\bar{r}$) and the r-factor are computed by Equations (3.22) and (3.23) respectively.

$$\bar{r} = \frac{1}{n}\sum_{ti}^{n}(y_{ti,97.5\%}^{M} - y_{ti,2.5\%}^{M}) \quad \text{Eqn. (3.22)}$$

$$r - factor = \frac{p-factor}{\sigma_{obs}} \quad \text{Eqn. (3.23)}$$

Where: ($y_{ti,97.5\%}^{M}$ and $y_{ti,2.5\%}^{M}$ represent the upper and lower boundaries of the 95 PPU and σ_{obs} is the standard deviation of the measured data.

3.12 Model Performance Evaluation

Hydrologic model behavior and performance evaluation is usually made and reported through evaluations of simulated and observed variables. The choice and use of specific efficiency criteria and the interpretation of the results can be a challenge for even the furthermost experienced hydrologist in the meantime each criterion may place not the same emphasis on different types of simulated and observed behaviors.

The performance evaluation criteria are used in this study:

A. Nash-Sutcliffe Efficiency

The Nash-Sutcliffe efficiency (NSE) is a stabilized statistic that defines the relative magnitude of the residual variance ("noise") compared to the measured data variance ("information"). NSE indicates how well the plot of observed versus simulated data fits the 1:1 line. If the measured value is the same as all predictions, NSE is 1. If the NSE is between 0 and 1, it indicates deviations between measured and predicted values. If ENS is negative, predictions are very poor, and the average value of output is better estimates the model prediction (Nash and Sutcliffe, 2007).

$$NSE = 1 - \frac{\sum_i (Q_m - Q_s)_i^2}{\sum_i \left(Q_{m,i} - \overline{Q_m}\right)^2} \quad (3.24)$$

Where, NSE is Nash-Sutcliffe efficiency, Q is a variable (e.g. Discharge), m and s stand for measured and simulated respectively and the bar stands for an average.

B. Coefficient of Determination

Coefficient of determination (R^2) is an indicator of the extent to which the model explains the total variance in the observed- data. A value shows how well a data fit into a statistical model. The range of coefficient of determination lies between 0 and 1. When R^2 is 1, it can be depicted that the regression line perfectly fits the data while R^2 is 0 indicates that the line does not fit the data at all. Major limitation of R^2 is that it refer to the linear relationship between the two data sets, and one may obtain large R^2 value with a poor model that consistently overestimates or underestimates the observations. (Muleta, and Nicklow, 2005)

$$R^2 = \frac{\left[\sum_i \left(Q_{m,i} - \overline{Q_m}\right)\left(Q_{s,i} - \overline{Q_s}\right)\right]^2}{\sum_i \left(Q_{m,i} - \overline{Q_m}\right)^2 \sum_i \left(Q_{s,i} - \overline{Q_s}\right)^2} \quad (3.25)$$

Where, R^2 is coefficient of determination, Q is a variable (e.g. Discharge), and m and s stand for measured and simulated, i is the i^{th} measured or simulated data.

C. Percentage bias (PBIAS)

Percentage bias (PBIAS) is nonconformity of simulated data from observed data being evaluated, which is expressed as a percentage. The low magnitude values show accurate simulation of the model. Percent bias measures the average tendency of the simulated data to be larger or smaller than the observations. The optimum value is zero where low magnitude values indicate better simulations. Positive values indicate model underestimation and negative values indicate model overestimation (Gupta *et al*., 1999).

$$PBIAS = 100 * \frac{\sum_{i=1}^{n}(Q_m - Q_s)_i}{\sum_{i=1}^{n} Q_{m,i}} \quad (3.26)$$

Where, Q is a variable (e.g. Discharge) and m and s stand for measured and simulated respectively.

Table 3.9: General performance rating statics for monthly time step **(**Moriasi *et al*., 2007**)**

Performance Rating	For stream flow	
	NSE	PBIAS (%)
Very good	0.75 < NSE < =1	PBIAS<10
Good	0.65 < NSE < = 0.75	10≤ PBIAS<15
Satisfactory	0.5 < NSE = 0.65	15≤ PBIAS<25
Unsatisfactory	NSE<=0.5	PBIAS≥25

4. RESULTS AND DISCUSSION

4.1. Land Use and Land Cover Change

4.1.1 Classification of Land use land Cover Map of 1986

The land use / land cover map of 1986 in shown in figure (4.1) and the histogram of the land class coverage shows that about 25% of the Upper awash watershed was enclosed by Grass Land, 21.8% by Forest land, 46.4% by cultivated land, 6.3% by Settlement and 0.5% by water.

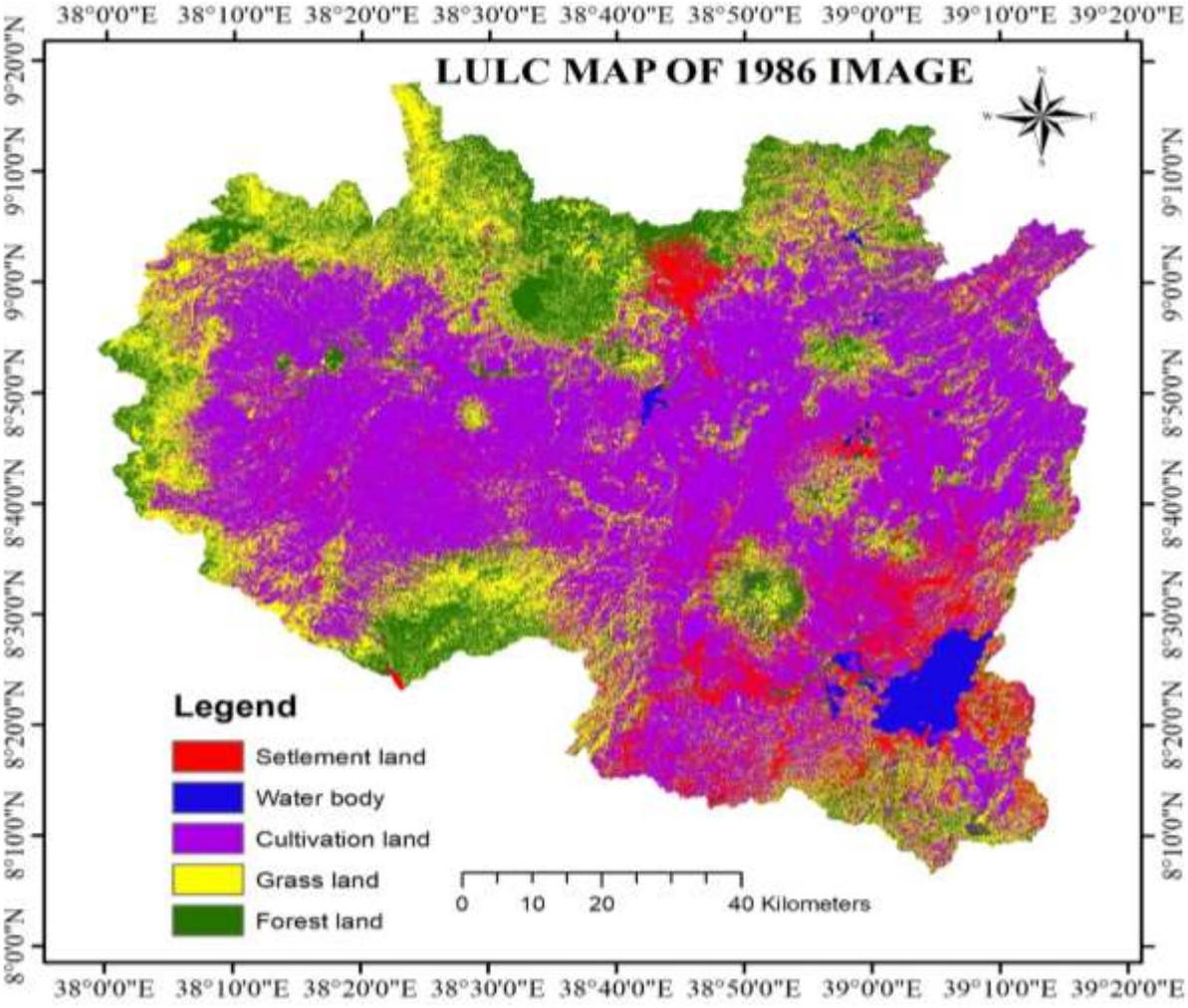

Figure 4.1: Land use / land cover map of Upper Awash watershed in the year 1986

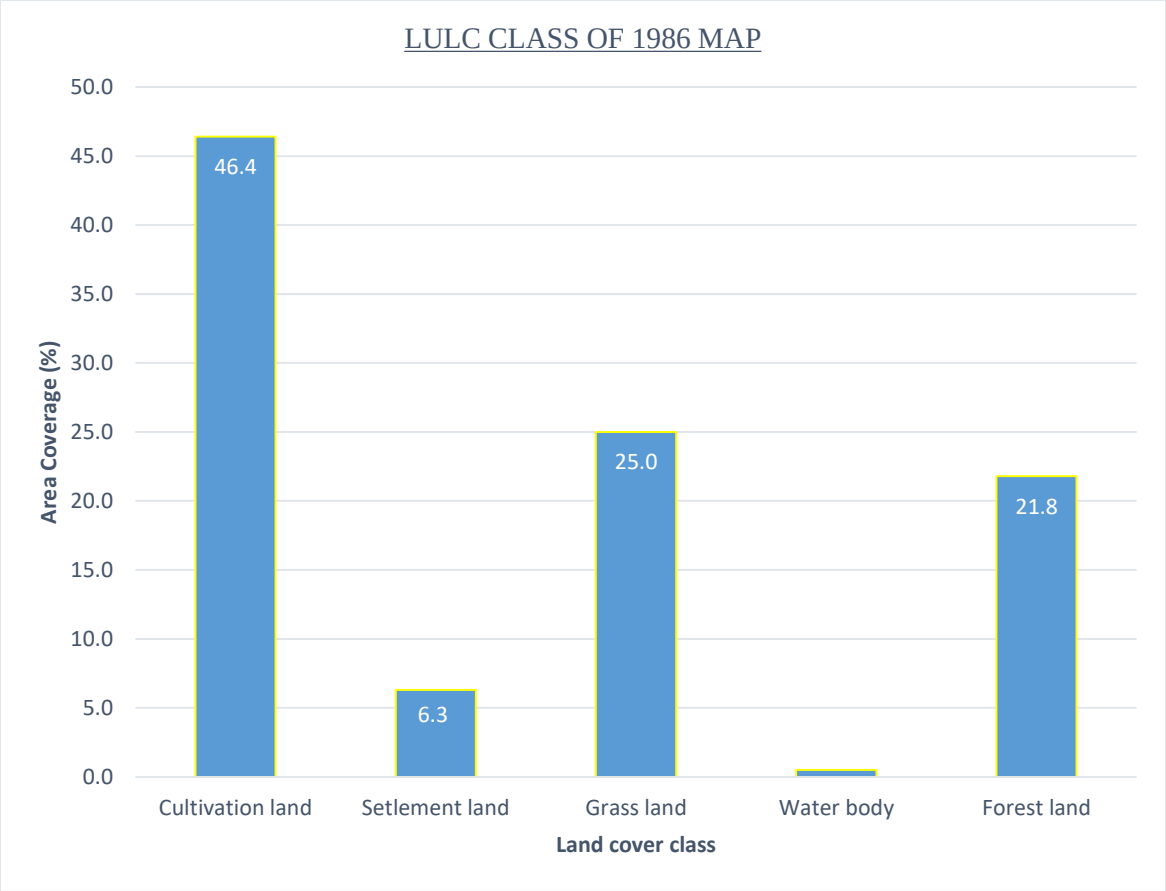

Figure 4.2: Percentage cover comparison of LU/LC classes 1986

Table 4.1: Area of LULC classes and percent of coverage for 1986 map

Land use/cover classes	LULC classes for 1986 map	
	Area(km^2)	Cover (%)
Grass land	2871.0	25.0
Forest land	2503.5	21.8
Settlement land	723.5	6.3
Water body	57.4	0.5
Cultivated land	5328.6	46.4
Total	11484.0	100.0

4.1.2 Land use land Cover Map of 2002

The land cover map of 2002 show that the watershed was covered by 20% Grass, 17% Forest, 52 % Cultivated land, 10% Settlement, and 1% of water body. All through this period, mostly the forest land and Grass land of the watershed was reduced. On contrast the cultivated land and Settlement land was extended in most parts of the watershed.

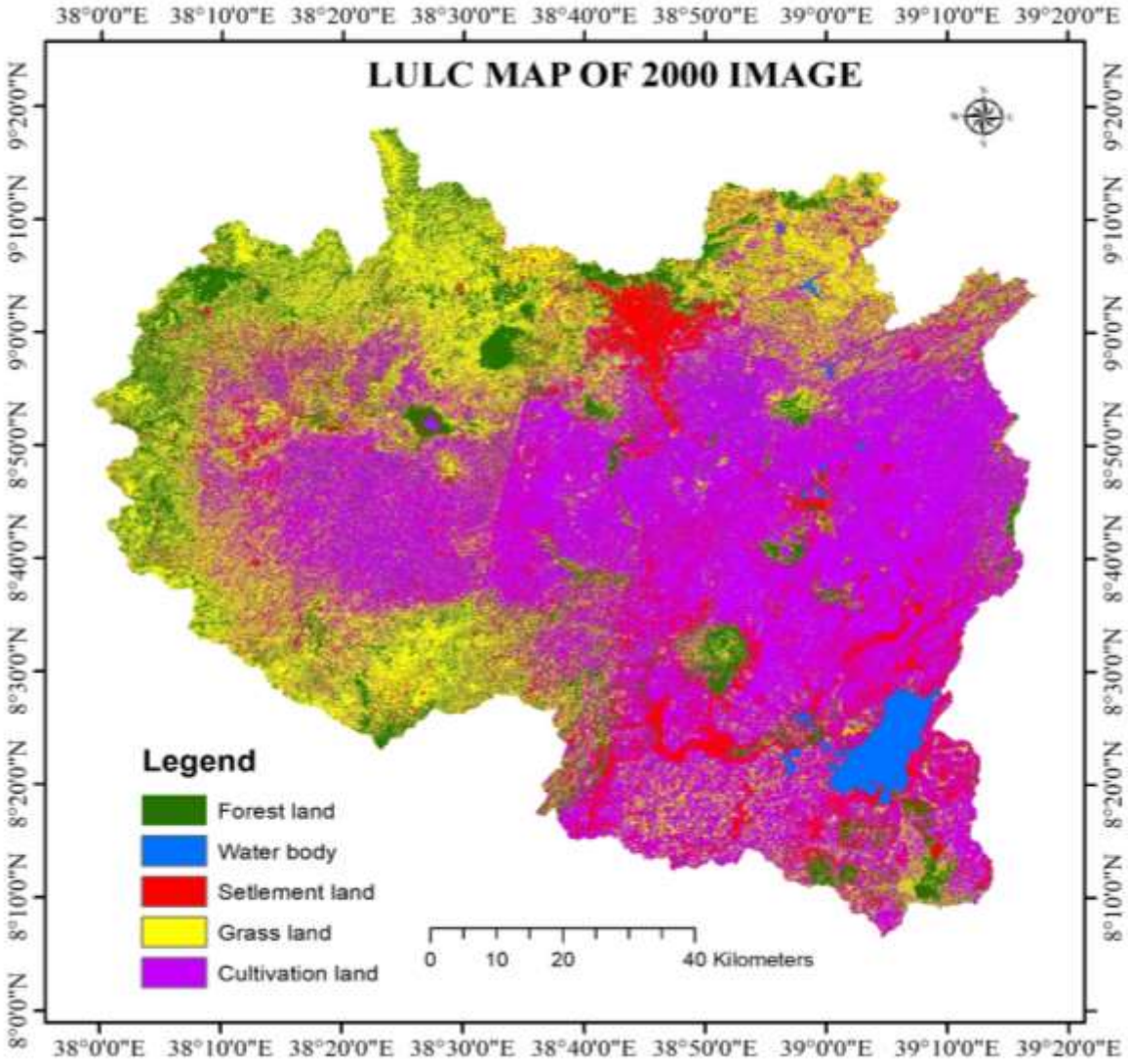

Figure 4.3: Land use land cover map of Upper Awash watershed in the year 2002

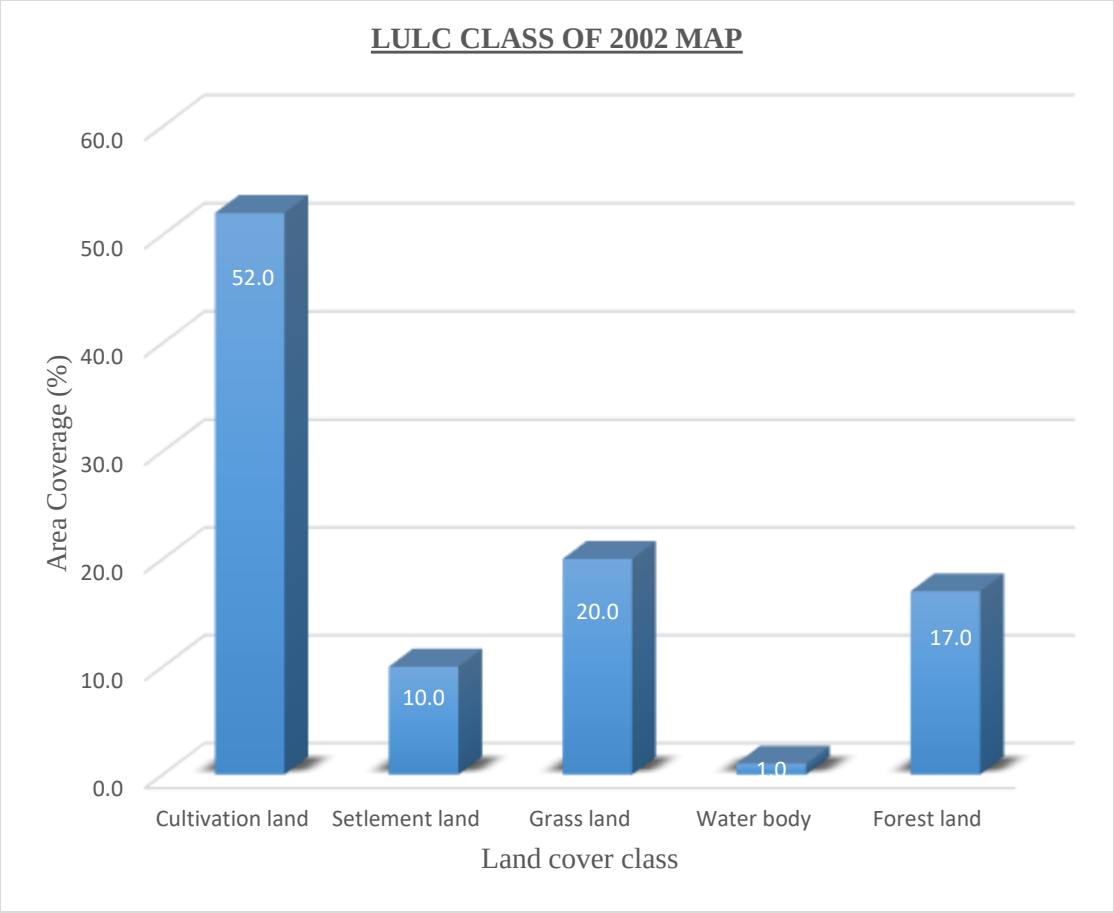

Figure 4.4: Percentage cover comparison of LU/LC classes 2002

Table 4.2: Area of LULC classes and percent of coverage for 2002 map

Land use/cover classes	LULC classes for 2002 map	
	Area(km^2)	Cover (%)
Grass land	2296.8	20
Forest land	1952.3	17
Settlement land	1148.4	10
Water body	114.8	1
Cultivated land	5971.7	52
Total	11484.0	100

4.1.3 Land use Land Cover Map of 2018

For the year 2018 the land cover map is shown in figure 4.5. The percentage coverage of each class is shown in figure and shows that cultivated land covered 56% whereas forest, Grass land, Settlement and water covered 8.9%, 11.6%, 21.9% and 1.6% respectively. Throughout this period and due to great growth of population density, the watershed area was converted into cultivated lands and Settlement in the central and outskirts part of the watershed, and only little forest cover leftovers through the Northern part of the watershed.

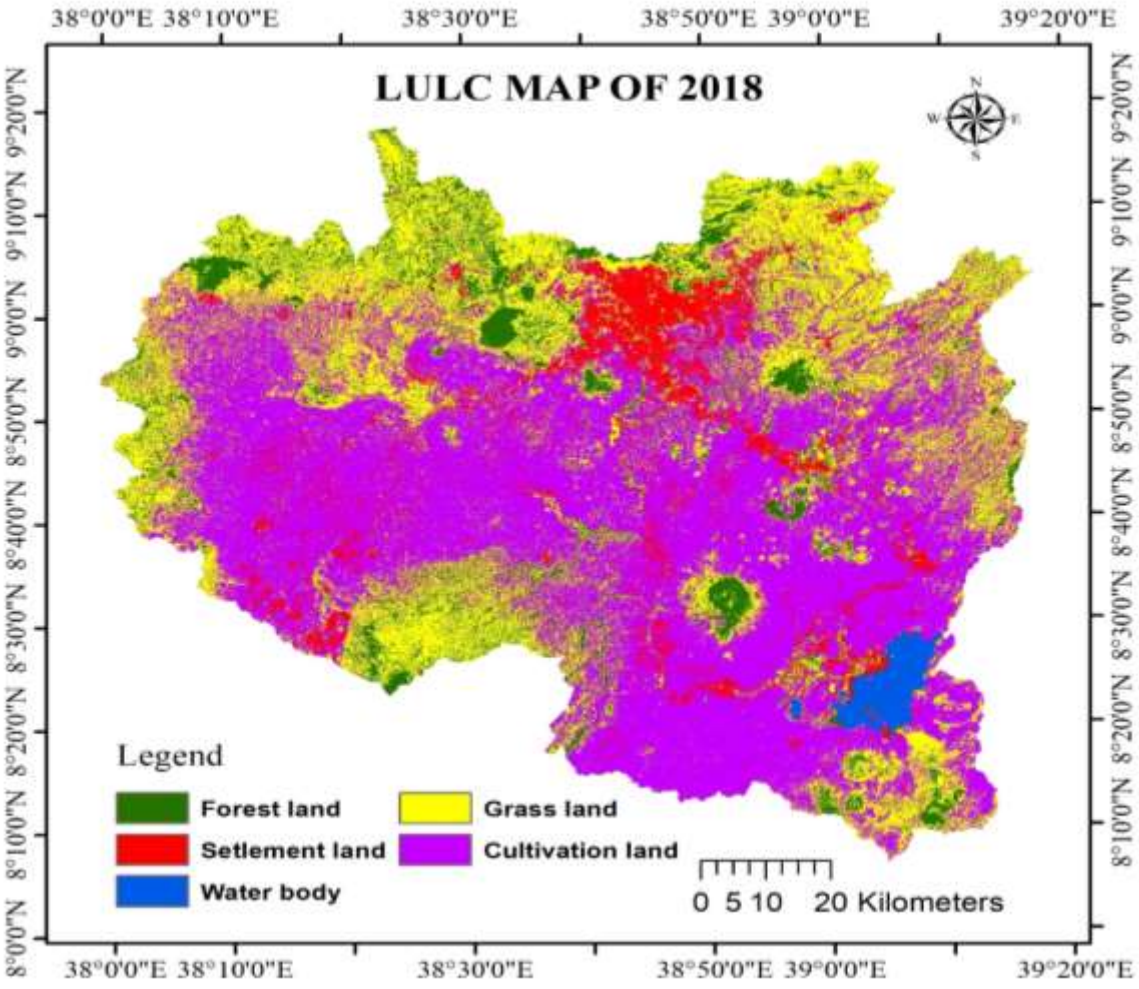

Figure 4.5: Land use land cover map of Upper Awash watershed in the year 2018

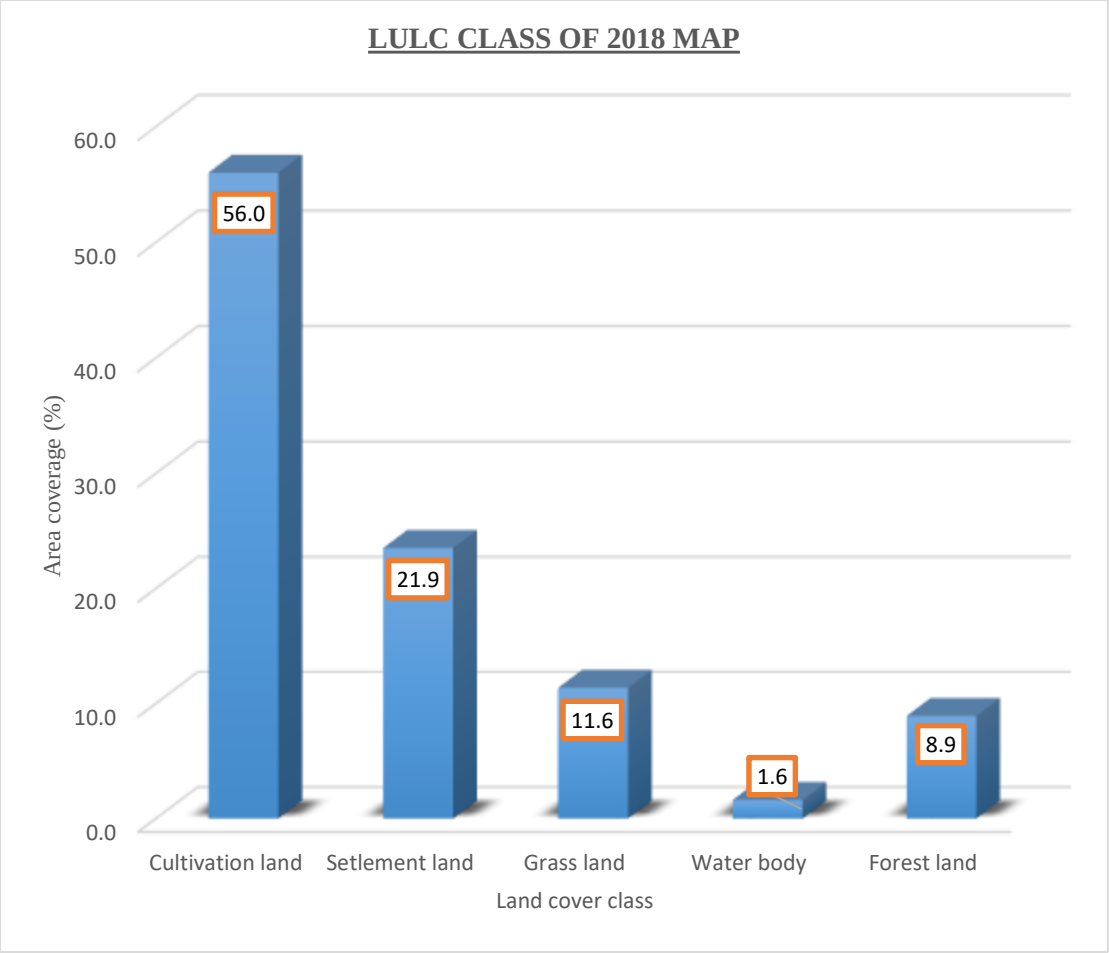

Figure 4.6: Percentage cover comparison of LU/LC classes 2018

Table 4.3: Area of LULC classes and percent of coverage for 2018 map

Land use/cover classes	LULC classes for 2018 map	
	Area(km^2)	Cover (%)
Grass land	1332.1	11.6
Forest land	1022.1	8.9
Settlement land	2515.1	21.9
Water body	183.7	1.6
Cultivated land	6431.0	56
Total	11484.0	100.0

Land use land cover classification maps of the study area were produced for three reference years 1986, 2002 and 2018 and reflect land cover for the given periods. The general land use and land cover changes at watershed level are summarized in table below.

Table 4.4: Land use and Land cover types and changes from1986-2018

Land use and land cover type	Land use and Land covers					
	1986		2002		2018	
	(km^2)	Cover (%)	(km^2)	Cover (%)	(km^2)	Cover (%)
Grass land	2871	25	2296.8	20	1332.1	11.6
forest land	2503.5	21.8	1952.3	17	1022.1	8.9
Settlement	723.5	6.3	1148.4	10	2515.0	21.9
Water	57.4	0.5	114.8	1	183.7	1.6
Cultivated land	5328.6	46.4	5971.7	52	6431.0	56
Total	11484.0	100.0	11484.0	100	11484.0	100.0

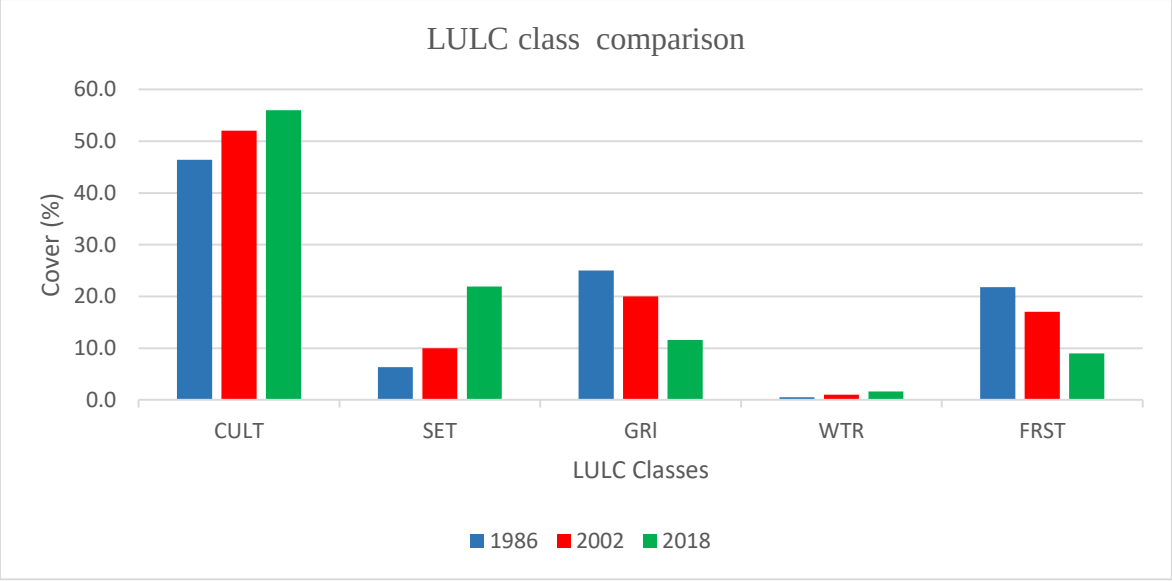

Figure 4.7: Comparison of land use category for the period 1986, 2000 and 2018

Note:-CLT is cultivated land, SET is settlement land, GRL is grass land, WTR is water body and FRST is forest land.

4.1.3. Land Use and Land Cover Change Detection

4.1.3. 1. Change Detection between 1986 and 2002

The lands use and land covers under cultivation, settlement land and water body were increased by 643.1km^2, 424.9km^2 and 57.42km^2 respectively. However the forest and grass land was reduced by 551.2km^2 and 574.2km^2 respectively. Generally, there was an increase in agricultural area and built-up areas in this period. This was caused by growth of population number to carry out deforestation for additional settlement and spreading out of agriculture.

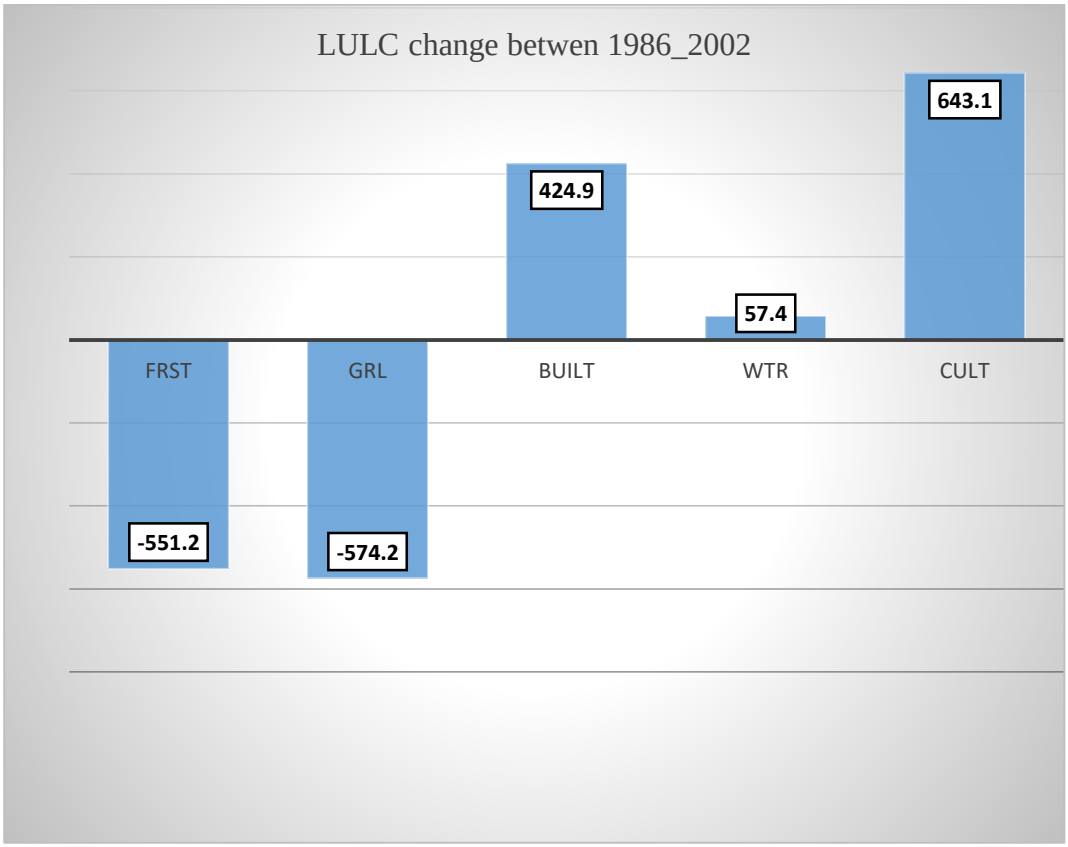

Figure 4.8: LULC change categories from 1986-2002

Note: FRST is forest land, GRL is grass land, BUILT IS Settlement, WTR is water body and CULT is cultivated land.

4.1.3. 2. Change Detection between 2002 and 2018

The lands uses under Cultivation, settlement/built-up and Water body were increased by 459.4km^2, 1366.6km^2 and 68.9km^2 respectively. Grazing land, and Forest land were reduced by 964.7km^2, and 930.2km^2 respectively.

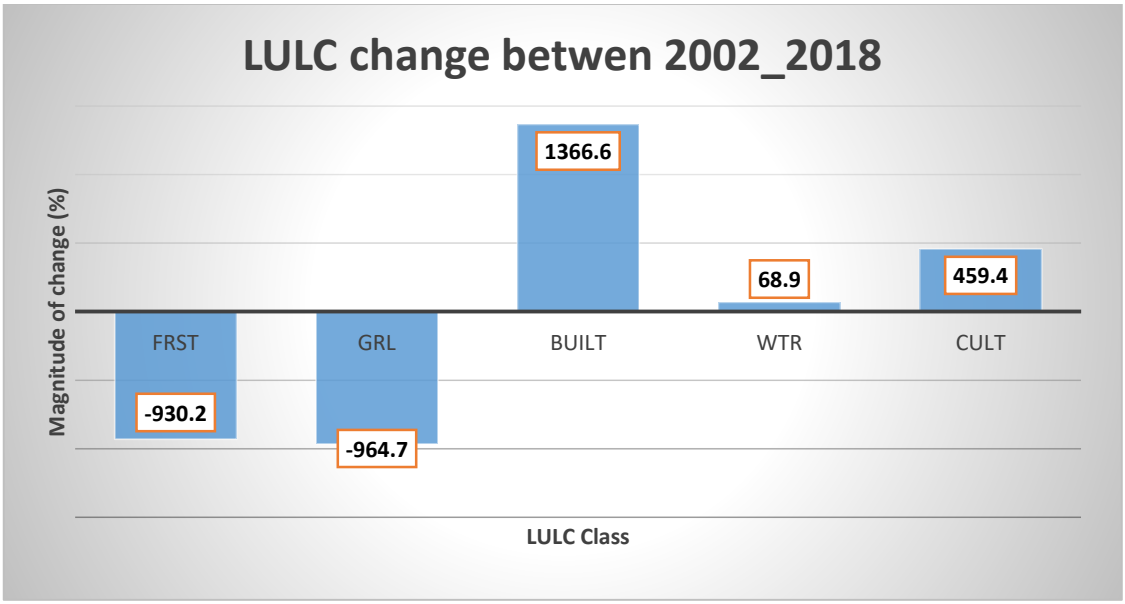

Figure 4.9: LULC change categories from 2002_2018

Note: FRST is forest land, GRL is grass land, BUILT IS Settlement, WTR is water body and CULT is cultivated land.

Table 4.5: Summary of LULC class changes

LULCC change detection									
LULC Classes	(1986-2002), Δyears =17			(2003-2018), Δyears =16			(1986-2018), Δyears =33		
	ΔArea(km^2)	Change(%)	Yearly change (%)	ΔArea(km^2)	Change (%)	Yearly change (%)	ΔArea(km^2)	Change (%)	Yearly change (%)
Grass land	-574.2	-20.0	-1.2	-964.7	-42.0	-2.6	-1538.9	-53.6	-1.6
Forest land	-551.2	-22.0	-1.3	-930.2	-47.6	-3.0	-1481.4	-59.2	-1.8
Settlement land	424.9	58.7	3.5	1366.6	119.0	7.4	1791.5	247.6	7.5
Water body	57.4	100.0	5.9	68.9	60.0	3.8	126.3	220.0	6.7
Cultivation land	643.1	12.1	0.7	459.4	7.7	0.5	1102.5	20.7	0.6

Note: Δ represented for land use land cover change

4.2 Accuracy Assessment

Using the original mosaic image and the Google Earth Image as a reference, randomly a selection of points were compared with the consistent classification. 182 points were collected for the accuracy assessment of each 1986 and 2002 maps respectively.

For land use land cover map of 2018, 182 points were collected from the ground for each period by using GPS. Table 4.6, 4.7 and 4.8 showed an error matrix for the three LULC maps. The results show that the overall accuracy for the maps of 1986, 2002 and 2018 were 89%, 90% and 97% respectively.

Table 4.6: Confusion Matrix for LU/LC Classification of 1986

Land Cover Class(1986)		Reference Data						User's accuracy (%)
		GRL	FRST	SET	WTR	CULT	Row total	
Classified Data	Grass land	56	2			7	65	86
	Forest land	1	36			1	38	95
	Settlement land			38		1	39	97
	Water body				23		23	100
	Cultivated land	1	5	1		10	17	60
	Column total	58	43	39	23	19		
	Producer's accuracy (%)	97	84	97	100	53	Overall accuracy (%) = 89	

Note: FRST is forest land, GRL is grass land, and SET IS Settlement, WTR is water body and CULT is cultivated land.

Table 4.7: Confusion Matrix for LU/LC Classification of 2002

Land Cover Class(2002)		Reference Data						User's accuracy (%)
		GRL	FRST	SET	WTR	CULT	Row total	
Classified Data	Grass land	44	5				49	90
	Forest land	6	51				57	89
	Settlement land	1	1	37			39	95
	Water body				23		23	100
	Cultivation land			5		9	14	64
	Column total	51	57	42	23	9		
	Producer's accuracy (%)	86	89	88	100	100	Overall accuracy (%) = 90	

Note: - FRST is forest land, GRL is grass land, and SET IS Settlement, WTR is water body and CULT is cultivation land.

Table 4.8: Confusion Matrix for LU/LC Classification of 2018

Land Cover Class(2018)		Referenced data						User's accuracy (%)
		GRL	FRST	SET	WTR	CULT	Row total	
Classified data	Grass land	49					49	100
	Forest land		49				49	100
	Settlement			50			50	100
	Water body				23		23	100
	Cultivation		2	2		7	11	64
	Column total	49	51	52	23	7		
	Producer's accuracy (%)	100	96	96	100	100	Overall accuracy (%) = 97	

4.3 Hydrological Modeling

4.3.1 Sensitivity Analysis of Stream Flow Parameters

Highlighting sensitive parameters was necessary for calibration to assess over and underestimation of output variables, a Sensitivity analysis was conducted using SWAT-CUP and a chosen algorithm was the Sequential Uncertainty Fitting version.2 (SUFI-2). Fifteen parameters were detected for sensitivity analysis of stream flow using the automated Latin Hypercube One-factor-At-a-Time (LH-OAT) sensitivity analysis provided that in SWAT-CUP. Parameters selected for calibration operation were listed in table 4.9. Using the LH-OAT analysis, a t-test was formed to identify the importance and sensitivity of each parameter. Based on p-value and t-value from twenty parameters fifteen parameters were selected as the most sensitive parameters. The parameters the absolute value of t-value is high and p-value close to zero that parameter is the most sensitive parameter the result was described in the table 4.9.

Table 4.9: Sensitive parameters used for Calibration and validation

No	Parameters name	Fitted value	Min	Max	t-Stat	P-Value	Rank
1	CN2	0.04	0.10	0.19	38.72	0.00	1
2	ALPHA_BF.gw	0.34	0.11	0.57	8.18	0.00	2
3	SURLAG. bsn	4.99	2.48	7.49	4.14	0.00	3
4	CANMX.hru	7.18	5.59	8.77	3.02	0.00	4
5	EPCO.hru	0.85	0.63	1.00	1.64	0.10	5
6	RCHRG_DP.gw	0.99	0.75	1.0	1.52	0.13	6
7	REVAPMN.gw	25.7	13.51	37.8	1.43	0.15	7
8	OV_N.hru	0.31	0.72	0.09	1.38	0.17	8
9	SOL_K	0.20	0.05	0.45	1.06	0.29	9
10	GWQMN.gw	715	658	773	0.78	0.44	10
11	SLSUBBSN. hru	0.39	0.05	0.84	0.48	0.63	11

No	Parameters name	Fitted value	Min	Max	t-Stat	P-Value	Rank
12	SOL_AWC	0.24	0.14	0.33	0.33	0.74	12
13	GW_DELAY.gw	38	31.9	44	0.77	0.7	13
14	ESCO. hru	0.41	0.28	0.53	0.11	0.91	14
15	SOL_Z	0.33	0.09	0.74	0.60	0.95	15

4.4 **Calibration and Validation of Stream Flow**

SWAT simulated of Upper awash watershed with default values of parameters was showed poor statistical parameters. For that reason, sensitivity analysis, manual calibration and auto calibration was carried out with SWAT CUP (SUFI-2) on monthly time steps (from 1986-2015).

Parameters were varied several times while simulating flows to obtain high NSE, R^2 and low PBIAS. This was done until simulated flow closely matched the observed flows. The results showed a good correlation between the predicted and observed flows. The calculated NSE showed that the predicted and the observed discharges have a good correlation and the model was very good in simulating the watershed. The three performance criteria indicated that the parameters modified during calibration represented the watershed hydrologic response.

Calibration and validation on monthly stream flow is performed by dividing stream flow from (1986_1995) for first class, (1996_2005) second and (2006_2015) 3rd class for LULC map of 1986, 2002 and 2018 respectively. For the first class of Calibration period, the model was run for period of 6 years from 1986 to 1991. However, the first year was considered for model warm up period, calibration was performed for 5 years from 1987 to 1991. The calibration result for monthly flow is shown in the figure 4.10. The result of calibration for monthly flow showed that there is a good agreement between the measured and simulated average monthly flows with Nash-Sutcliffe simulation efficiency (ENS) of 0.78 and coefficient of determination (R^2) of 0.84 as shown in Table 4.10. The model validation was also performed for 4 years from 1992 to 1995 without further adjustment of the calibrated parameters. The validation result for monthly flow is shown in the figure 4.11. The validation simulation also showed good agreement between the simulated and measured monthly flow with the ENS value of 0.60 and R^2 of 0.76 as shown in Table 4.10.

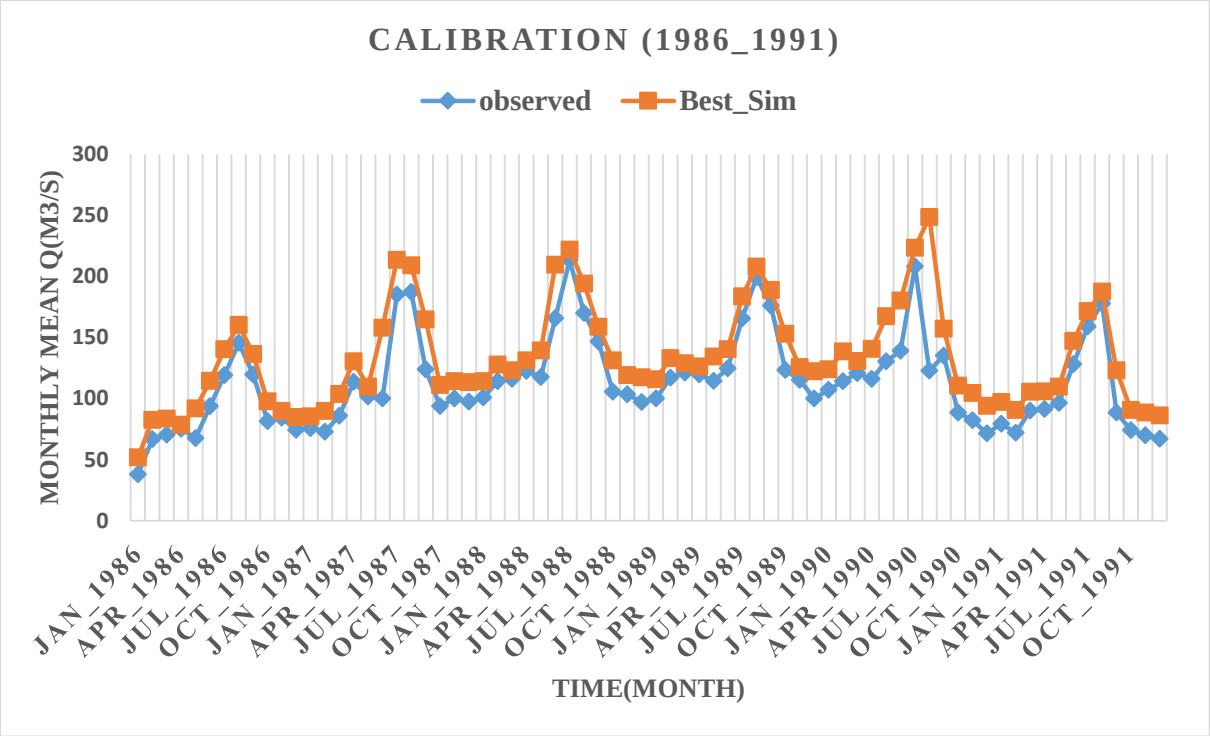

Figure 4.10: Measured and simulated hydrograph for 1986 land use and land cover at awash Hombole Calibration (1986_1991)

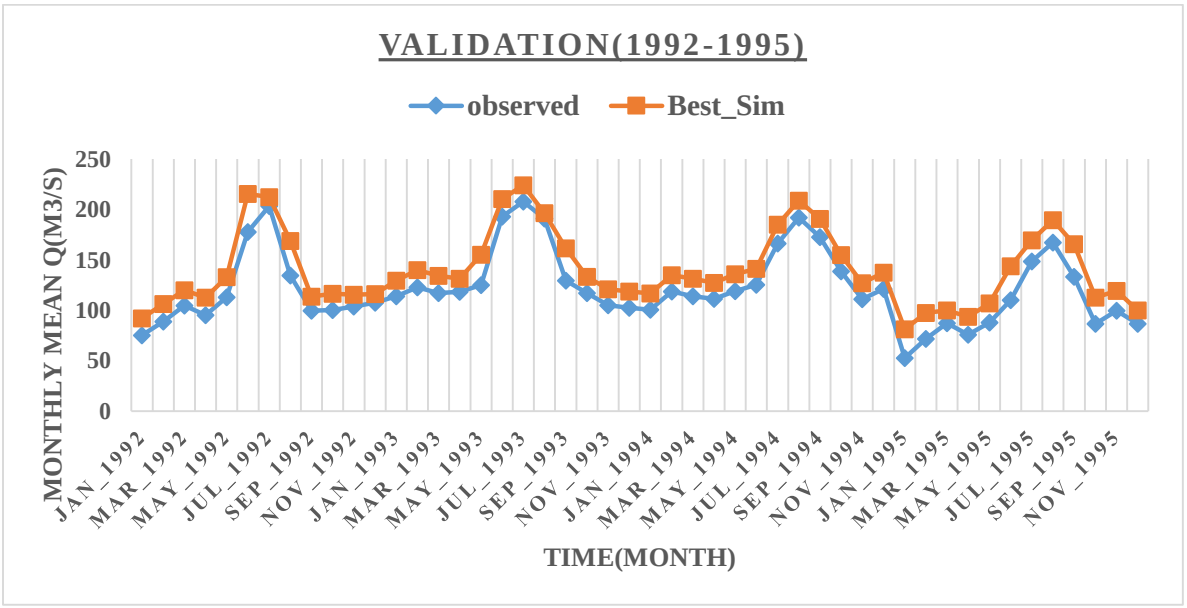

Figure 4.11: Measured and simulated hydrograph for 1986 land use and land cover at awash Hombole Validation (1992-1995)

Table 4.10: measured and simulated stream flow at awash Hombole station for 1986 land use and land cover.

Method	period	Average monthly stream flow(m3/s)		Evaluation Criteria		
		Observed	Simulated	R^2	NSE	PBIAS
SUFI-2	Calibration (1986_1991)	113.2	133.1	0.83	0.78	-3.06
	Validation (1992_1995)	121.7	140.6	0.76	0.62	-13.04

For the second class of Calibration period, the model was run for period of 6 years from 1996 to 2001. However, as the first year was considered for model warm up period, calibration was performed for 5 years from 1997 to 2001. The calibration result for monthly flow is shown in the figure 4.12.

The result of calibration for monthly flow showed that there is a good agreement between the measured and simulated average monthly flows with Nash-Sutcliffe simulation efficiency (ENS) of 0.81 and coefficient of determination (R^2) of 0.86 as shown in Table 4.11

The model validation was also performed for 5 years from 2002 to 2005 without further adjustment of the calibrated parameters. The validation result for monthly flow is shown in the figure 4.13. The validation simulation also showed good agreement between the simulated and measured monthly flow with the ENS value of 0.62 and R^2 of 0.82 as shown in Table 4.11.

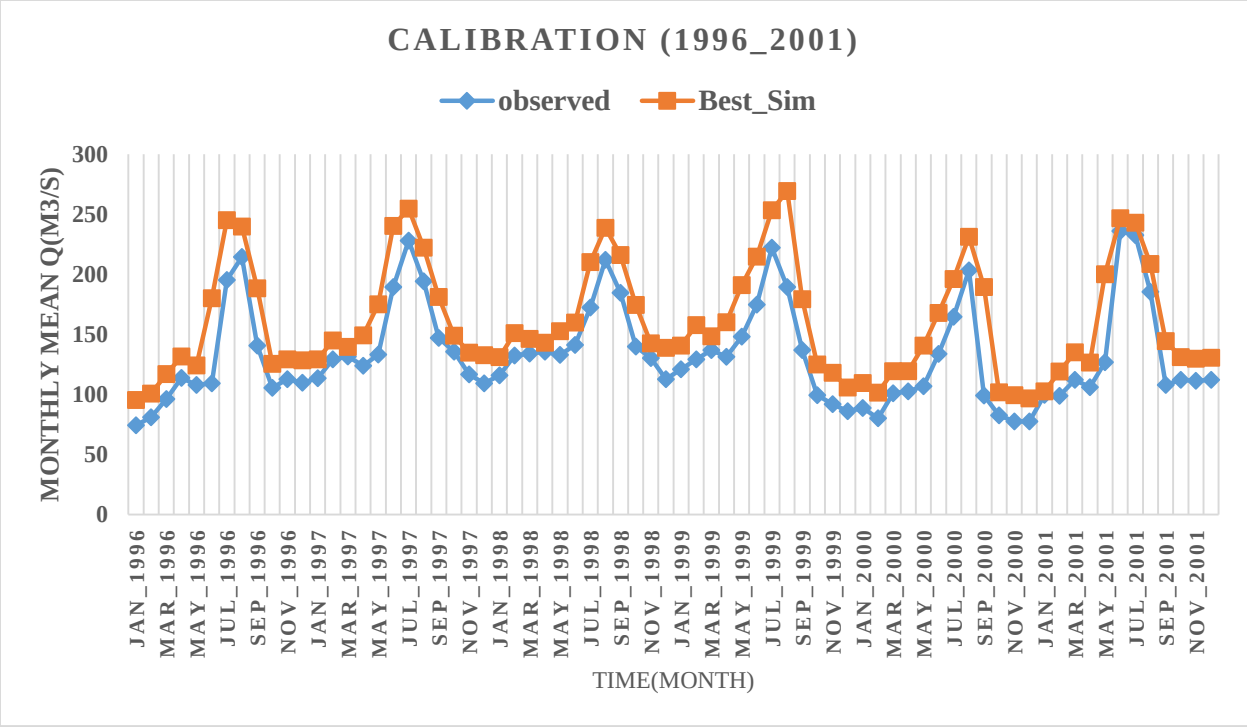

Figure 4.12: Measured and simulated hydrograph for 2002 land use and land cover at awash Hombole Calibration (1996_2001)

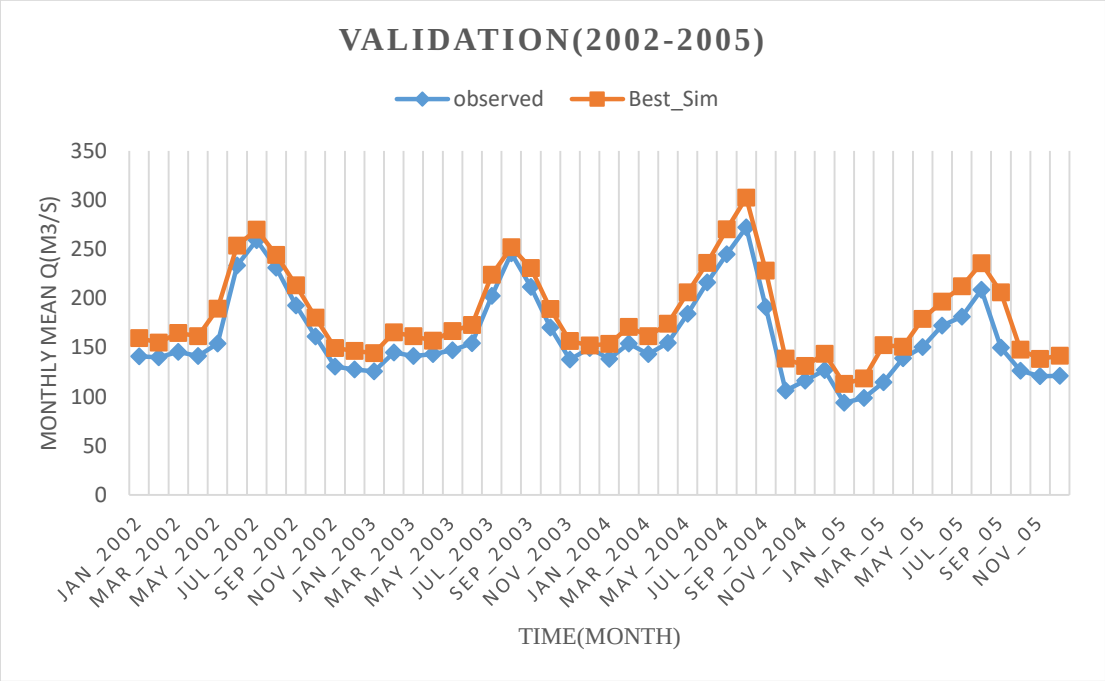

Figure 4.13: Measured and simulated hydrograph for 2002 land use and land cover at awash Hombole validation (2002-2005)

Table 4.11: measured and simulated stream flow at awash Hombole station for 2002 land use and land cover.

Method	period	Average monthly stream flow(m3/s)		Evaluation Criteria		
		Observed	Simulated	R^2	NSE	PBIAS
SUFI-2	Calibration (1996_2001)	133.1	160.0	0.86	0.81	-9.8
	Validation (2002_2005)	161.6	182.7	0.82	0.62	-12.4

For the 3rd class of Calibration period, the model was run for period of 6 years from 2006 to 2011. However, as the first year was considered for model warm up period, calibration was performed for 5 years from 2007 to 2011. The calibration result for monthly flow is shown in the figure 4.14. The result of calibration for monthly flow showed that there is a good agreement between the measured and simulated average monthly flows with Nash-Sutcliffe simulation efficiency (ENS) of 0.85 and coefficient of determination (R^2) of 0.89 as shown in Table 4.12.

The model validation was also performed for 5 years from 2012 to 2015 without further adjustment of the calibrated parameters. The validation result for monthly flow is shown in the figure 4.15. The validation simulation also showed good agreement between the simulated and measured monthly flow with the ENS value of 0.64 and R^2 of 0.84 as shown in Table 4.12.

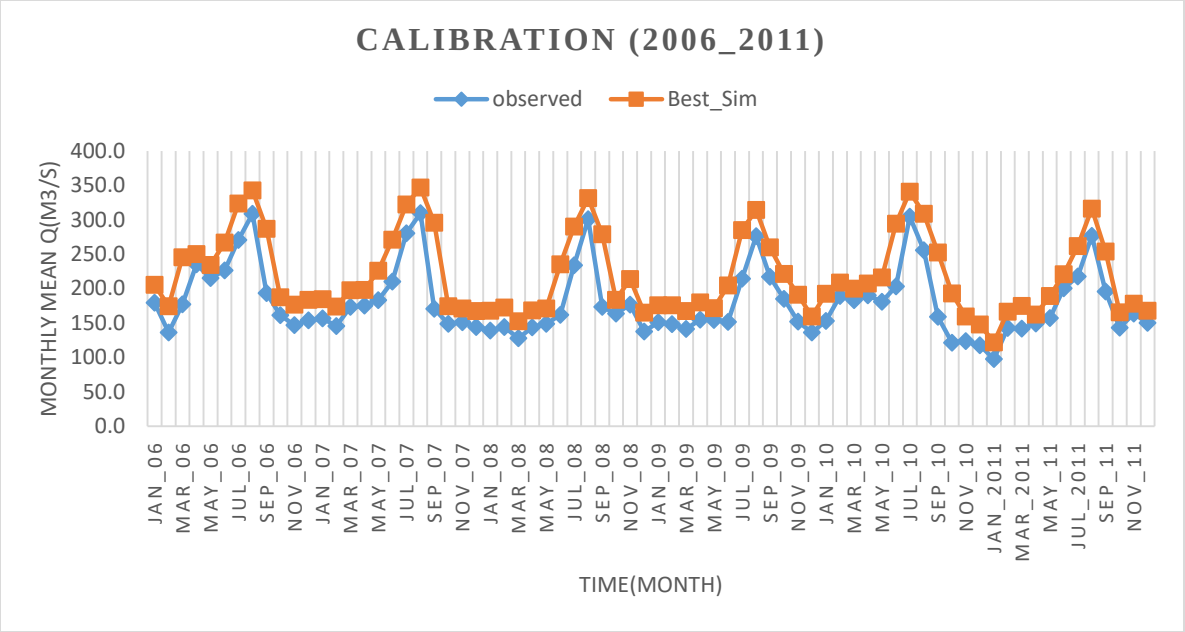

Figure 4.14: Measured and simulated hydrograph for 2018 land use and land cover at awash Hombole Calibration (2006_2011)

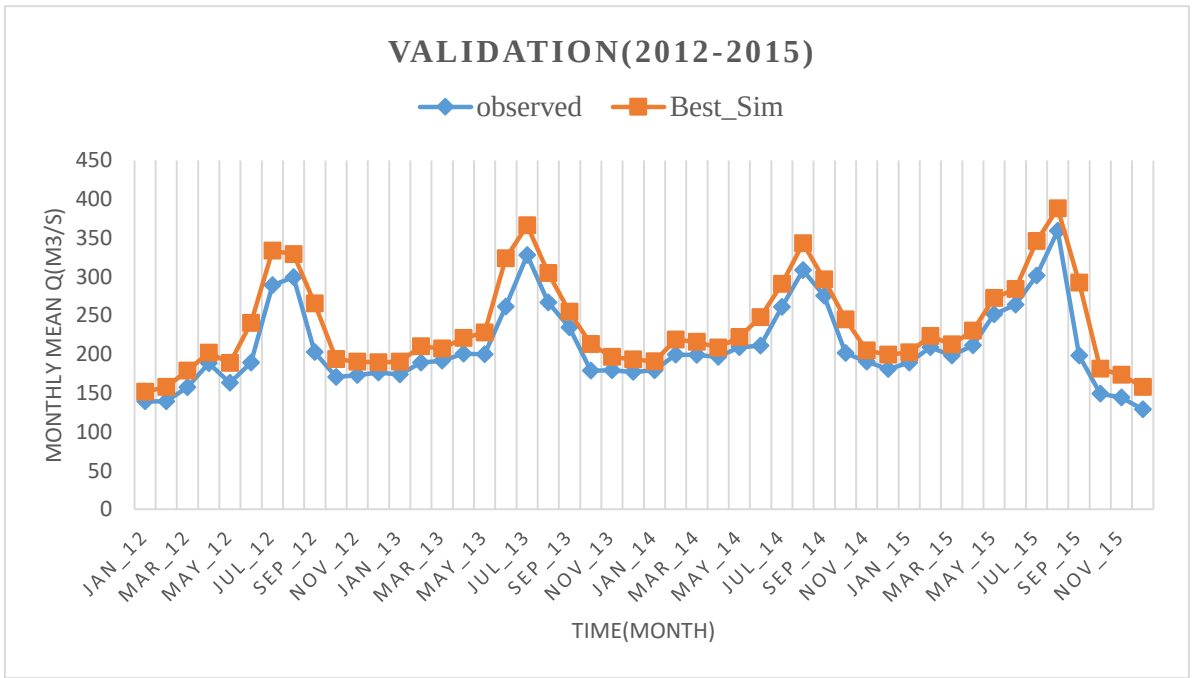

Figure 4.15: Measured and simulated hydrograph for 2018 land use and land cover at awash Hombole Validation (2012-2015)

Generally, the graphical and statistical results both during calibration and validation period displayed adequate model performance.

Table 4.12: measured and simulated stream flow at awash Hombole station for 2018 land use and land cover.

Method	period	Average monthly stream flow(m3/s)		Evaluation Criteria		
		Observed	Simulated	R^2	NSE	PBIAS
SUFI-2	Calibration (2006_2011)	162.6	196.9	0.89	0.85	-0.84
	Validation (2012_2015)	175.0	197.5	0.84	0.64	-13.5

Table 4.13: Change in Mean monthly stream flow for 1986, 2002 and 2018 land use land cover at awash Hombole station

Period	Average monthly flow (m^3/s)			Change in Mean monthly stream flow		
	For 1986 Land use	For 2002 Land use	For 2018 Land use	(1986_2002)	(2002_2018)	(1986_2018)
Calibration	113.2	133.1	162.6	19.9	29.5	49.4
Validation	121.7	161.6	175.0	39.9	13.4	53.3

As table 4.13 shows from (1986_2002) Land use Land cover the observed stream flow change was increased by19.9 m^3/s and 39.9 m^3/s for calibration and validation period respectively. This shows that stream flow is increasing due to land use and land cover changes. From (2002 to 2018) Land use Land cover the observed stream flow change was increased by 29.5 m^3/s and 13.4 m^3/s and for (1986 to 2018) Land use Land cover the observed stream flow was also increased by 49.4 m^3/s and 53.3 m^3/s calibration and validation period respectively. This shows that significant change in stream flow due to change in land use land cover of Awash River basin for long period of time.

4.4.2 Uncertainty Analysis

All sources of uncertainty were planned to a set of parameter ranges. Two different indices were used to quantify the goodness of calibration uncertainty performance. The percentage of data bracketed by the 95% prediction uncertainty (95PPU) band (P-factor) and a measure of the average width of the 95PPU (R-factor), Abbas pour (2015) suggested for P-factor, a value of >70% and R-factor of around 1.

For this study, the P-factor and R-factor result showed that the observed flow was bracketed in the 95PPU suggesting very good results or a minimal uncertainty in the model, which indicates SUFI-2 was able to capture most uncertainties.

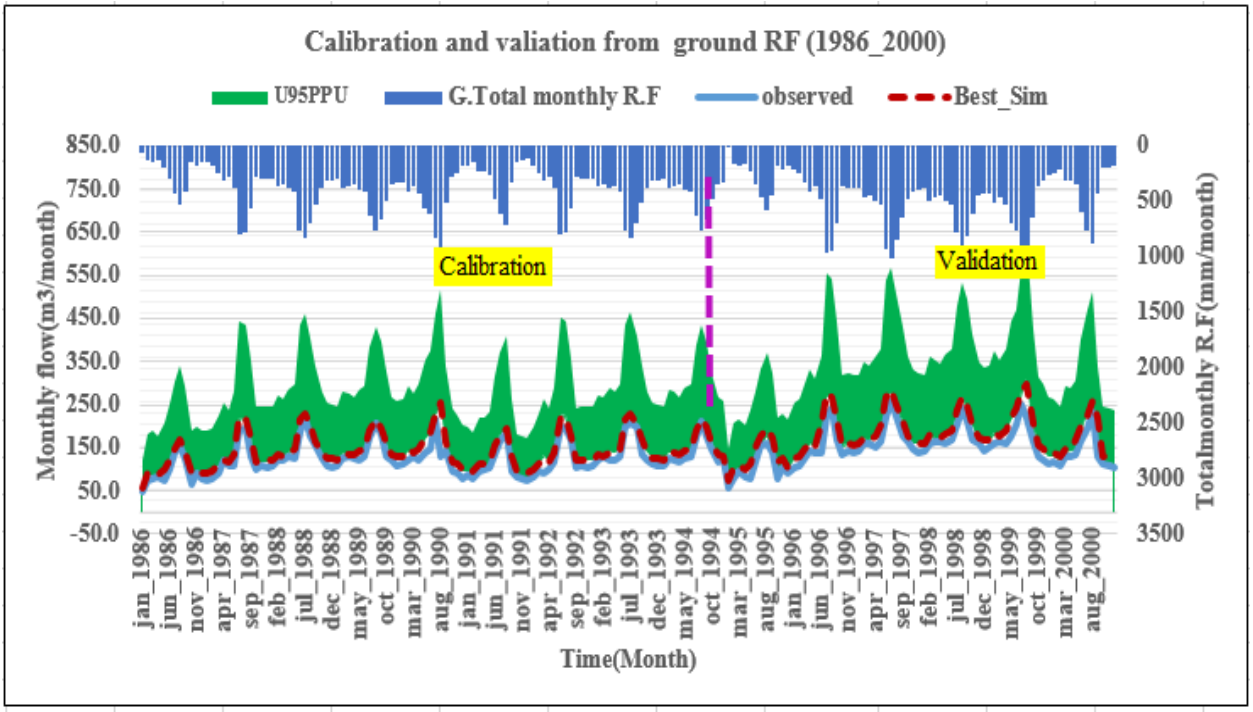

Figure 4.16: Calibration and Validation analysis results

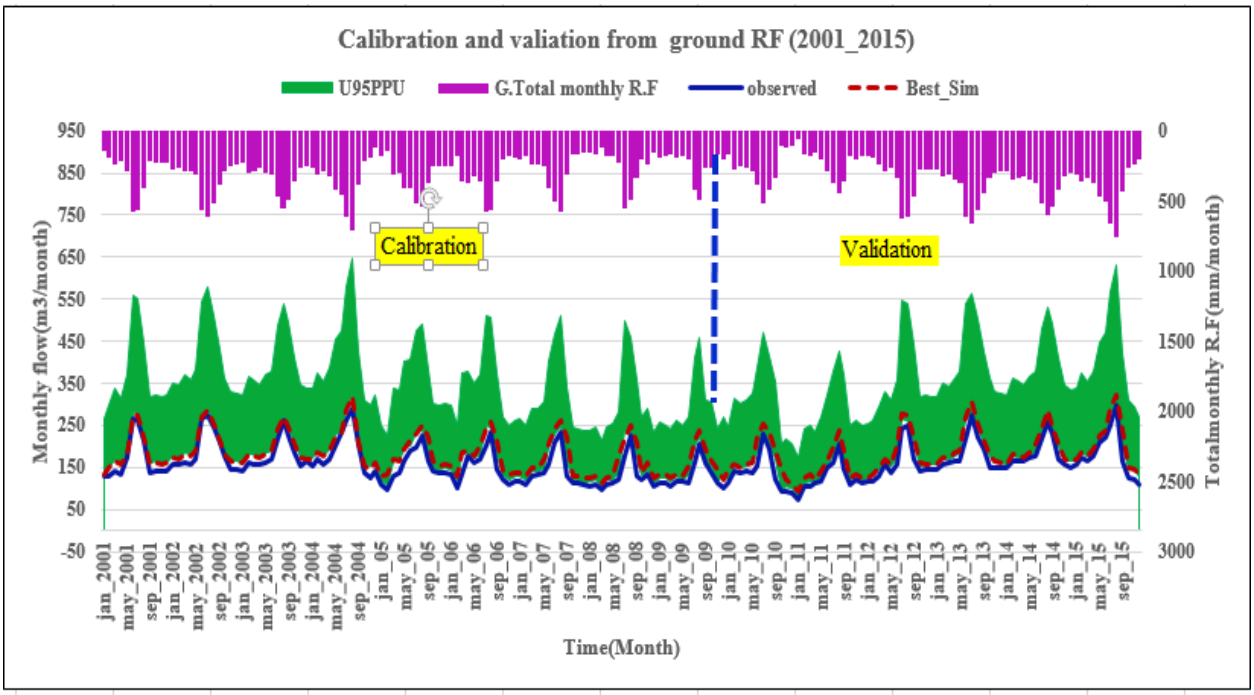

Figure 4.17: Calibration and Validation analysis results

4.5. Impact of land use and land cover change on seasonal and annual stream flow variability

Annual observed stream flow, for the period from 1986-2015 at Awash Hombole gauging station, the Mann-Kendall's test results showed that there is statistically significant trend in the time series, and the result is statistically significant trend for annual stream flow. Thus, the values of Z were positive for this stations indicating that the number of annual stream flow is increasing. This increasing trend with z value is 2.12 at α =0.05 is statistically significant with a robust estimate of the slope β value 2.11, and the Mann-Kendall S Statistic values is 10. The stream flow analysis result identified that the flow is generally increasing from time to time.

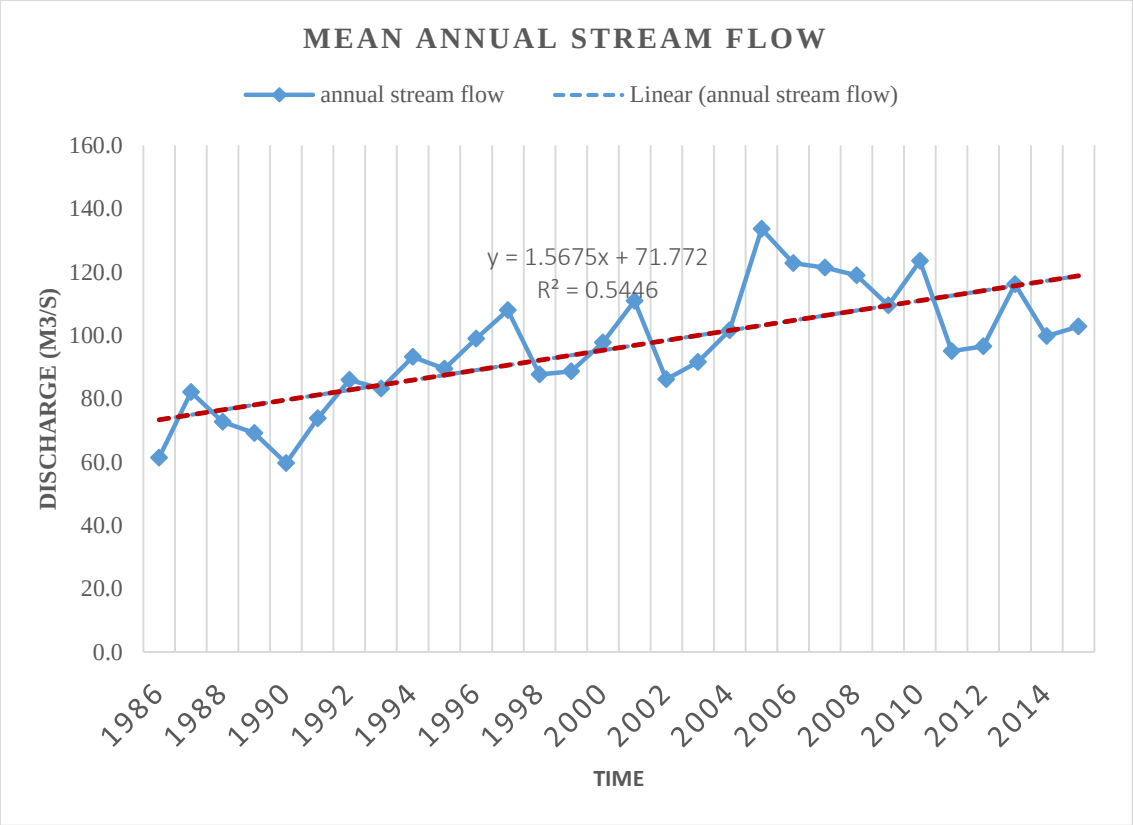

Figure 4.18: Trends in mean annual stream flow over the study period (1986-2015)

The analysis of the effects of land cover change on the stream flow variability in the period 1986–2015 shows that mean annual stream flow in wet month's shows increasing trained while in the dry seasons decreased trained. The expansion of agricultural land results in the reduction of water infiltrating into the ground and supplying the shallow aquifer. Therefore, discharge during the dry months (which mostly comes from base flow) decreases, whereas discharge during the wet months increases. The MK test was also applied to the seasonal observed stream flow pattern at the indicated watershed outlet. From the statistical analysis results, there were significant variability in simulated stream flow during wet (July, August and September) and dry (January, February and March) seasons (Fig. 4.19 and Fig.4.20). The results in Table 4.14 show a significant increasing trend of stream flow during the wet season, and a decreasing trend of at dry season.

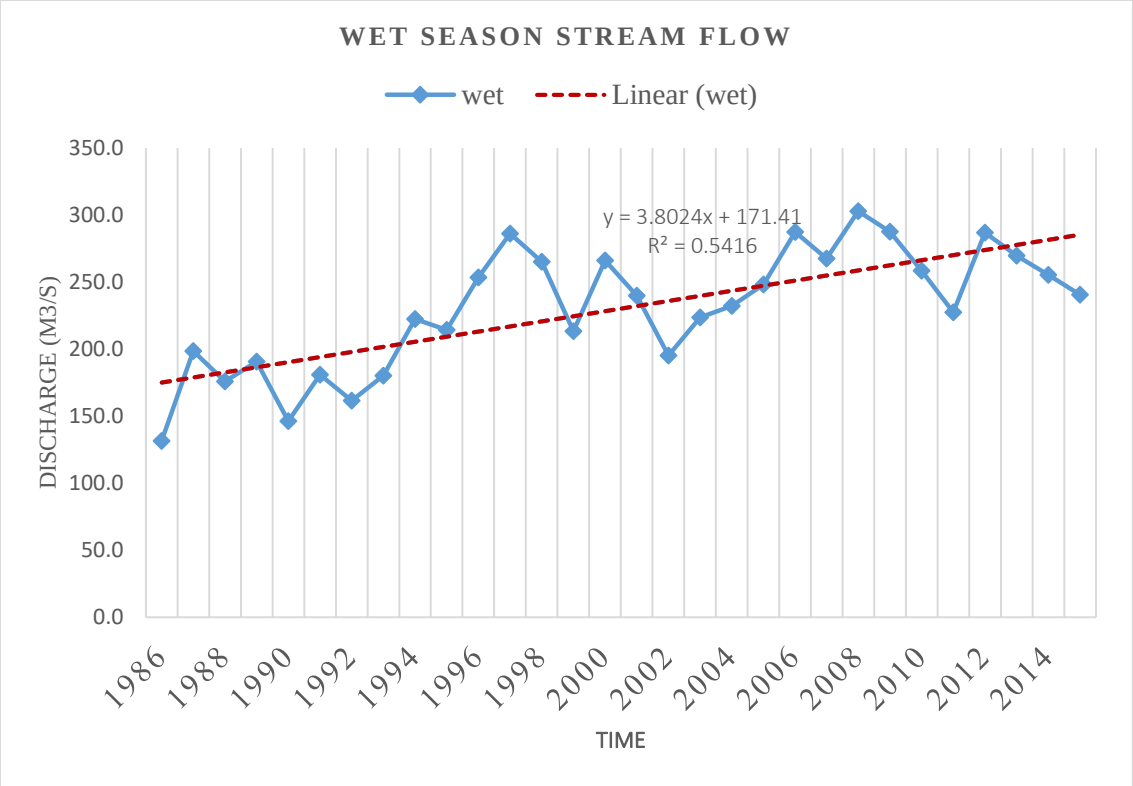

Figure 4.19: Wet season stream flow

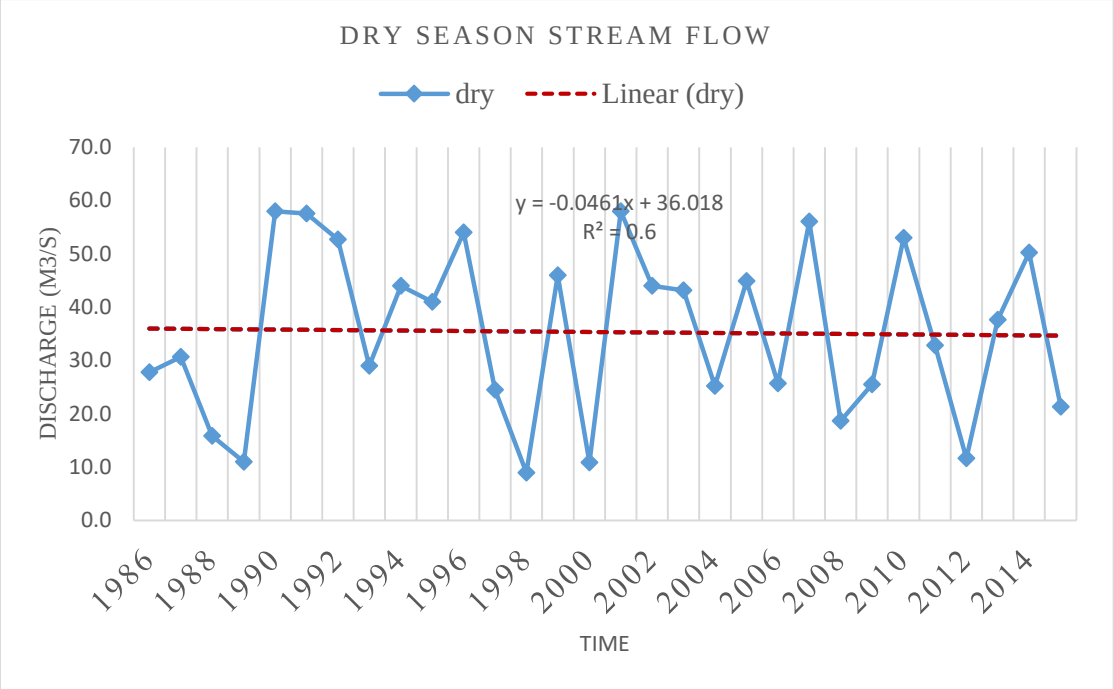

Figure 4.20: Dry season stream flow

Table 4.14: Mean monthly dry and wet season stream flow and their variability with Man-Kendall trend test and statistical summary (1986-2018)

years	1986_LULC	2002_LULC	2018_LULC	Change (1986_2002)	Change (2002_2018) (m^3/s)	Change (1986_2018) (m^3/s)	Trend
Wet season (m^3/s)	180.3	242.4	268.4	62.2	26.0	88.1	Significantly increasing t rend
Dry season (m^3/s)	36.7	35.0	32.6	-1.7	-2.4	-4.1	Significantly decreasing trend

4.6. Annual Rainfall Trend Analysis

The results of the Mann-Kendall test and null hypothesis test at 95% confidence level (α=0.05) on the rainfall for the four stations reflected in this work. As illustrated in table 4.15, by organization Mann-Kendall test on the number of years for the four stations, the test results in accepting the null hypothesis H_o for all of the stations. Accepting H_o indicates that there is no statistically significant trend in the time series, and the result is statistically insignificant. On the other hand, the values of Z were all negative for all stations indicating that the number of rainy year decreases with time. The value of Sen's slope estimates β and trend statistic Z for annual rainfall recorded at four weather stations from 1986 to 2018 were displayed in Table 4.15. The annual precipitation showed a decreasing trend at all the meteorological stations from 1986 to 2018.

Table 4.15. Results of the MK test for annual rainfall from 1986 to 2018

Weather stations	Annual Total Precipitation		Significance at α=0.05
	Z	β	
Akaki	-0.07	-1.12	NS
Hombole	-1.18	-2.05	NS
Ginchi	-1.15	-6.72	NS
Teji	-3.75	-23.03	NS
Adama	-0.31	-1.37	NS

Note:-NS is non-significant and SG is significant

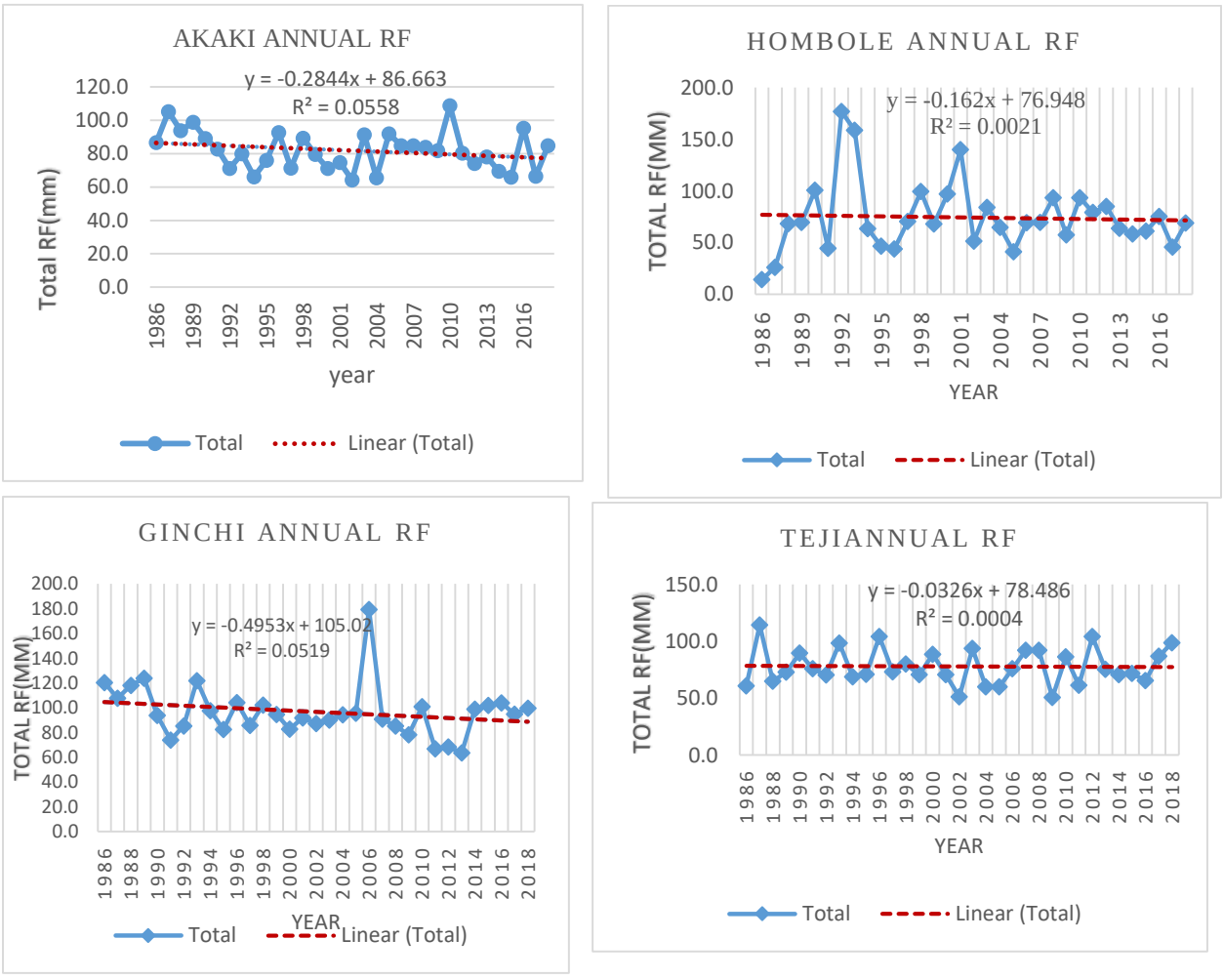

Figure 4.21: Trends in the annual rainfall over the study period (1986-2018)

Advanced investigation concentrated on the LULCC contributions on annual surface runoff, lateral flow, total aquifer recharge, total water yield, and evapotranspiration as characteristics of the hydrological process of the watershed were presented in table 4.16.

Table 4.16: Hydrological process from simulated annual stream flow of 1986, 2002 and 2018 land covers

Hydrological components	LULC-1986	LULC-2002	LULC-2018
Surface runoff (mm)	78.0	89.3	106.5
Lateral flow (mm)	20.7	30.2	45.5
Ground water flow (mm)	44.2	39.4	27.3
Total aquifer recharge (mm)	113.6	106.4	91.0
Water yield (mm)	142.2	156.3	167.5
Evapotranspiration (mm)	631.1	612.2	595.9

The simulated stream flow result showed that, surface runoff and lateral flow were increased from 78.0 mm, to 89.3 mm and 20.7 mm, to 30.2 mm, for (1986 to 2002) land use and land cover respectively. Also surface runoff and lateral flow were increased from 89.3mm, to 106.5mm and 30.2mm, to 45.5mm for (2002 to 2018) land use and land cover respectively. While ground water has decreased from 44.2 mm to 39.9 mm, for (1986 to 2002) land use land cover and from 39.4mm to 27.3mm for (2002 to 2018) land use and land cover respectively. This attributed by the expansion of agricultural land over others affecting the variation of soil moisture condition and ground water storage. From the result of land use and land cover map, areas of forest and grass land have decreased from 1986 to 2002 and 2002 to 2018 respectively which has contributed to the increased surface runoff and reduction of water infiltrating into the ground. Thus, the rate of evapotranspiration has decreased resulting in increased water yield. As a result of decreasing percolation rate, total aquifer recharge has decreased throughout the study period from 1986 to 2002 and 2002 to 2018 respectively.

5. SUMMARY AND CONCLUSION

5.1. Summary

This study was aimed at assessing the effects of the land use and land covers changes on stream flow of upper Awash River basin between the years 1986 and 2018 using distributed hydrological model (SWAT). The integrated method of GIS and remote sensing are used to map different types of land cover classes and to identify and examines spatiotemporal land cover dynamics.

The impacts of land use and the land cover change on stream flow was studied statistically using the hydrological model, SWAT. To do this analysis, first land use and land cover alteration during the past 33 years (1986 –2018) was examined; then SWAT model was verified for its performance at the upper awash river basin in order to examining the hydrological response of the watershed to alterations in land use and land cover. The land use and land cover maps of the year 1986, 2002 and 2018 were formed and the accuracy assessments of the three maps was tested using the Confusion Matrix. On the other hand, sensitivity analysis, calibration, validation and evaluation of model performance were performed on the selected SWAT CUP, model. The GIS used for the processing of DEM, land use and land cover, soil data layers and showing model results. Based on the results, the following decisions are drawn:

Land use and land cover indicated that an increasing variation in cultivation land, built-up and Water body with the magnitude of change 1102.5km^{2,} 1791.5km^2 and 126.3km^2 by the annual rate of change 0.6%, 7.5% and 6.7% respectively. Areas under Grass land, and Forest land were reduced by 1538.9km^2, and 1481.4km^2 by the annual rate of change -1.6%, and -1.8% respectively of the total watershed area. The SWAT model was used to simulate the effects of Land use and land cover variations on stream flow in upper awash basin.

The performance of the SWAT model was evaluated through sensitivity analysis, calibration, and validation. Fifteen flow parameters were identified to be sensitive for the stream flow of the study area and used for model calibration.

Calibration and validation on monthly stream flow is performed by dividing stream flow from (1986_1995) first class for1986 land use and land cover, (1996_2005) second class, for 2002 land use and land cover and (2006_2015) 3rd class for 2018 land use and land cover respectively.

For 1986 LULC class of Calibration period, Nash-Sutcliffe efficiency (ENS) of 0.78 and coefficient of determination (R^2) of 0.84 and validation ENS value of 0.60 and R^2 of 0.76

respectively. For 2002 LULC class of Calibration period, Nash-Sutcliffe efficiency (ENS) of 0.81 and coefficient of determination (R^2) of 0.86 and validation with the ENS value of 0.62 and R^2 of 0.82 respectively. For the 2018 LULC class of Calibration period, Nash-Sutcliffe efficiency (ENS) of 0.85 and coefficient of determination (R^2) of 0.89 and validation with the ENS value of 0.64 and R^2 of 0.84 respectively.

The analysis of the effects of land cover change on the stream flow variability in the period 1986–2015 shows that mean annual stream flow in wet month's shows increasing trained while in the dry seasons decreased trained. This is because, the diminishing rate of forest land, and grass land cover over the analysis period aggravated runoff generation and decreased base flow in studied watershed. The expansion of agricultural land results in the reduction of water infiltrating into the ground and supplying the shallow aquifer. The simulated stream flow result showed that, surface runoff and lateral flow were increased from 78.0 mm to 89.3 mm and 20.7 mm to 30.2 mm, for (1986 to 2002) land use and land cover respectively. Also surface runoff and lateral flow were increased from 89.3mm, to 106.5mm and 30.2mm, to 45.5mm for (2002 to 2018) land use and land cover respectively. While ground water has decreased from 44.2 mm to 39.9 mm, for (2002 to 2018) land use /land cover and from 39.4mm to 27.3mm for (2002 to 2018) land use and land cover respectively. This attributed by the expansion of agricultural land over others affecting the variation of soil moisture condition and ground water storage. From the result of land use and land cover map, areas of forest and grass land have decreased from 1986 to 2002 and 2002 to 2018 respectively which has contributed to the increased surface runoff and reduction of water infiltrating into the ground. Thus, the rate of evapotranspiration and potential evapotranspiration has decreased resulting in increased water yield. As a result of decreasing percolation rate, total aquifer recharge has decreased throughout the study period from 1986 to 2002 and 2002 to 2018 respectively. Therefore, discharge during the dry months (which mostly comes from base flow) decreases, whereas discharge during the wet months increases.

Generally, the results indicated that Land use and land cover has high effect on stream flow components such as surface runoff, lateral flow and base flow in the study of awash watershed.

5.2. Conclusion

Based on this research the following finding was concluded:

- ✓ LULC map of 1986,2002 and 2018 indicate change in cultivation land, built-up and Water body were increasing and Grass land, and Forest land were reduced.
- ✓ LULCC on the stream flow in the period 1986–2015 shows that mean annual stream flow in wet month's shows increasing trained while in the dry seasons decreased trained.
- ✓ The simulated stream flow result showed that, surface runoff and lateral flow were increased, while ground water has decreased from 1986 to 2002 and 2002 to 2018 LULCC.
- ✓ Therefore, discharge during the dry months (which mostly comes from base flow) decreases, whereas discharge during the wet months increases.

Generally, based on the finding the following recommendations were forwarded:

- ✓ In this research the model simulation deliberated only land use and land cover change properties by assuming all other variables constant on the stream flow. However, change in climate can similarly contribute excessive effect on rainfall runoff method of the watershed. Hence, there is an essential for further research to determine the hydrological influences of climate change in the watershed.
- ✓ Land use and land cover fluctuations of the awash watershed are generally affected by increasing population. Currently, number of population and its annual crop production are not proportional. Furthermore, the farmers are not capable to increase the amount of the production by the current farming practices. Hence, increase of household awareness with the effect of population growth on their living status has paramount meaning. Thus, family planning must be given widely and continuously through formal and informal education in school and some other social assembly area.
- ✓ Policy maker must be established from bottom to top approach for appropriate land use planning and sustainable water resources management system in the watershed. This helps for stakeholders and decision makers to create better choosing for land and water resource planning and management.
- ✓ The weather and hydrological stations must be improved both in quality and quantity in order to increase the performance of the model. Therefore, it is extremely recommended to form good meteorological and hydrometric stations.

6. REFERENCES

Abbaspour, K.C. (2005). Calibration of hydrologic models: when is a model calibrated: In Zerger, A. and Argent, R.M. (eds) MODSIM 2005 International Congress on Modelling and Simulation. Modelling and Simulation Society of Australia and New Zealand, pp. 2449-12455. http://www.mssanz.org.au/modsim05/papers/abbaspour.pdf.

Adamu, A. (2013), Assessing the Impacts of Land Use and Cover Change on Hydrology of Watershed: The Case Study on Gilgel Abbay Watershed, Lake Tana Basin, Ethiopia.

Adeogun G. Adeniyi, (2014). Validation of SWAT Model for Prediction of Water Yield and Water Balance: Case Study of Upstream Watershed of Jebba Dam in Nigeria.

Ambachew Getnet and Fungai Svondo, (2010), Effect of Agricultural Land Expansion on Deforestation and Its Implication on Climate Change in Ethiopia and Zimbabwe. Anger Watershed, Ethiopia, International Journal of Water Sciences.

Arnold, J. G. (1998). Large area hydrologic modeling and assessment Part I: Model

Arnold, J. G., srinivasan, R., Muttiah, R. S and Williams, J. R. (1998). Large area hydrologic modeling and assessment Part I: Model Developmentd.

Atasoy, M., R.B. Palmquist, and D.J. Phaneuf. (2006). Estimating those effects of urban residential development on water quality using micro data. Journal of Environmental Management 794: 399 408.

Baker, T. J., and MillerS. N. (2013). Using the Soil and Water Assessment Tool (SWAT) to assess land use impact on water resources in an East African watershed. Journal of Hydrology, 486,100-111.

Baldyga, J. T. (2005), Assessing Land Cover Change Impacts in Kenya's River Njoro.

Barkhordari, J. (2003). Assessing the Effects of Land Use Change on Hydrologic Regime by Remote Sensing and GIS: A case study in the Minab watershed, Hormozgan Province Iran, Master's Thesis.

Bawahidi, K. S. Y. (2005). Integrated land use change analysis for soil erosion study in ulu kinta attachment. University Sains Malaysia.

Berga, A. (2011) 'Institute of Technology School of Graduate Studies Department of Civil Engineering Addis Ababa University the Effect of Land Use Change on Hydrology of Akaki Watershed the Effect of Land Use Change on Hydrology of Akaki Watershed'.

Belihu, M., Abate, B., Tekleab, S., and Bewket, W. (2018). Hydro-meteorological trends in the Gidabo Watershed of the Rift Valley Lakes Basin of Ethiopia. Physics and Chemistry of the Earth. 104, 84-101.

Beven, (2000), Rainfall Runoff Modelling. *The primer.Wiley. 360 p.*

Briley, L. (2010) 'Data Pre-Processing for SWAT', University of Michigan/NOAA/CIRES, pp. 1–10.

Caetano, M., Mata, F., Freire, S. (2005). Accuracy assessment of the Portuguese CORINE Land cover map.

Chien, H., Yeh, P. and Knouft, J. (2013). Modeling the potential impacts of climate change on stream flow in agricultural watersheds of the Midwestern United States. Journal of Hydrology, 491, 73-88.

Cunderlik, J. (2003), Hydrological Model Selection for CFCAS Project, Assessment of Water Resource Risk and Vulnerability to Change in Climate Condition, University of Western Ontario.

Chemelil, M. C. (1995). The Effects of Human-Induced Watershed Changes on Stream Flows, Doctoral Thesis.

Chorley, R.J. (1977). Introduction to physical hydrology. Methuen and Co. Ltd. London, England.

Damtew Fufa. (2015). SWAT Based Hydrological Modeling of Ketar Watershed Lake Ziway Watershed, Ethiopia. International Journal of Civil, Structural, Environmental and Infrastructure Engineering Research and Development (IJCSEIERD), 5, 33-44.

DeFries RS, Eshleman KN (2004). Land-use change and hydrologic processes: A major focus for the future. Hydrologic Process 18:2183–2186.

De Roo, A. P. J., Wesseling, C. G., & Van Deursen, W. P. A. (2000). Physically Based River Basin Modelling within a GIS: The LISFLOOD Model. Hydrological Processes, 14(11-12), 1981-1992.

Donizete, R., Mauro, A., Demetrius, D. and Fernando, F. (2016). Hydrological simulation in a basin of typical tropical climate and soil using the SWAT Model Part II: Simulation of hydrological variables and soil use scenarios. *Journal of Hydrology: Regional Studies* 5,149-163.

Efrem, G. (2010). Land Use and Land Cover Dynamics and Rural Livelihood Perspectives, in the SemiArid Areas of Central Rift Valley of Ethiopia.

FAO, (1998): The Soil and Terrain Database for northeastern Africa (CDROM) FAO, Rome.

Fohrer, N. H. (2001), Hydrologic Response to Land Use Changes on the Watershed Scales. Phys. Chem. Earth. 26, 577-582.

Foody, M. G. (2002). Status of land cover Classification accuracy assessment. Remote sensing of the environment. Elsevier science increment, 80, 185 – 201.

Geremew, a. A. (2013) 'assessing the impacts of land use and land cover change on hydrology of watershed : a case study on gilgel – abbay watershed , lake tana', p. 82.

Ghaffari, G., Keesstra, S., Ghodousi, J. and Ahmadi, H. (2010). SWAT simulated hydrological impact of land use change in the Zanjanrood basin, Northwest Iran. Hydrological Processes, 24(7), 892-903.

Gobena, M. (2010). Effects of Large Scale Land Acquisition in Rural Ethiopia. The Case of Bako Tibe Woreda Master's Thesis, Swedish University of Agriculture.

Gobena,S.(2010) daily rainfall-runoff modelling of upper awash sub basin using conceptual rainfall addis ababa university.

Golmar, G., Ramesh, R., Trevor, D., Pradeep, G. and Mari, V. (2017). Predicting the temporal variation of flow contributing areas using SWAT. *Journal of Hydrology*. 547, 375-386.

Golosov, V. and Panin A. (2006). Century-scale Stream Network Dynamics in the Russian Plain in Response to Climate and Land Use Change. 66, 74-92.

Guo, H. H. (2008). Annual and Seasonal Stream Flow Responses to Climate and Land-Cover Changes in the Poyang Lake Basin, China. Journal of Hydrology, vol. 355, 106-122.

Gupta, V., Sorooshian, S. and Yapo, P. (1999). Status of automatic calibration for hydrologic models: Comparison with multilevel expert calibration. Journal of Hydrology engineering, 4, 135-143.

Halcrow (1989): Awash Master Plan Project MoWR, Addis Ababa, Ethiopia.

Halcrow. (2006). Awash River Basin Flood Control and Watershed Management Study Project. Halcrow and MoWE, Addis Ababa, Ethiopia.

Han, E., Merwade, V., Heathman, G.C. (2012). Implementation of surface soil moisture data assimilation with watershed scale distributed hydrological model. J. Hydrol. 416-417, 98-117.

Hanson, R. L. (1988). Evapotranspiration and droughts. Paulson, RW, Chase, EB, Roberts, RS and Moody, DW, Compilers, National Water Summary: 99-104.

IPCC (Intergovernmental panel on climate change). (2014). Climate Change. Synthesis Report. Contribution of Working Groups I, II and III to the Fifth Assessment Report of the Intergovernmental Panel on Climate Change. Geneva, Switzerland, pp. 151.

Jemberye M (2016) 'Evaluation of Land Use Land Cover Change on Stream Flow : a Case Study Ofdedissa Sub Basin ', *International Journal of Innovations in Engineering Research and Technology [Ijiert*, 3(8), pp. 44–60.

Jha, K. (2011). Evaluating hydrologic response of an agricultural watershed for watershed analysis. Water 3, 604-617.

Kannan, N., White, S.M., Worrall, F., Whelan, M.J. (2007). Hydrological modeling of a small watershed using SWAT-2000 Ensuring correct flow partitioning for contaminant modeling. J. Hydrol 334, 64-72.

Kassa, T. (2007), Impact of Land Use/Cover Change on Stream Flow: The Case of Hare River Watershed, Ethiopia, Arba Minch Water Technology Institute, Arba Minch University.

Kendall, M.G. (1975). Rank Correlation Methods, fourth ed. Charles Griffin, 212 pp.

Khalid, K., Ali, M., Rahman, N., Mispan, M., Haron, S., Othman, Z. and Bachok, M. (2016). Sensitivity analysis in watershed model using SUFI-2 algorithm. Procedia Engineering 162, 441-447.

Kindu, M., Schneider, T., Teketay, D. and Knoke, T. (2015). Drivers of land use/land cover changes in Munessa Shashemene landscape of the south-central highlands of Ethiopia. Environmental monitoring and Assessment187:452.

Legesse, D. and Ayenew, T. (2006), Effect of Improper Water and Land Resource.

Li,Y.K., & Wang, C.Z. (2009). Impacts of urbanization on surface runoff of the Dardenne Creek watershed, St. Charles County, Missouri. Physical geography, 30(6), 556–573.

Manandhar, R., Odeh, I., and Ancev, T. (2009). Improving the Accuracy of Land use and land cover classification of Landsat Data using Post-Classification Enhancement.

Mann, H.B. (1945). Non-parametric tests against trend. Econometrica 13, 245-259.

Meyer, and Turner, (1994), Changes in Land Use and Land Cover: A Global Perspective. Cambridge: Cambridge University Press. New York.

Molla, (2014), Land Use/land Cover Dynamics in the Central Rift Valley Region of Ethiopia.

Moriasi, D.N, J. G. Arnold, M. W. Van Liew, R. L. Bingner, R. D. Harem, T. L.Veith, (2007): Model evaluation guidelines for systematic quantification of accuracy in Watershed simulations.

Muleta, M. K., and Nicklow, J. W. (2005). Sensitivity and uncertainty analysis coupled with automated calibration for a distributed watershed. J. Hydrol. (Amsterdam), 306(1–4), 127–145.

Ndomba, P. (2002). SWAT Model Application in a Data Scarce Tropical Complex Watershed in Tanzania. Physics and chemistry of the Earth.

Neitsch SL, (2005). Soil and Water Assessment Tool, Theoretical Documentation: Version 2005.

Nigussie, A. (2012) 'Impact of Land use Land cover change on Stream flow (case study gilgel Gibe III)'.

Pai, N. and Saraswat, D. (2011). SWAT 2009 _LUC: A Tool to Activate the Land Use Change Module in SWAT 2009. Transactions of the ASABE 54(5), 1649-1658.

Rientjes, T. H. M. *et al.* (2011) 'Changes in land cover , rainfall and stream flow in Upper Gilgel Abbay catchment , Blue Nile basin – Ethiopia', (2008), pp. 1979–1989. doi: 10.5194/hess-15-1979-2011.

Schilling, E., Gassman, P., Kling, C., Campbell, T., Jha, M., Wolter, C. and Arnold, J. (2014). The potential for agricultural land use change to reduce flood risk in a large watershed. Hydrological Processes, 28(8), 3314-3325.

Setyorini, A., Khare, D. and Pingale, S.M. (2017). Simulating the impact of land use/land cover change and climate variability on watershed hydrology in the upper Brantas basin, Indonesia. Appl. Geomatics.

Shimaa, M. (2015). Hydrological modeling of the Simly Dam watershed (Pakistan) using GIS and SWAT model. *Alexandria Engineering Journal.*54, 583-594.

Shimelies and Yilma. (2015). Charcterization of runoff generation mechanisms for modeling of flow , soil erosion and sedimentation of upper awash river basin.

Shrestha, R.P., Binhn. D. and Son N.T. (2015). Effect of runoff and sediment yield in Da river basin of Hoahbinh province, Northwest Vietnam: *Journal of Metrological sciences.*12 (4), 1051-1064.

Stefanov, W. L., Ramsey, M. S., Christensen, P. R. (2001). Monitoring urban land cover change: An expert system approach to land cover classification of semiarid to arid urban centers. Remote sensing of Environment 77 (2001) 173 - 185.

Srinivasan, R. (2015). Soil and Water Assessment Tool Beginner SWAT Training Manual. Workshop at Spatial Science Laboratory, Texas A, and M University. January 26-28th 2015.

Surur, A. (2010). Simulated Impact of Land Use Dynamics on Hydrology During a 20-65 Year Period of Beles Basin in Ethiopia. M.Sc. Thesis, Royal Institute of Technology (KTH), Sweden.

Tadele, K. (2007). *Impact of Land use/cover change on stream flow: the case of* Hare *River Watershed, Ethiopia.* Arba Minch Water Technology Institute, Arba Minch University.

Tekleab, S., Kassew A. (2019) Hydrologic responses to land use/Land cover change in the Kesem Watershed, Awash basin, Ethiopia. Journal of spatial hydrology, vol 15 (No.1, spring), 2019.

Tibebe and Bewket (2010), Surface Runoff and Soil Erosion Estimation Using the SWAT Model in the Keeta Watershed, Ethiopia. Land Degradation and Development.

Taye Aduna (2009): The impact of land use/ land cover change on watershed hydrology and Water quality of Legedad-Dire watersheds. Addis Ababa University Addis Ababa Ethiopia.

Tibebe D. and Bewket W. (2010). Surface Runoff and Soil Erosion Estimation Using the SWAT Model in the Keeta Watershed, Ethiopia. Land Degradation and Development.

Veith, T.L. and L.T. Ghebremichael (2009). How to: applying and interpreting the SWAT Auto calibration tools. In: Fifth International SWAT Conference Proceedings. August 5-7, 2009 (Proceedings).

White K. L. and Chaubey I., 2005. Sensitivity Analysis, Calibration and Validations for a Multisite and Multivariable SWAT Model. Journal of the American Water Resources Association (JAWRA), 41(5):1077-1089.

Wohlrab, B. Ernstberger, H. Meuser, A. & Sokollek, V. (1992). Landschaftswasserhaushalt.- Hamburg, Berlin.

Yesserie, A. (2009). Spatio-temporal land use/land cover changes analysis and monitoring in the Valencia municipality, Spain. MSc. thesis, University of Nova.

Zhang, T., Zhang, X., Xia, D. and Liu, Y. (2014). Analysis of land use change dynamics and its impacts on hydrological processes in the Jialing River Basin. Water, 6(12), 3758-3782.

LIST OF TABLE IN APPENDICES

Table.1 Soil parameter values used in SWAT model

Appendix	MUID	SEQN	SNAM	S5ID	CMPPCT	NLAYERS	HYDGRP	SOL_ZMX	ANION_EXCL	SOL_CRK	TEXTURE	Appendix	MUID	SEQN	SNAM	S5ID
216	VT041	108	LVx	ET085	0	3	D	1600	0.5	0.5	C	2.64	3.77	56.91	32.64	10.45
216	VT011	108	LVx	MA0080	0	3	D	1600	0.5	0.5	C	2.64	3.77	56.91	32.64	10.45
221	ET088	178	VRe	ME0105	0	3	D	1450	0.5	0.5	C	1.77	3.59	68.04	24.64	7.32
214	ET083	103	LPq	NY0025	0	3	C	1100	0.5	0.5	L	13.06	2.84	23.31	32.57	44.13
5	VT021	5	CMx	VT0008	1	3	B	1800	0.5	0.5	SIL	38.4	1.2	11	67	22
3	VT023	3	CMe	VT0008	1	3	C	1651	0.5	0.5	FSL-S-VFSL	450	2.62	3	35.21	61.79
1	VT025	1	LVv	VT011	3	4	B	1651	0.5	0.5	VFSL-SI-VFSL-FSL	270	2.91	6.5	29.39	64.11

Appendix	MUID	SEQN	SNAM	S5ID	CMPPCT	NLAYERS	HYDGRP	SOL_ZMX	ANION_EXCL	SOL_CRK	TEXTURE	Appendix	MUID	SEQN	SNAM	S5ID
6	VT017	6	FLc	VT0012	1	3	D	1651	0.5	0.5	SICL-C-C	7.9	5.81	35	47.76	17.24
4	VT021	4	CMv	VT0007	5	3	C	1651	0.5	0.5	LFS-S-VFSL	700	1.74	3	16.7	80.3
7	VT023	7	FLe	NY0006	3	4	B	736.6	0.5	0.5	SIL-CN--SIL-CNV-SIL-UWB	26	3.49	11.5	56.14	32.36

Table. 2 Accuracy assessment points collected by GPS for LULC map 2018

Cultivation Land			Forest Land			Water body		
x	y	Altitude	x	y	Altitude	x	Y	Altitude
416788	1000259	2229	450979	993775	2619	510154	932663	1573
416919	1000285	2228	450987	993804	2618	510841	932684	1573
416840	1000067	2227	450987	993849	2611	511351	933320	1573
416912	999870	2227	450959	993591	2611	511900	933300	1573
416988	999640	2212	450970	993651	2610	512439	932385	1573
417105	999690	2209	450970	993746	2609	513034	932486	1573
417106	999532	2204	450876	993762	2609	513626	932993	1573
416975	999493	2205	450894	993616	2604	513580	933274	1573
417106	999192	2207	450837	993646	2599	513163	932871	1573
417317	999138	2178	450895	993561	2598	512601	932443	1573
417139	999025	2205	450934	993890	2597	511413	932053	1573
417324	998966	2190	450834	993674	2597	510671	931895	1573
417535	999023	2206	450873	993920	2595	510319	931988	1573
417344	999342	2202	450766	993537	2595	510413	931973	1573
417551	999336	2209	450794	993617	2594	510591	931957	1573
417278	999719	2215	450799	993684	2592	510837	931941	1573
417496	999799	2215	450796	993810	2590	510823	932060	1573
417150	1000225	2229	450804	993961	2587	511115	932217	1573
417567	1000379	2249	450743	993596	2582	511353	932423	1573
417986	1000277	2277	450764	993685	2579	511833	932385	1573
417884	999741	2238	450692	993658	2575	511909	932320	1573

Cultivation Land			Forest Land			Water body		
x	y	Altitude	x	y	Altitude	x	y	Altitude
417697	999686	2228	450723	993683	2575	512457	932385	1573
417715	999377	2215	450581	993616	2569	512578	932759	1573
418076	999506	2247	450664	993549	2569			
418344	999540	2260	450719	993993	2568			
418329	999462	2250	450613	993698	2566			
418481	999526	2259	450593	993579	2566			
418468	999321	2255	450635	993797	2559			
418089	999225	2219	450589	993771	2553			
418108	999356	2230	450577	993820	2551			
417969	999217	2221	450634	994021	2546			
417693	999188	2214	450588	994040	2533			
417725	999096	2214	450536	994048	2522			
417984	999023	2223	450501	994057	2518			
418289	999127	2228						

Grazing Land			Built Up Areas		
x	y	Altitude	x	y	Altitude
410661	1010446	2716	470413	994855	2319
410815	1010451	2690	470622	994230	2306
410713	1010231	2708	470813	993727	2291
410836	1010204	2701	471091	993131	2277
410965	1010353	2697	471248	993069	2275
411014	1010449	2692	471203	993216	2267
411074	1010363	2683	471076	993573	2282
411020	1010202	2701	470975	993801	2277
410805	1010013	2714	471089	993874	2291
410740	1009857	2706	470943	994195	2310
410749	1009709	2697	470761	994826	2303
410802	1009685	2702	470804	995343	2300
410911	1009796	2699	471004	995441	2323
410949	1010018	2712	471154	995005	2304
411082	1010090	2699	471285	994389	2307
411227	1010016	2690	471344	993929	2291
411084	1009788	2693	471364	993643	2281
410871	1009651	2711	471471	993504	2291
410905	1009554	2709	471462	993270	2276
410992	1009568	2691	471510	993027	2272
411104	1009644	2696	471777	993005	2241
411199	1009790	2684	471754	993187	2264

Grazing Land			Built Up Areas		
x	y	Altitude	x	y	Altitude
411238	1009619	2687	471627	993735	2285
411231	1009563	2680	471410	994496	2293
411071	1009541	2699	471394	995085	2317
410918	1009482	2705	471624	995173	2337
410990	1009462	2700	471737	994733	2306
411108	1009463	2693	471847	994058	2282
411187	1009450	2688	471977	993390	2250
411277	1009451	2689	471969	993042	2248
411277	1009509	2686	472317	993019	2279
411270	1009653	2694	472361	993423	2273
411230	1009792	2681	472219	994366	2280
411227	1009876	2688	472084	994858	2312
411271	1009993	2682	471966	995326	2326

Table.3: Monthly rainfall (mm) of Ginchi station

Year	Jan	Feb	Mar	Apr	May	Jun	Jul	Aug	Sep	Oct	Nov	Dec
1986	0.00	98.40	103.00	92.20	141.70	270.20	276.00	236.60	159.10	67.70	0.00	0.00
1987	16.00	50.80	219.90	91.10	249.30	105.60	216.40	179.40	97.20	58.40	2.20	5.90
1988	35.90	108.20	51.10	74.80	21.60	135.20	274.80	375.90	287.40	49.80	0.00	2.70
1989	12.60	120.20	151.10	126.10	14.50	134.10	334.70	253.80	157.00	86.50	10.20	85.60
1990	0.00	184.20	101.80	65.60	69.90	126.10	118.90	279.90	141.20	22.10	10.90	5.00
1991	11.70	39.70	27.80	9.00	54.50	165.10	189.80	264.80	121.30	0.00	0.00	4.20
1992	21.10	112.90	43.60	60.70	70.70	127.50	243.80	180.40	93.10	54.50	15.30	0.00
1993	22.80	87.80	33.00	157.00	153.50	137.50	208.90	374.50	264.60	23.40	0.00	0.00
1994	0.00	0.00	98.30	77.50	91.90	138.60	214.80	361.10	167.00	12.30	12.00	0.00
1995	3.50	30.20	14.90	280.70	84.10	61.80	171.60	210.40	106.80	0.00	0.00	27.80
1996	27.90	2.90	116.80	90.60	108.50	151.50	254.70	285.10	190.90	19.70	1.20	0.00
1997	64.40	0.00	0.00	131.30	47.10	118.20	199.60	188.20	101.70	101.00	74.90	2.80
1998	71.50	18.80	99.40	25.70	79.80	172.20	242.70	267.00	182.80	66.60	0.00	0.00
1999	16.30	0.00	26.50	163.40	72.10	150.30	226.40	196.00	101.60	178.70	4.20	0.00
2000	0.00	0.00	8.30	129.40	85.80	159.40	141.60	236.20	146.30	45.70	37.00	3.50
2001	7.10	40.30	118.60	33.80	113.00	270.70	238.00	151.00	96.50	31.10	2.50	0.00
2002	112.70	76.50	88.70	40.50	38.20	182.00	209.40	158.10	79.90	0.00	0.00	61.40
2003	19.60	61.20	107.00	162.50	15.40	147.60	227.80	207.00	117.70	0.00	2.10	14.90
2004	107.80	6.70	21.40	214.10	57.90	123.60	198.40	200.40	178.00	19.10	4.90	1.00
2005	65.60	2.50	119.50	45.60	85.50	116.40	260.50	241.60	185.80	12.80	12.50	0.00
2006	0.00	15.30	320.40	191.50	133.50	237.80	434.20	629.20	157.10	19.50	0.00	14.10
2007	19.90	24.10	37.30	31.60	157.40	248.10	232.30	182.60	122.10	35.30	0.00	0.00
2008	0.00	5.70	0.00	18.10	100.60	152.70	294.90	236.60	111.20	41.70	62.60	0.00
2009	57.50	5.30	11.40	50.90	43.60	101.10	210.60	274.20	144.80	0.00	0.00	41.00
2010	45.50	74.50	90.50	136.50	68.00	161.70	262.30	213.50	103.50	17.50	0.00	37.90
2011	8.50	12.30	60.40	11.20	94.50	182.10	144.10	185.30	52.90	0.00	52.30	0.00
2012	0.00	0.00	5.00	67.70	22.70	101.80	221.30	188.80	215.10	0.00	0.00	0.00
2013	8.50	13.40	5.00	67.70	108.50	159.40	141.60	111.20	41.70	62.60	2.10	41.00
2014	0.00	0.00	0.00	102.60	119.30	145.50	232.40	250.60	190.02	145.50	0.00	0.00
2015	19.60	61.20	107.00	162.50	15.40	150.30	226.40	196.00	101.60	178.70	4.20	0.00
2016	27.90	2.90	116.80	90.60	108.50	152.70	294.90	236.60	111.20	41.70	62.60	0.00
2017	5.10	0.00	26.60	116.30	162.30	116.40	260.50	241.60	185.80	12.80	12.50	0.00
2018	112.70	76.50	88.70	40.50	38.20	54.10	297.40	299.50	171.40	7.30	5.70	4.10

Table.4: Monthly rainfall (mm) of Adama station

Year	Jan	Feb	Mar	Apr	May	Jun	Jul	Aug	Sep	Oct	Nov	Dec
1986	0.00	96.50	41.00	6.20	54.40	152.40	263.30	95.00	20.40	0.00	0.00	0.00
1987	0.00	11.20	80.20	81.10	259.60	0.00	161.60	243.40	30.80	0.00	0.00	0.00
1988	34.00	31.30	6.80	50.90	9.40	50.30	185.40	171.40	186.90	52.90	0.00	0.00
1989	0.00	29.90	21.70	95.40	0.00	54.70	182.50	281.20	80.30	5.70	0.00	3.50
1990	0.70	183.90	83.00	114.70	13.30	12.00	337.80	168.70	153.70	7.00	0.00	0.00
1991	0.00	29.90	111.00	13.50	22.30	74.40	322.00	232.80	89.00	14.10	0.00	1.70
1992	41.20	27.80	0.00	47.30	8.60	69.90	233.80	210.00	160.30	43.90	0.00	3.50
1993	16.40	51.90	0.00	102.60	72.70	64.10	345.20	142.40	79.30	20.00	0.00	0.00
1994	0.00	0.00	2.60	49.10	26.50	70.10	229.60	171.50	173.80	13.80	35.60	51.00
1995	0.00	36.50	46.90	127.20	33.00	46.50	203.10	251.40	88.20	14.70	0.00	2.80
1996	27.20	0.00	111.50	65.10	115.20	120.20	220.20	250.00	93.90	0.00	7.90	0.00
1997	14.40	0.00	75.30	28.50	6.90	94.00	193.10	240.90	75.50	116.50	31.50	0.00
1998	11.80	25.60	105.20	19.80	49.30	55.30	196.50	220.60	144.70	132.80	0.00	0.00
1999	9.20	0.00	34.60	1.20	18.60	74.00	283.20	194.40	66.30	164.70	3.10	0.00
2000	0.00	0.00	20.20	16.10	51.50	60.80	355.10	269.00	133.60	85.70	57.80	12.90
2001	0.00	6.20	108.30	28.70	177.00	51.20	216.80	145.30	107.80	1.70	0.00	6.60
2002	20.90	11.10	21.90	51.30	22.50	50.20	129.90	205.70	65.30	1.10	0.00	34.50
2003	46.50	69.10	151.20	88.90	3.60	75.20	235.60	279.70	122.80	0.00	5.30	48.80
2004	28.80	3.30	77.40	53.10	1.90	63.30	114.40	227.30	77.10	58.60	12.80	1.60
2005	72.50	6.30	90.10	41.30	71.10	50.20	144.30	165.00	68.40	6.00	5.30	0.00
2006	17.60	88.40	64.60	88.70	27.80	58.70	173.50	225.00	128.80	10.10	0.50	28.50
2007	23.10	31.60	82.10	101.70	64.70	62.80	225.70	344.40	138.00	25.40	6.70	0.00
2008	34.60	0.00	0.00	79.90	69.20	58.70	353.10	302.20	100.30	37.50	69.50	0.00
2009	62.60	0.00	0.00	25.30	22.10	50.00	156.10	113.30	34.00	132.70	0.40	12.50
2010	0.00	97.30	88.80	27.40	68.10	100.60	227.80	242.90	164.70	0.00	17.60	0.30
2011	22.00	0.00	10.40	17.60	68.70	54.80	215.10	155.80	192.10	0.00	0.00	0.00
2012	56.00	28.80	39.80	107.40	48.80	93.50	533.30	327.10	130.20	1.40	0.50	3.90
2013	4.40	0.20	69.20	35.10	36.00	38.90	443.20	105.20	132.80	34.00	5.20	0.00
2014	0.00	4.80	123.00	7.10	62.30	7.70	211.70	180.00	150.60	91.70	8.90	0.00
2015	0.00	36.50	46.90	127.20	33.00	46.50	220.20	250.00	93.90	0.00	7.90	0.00
2016	0.70	183.90	83.00	114.70	13.30	12.00	263.30	96.00	20.40	0.00	0.00	0.00
2017	28.80	3.30	77.40	53.10	64.70	62.80	225.70	344.40	164.70	0.00	17.60	0.30
2018	3.00	0.00	23.10	183.40	67.30	8.00	399.40	327.40	174.00	0.00	0.00	0.00

Table.5: Monthly rainfall (mm) of Akakai station

Year	Jan	Feb	Mar	Apr	May	Jun	Jul	Aug	Sep	Oct	Nov	Dec
1986	0.00	95.40	67.70	148.70	83.20	143.40	189.40	216.50	86.10	9.40	0.00	0.00
1987	0.00	77.80	221.52	99.08	196.43	78.99	234.70	250.47	99.10	4.40	0.00	0.00
1988	0.00	44.50	0.00	96.00	38.14	124.60	255.90	278.10	253.50	35.40	0.00	0.00
1989	2.10	63.80	53.80	226.30	7.10	58.60	264.20	301.00	170.90	37.90	0.00	0.00
1990	7.70	120.60	48.40	159.10	37.30	78.90	280.70	222.90	107.30	5.80	1.20	0.00
1991	0.00	37.60	62.40	11.60	45.60	90.40	263.70	308.50	113.30	4.40	0.00	56.50
1992	33.50	24.20	30.50	15.50	25.60	100.40	218.40	276.00	86.70	43.30	0.20	0.00
1993	1.20	53.90	5.60	118.40	54.60	116.50	218.00	251.50	118.30	20.50	0.00	0.00
1994	0.00	0.00	62.70	72.20	20.20	131.20	219.30	181.00	94.50	0.00	11.00	0.00
1995	0.00	25.40	62.70	102.10	20.90	95.70	279.00	242.30	79.50	0.00	0.00	4.80
1996	15.30	0.30	79.70	38.80	90.50	240.10	292.50	234.10	119.00	1.90	0.00	0.00
1997	27.60	0.00	29.50	102.70	25.20	57.00	203.60	203.40	82.50	114.90	10.30	0.00
1998	32.70	30.20	19.60	69.30	159.90	116.90	207.80	280.00	118.50	36.90	0.00	0.00
1999	1.30	1.80	91.80	12.10	45.40	92.80	282.60	300.70	61.70	65.00	0.00	0.00
2000	0.00	0.00	29.10	93.00	64.90	100.10	188.90	210.00	124.10	17.20	23.40	3.80
2001	0.00	20.70	121.20	23.60	118.00	142.60	257.50	145.00	64.90	2.20	0.00	0.00
2002	31.10	10.50	87.80	53.90	76.60	108.00	167.10	166.30	52.30	0.00	0.00	17.70
2003	19.60	24.80	23.90	114.00	1.40	125.40	325.10	307.40	113.40	0.00	0.00	40.80
2004	15.60	15.80	61.40	154.50	15.40	95.20	150.30	189.10	80.90	4.80	3.40	0.70
2005	28.80	7.30	47.90	112.20	140.70	139.90	218.70	231.40	152.70	9.10	15.20	0.00
2006	2.60	44.20	56.30	79.70	22.00	84.30	276.40	262.60	148.10	38.00	0.00	3.20
2007	34.20	24.70	25.60	96.80	64.60	132.70	254.20	221.80	148.50	14.30	1.30	0.00
2008	0.00	0.00	0.60	34.20	62.40	140.20	253.50	252.30	191.40	7.20	64.80	0.00
2009	60.20	0.00	10.00	118.70	47.70	63.50	235.30	322.40	71.30	32.80	4.00	16.80
2010	0.00	63.80	126.20	170.00	95.20	164.80	334.40	169.80	154.10	5.20	14.80	7.80
2011	0.00	2.50	45.20	20.70	128.70	60.00	204.30	304.00	194.50	0.00	4.70	0.00
2012	0.00	0.00	126.20	61.00	26.10	80.60	228.00	243.90	122.90	0.00	0.00	0.00
2013	0.00	0.00	77.00	89.10	73.40	111.50	179.60	242.40	142.50	20.60	0.00	0.20
2014	0.00	39.40	76.00	13.90	26.10	52.60	176.80	281.60	115.30	52.30	0.00	0.00
2015	0.00	0.00	13.70	2.30	96.50	158.00	187.80	247.50	70.00	0.00	14.50	0.00
2016	0.00	46.00	39.30	184.50	134.20	105.70	179.60	242.40	119.10	83.24	9.30	0.00
2017	0.00	25.40	46.10	22.50	62.40	140.20	253.50	70.30	177.20	0.00	0.00	0.00
2018	0.00	0.00	37.60	121.20	23.60	118.00	84.30	276.40	262.60	94.50	0.00	0.00

Table.6: Monthly rainfall (mm) of Hombole station

Year	Jan	Feb	Mar	Apr	May	Jun	Jul	Aug	Sep	Oct	Nov	Dec
1986	0.00	10.80	11.70	3.20	6.50	26.80	72.80	24.60	12.90	0.00	0.00	0.00
1987	0.00	0.00	17.90	16.60	103.80	14.30	70.70	76.70	12.80	0.00	0.00	0.00
1988	16.40	21.20	15.00	64.00	8.50	48.70	237.00	244.80	132.40	29.90	0.00	1.00
1989	0.50	22.80	64.90	185.90	2.70	55.20	107.10	283.70	95.70	14.00	0.00	0.50
1990	0.00	152.80	292.00	151.20	0.50	5.00	225.10	213.40	168.40	0.00	0.00	0.00
1991	0.00	8.80	43.70	0.00	0.00	0.00	164.40	220.90	95.70	0.00	0.00	0.00
1992	16.40	21.20	15.00	151.30	90.40	249.10	433.40	733.10	410.60	0.00	0.00	0.00
1993	47.00	133.00	68.00	293.00	143.00	75.00	274.80	690.40	145.00	36.80	0.00	0.00
1994	0.00	0.00	19.00	293.00	143.00	20.40	113.60	102.90	58.20	0.00	10.20	0.00
1995	0.00	29.20	6.50	48.10	143.00	9.20	225.40	84.00	13.70	0.00	0.00	0.00
1996	0.00	0.00	1.60	48.10	10.20	29.00	114.40	258.40	63.30	0.00	0.00	0.00
1997	25.70	0.00	11.70	39.30	10.70	143.60	201.00	270.90	51.50	66.60	24.70	0.00
1998	31.00	37.60	5.60	39.50	128.80	61.70	249.10	355.80	112.30	172.30	0.00	0.00
1999	15.60	0.00	3.50	0.00	10.00	110.20	219.30	211.40	54.50	190.10	0.00	0.00
2000	0.00	0.00	1.60	57.90	111.20	102.10	337.00	264.90	212.10	0.00	67.80	10.10
2001	0.00	69.02	141.20	40.90	144.90	188.10	489.80	447.20	97.10	35.20	5.90	21.70
2002	19.80	32.30	11.40	60.00	8.90	13.00	217.00	175.60	56.60	7.10	0.00	13.90
2003	46.10	65.60	104.20	28.20	1.30	121.30	252.60	295.50	33.20	0.00	3.80	55.70
2004	6.30	0.00	68.80	54.10	30.40	103.40	153.90	272.10	47.50	35.70	4.20	0.00
2005	47.90	0.00	34.80	30.40	10.60	69.10	92.40	137.90	65.40	0.00	5.80	0.00
2006	0.30	11.00	38.10	60.80	69.50	131.30	234.50	171.40	60.90	30.20	0.00	23.00
2007	46.70	8.50	83.20	37.20	94.40	69.10	144.20	187.10	135.00	28.20	1.30	0.00
2008	5.10	0.00	0.00	26.50	100.30	94.20	299.30	295.00	165.70	59.00	67.30	9.70
2009	27.80	0.00	1.50	23.10	37.20	65.70	181.50	165.50	45.40	93.20	1.50	47.10
2010	0.00	69.70	90.10	80.40	80.20	87.50	236.80	272.30	196.50	5.20	1.40	0.00
2011	0.00	0.00	72.10	18.20	51.40	100.30	256.80	191.50	221.90	0.00	38.80	0.00
2012	0.00	0.00	0.00	33.30	42.20	38.40	494.20	297.70	113.10	0.00	0.00	0.00
2013	0.00	0.00	36.70	12.60	54.90	55.20	287.80	182.80	101.60	27.80	5.30	0.00
2014	0.00	3.50	87.30	0.50	54.90	5.30	260.50	195.90	76.03	14.00	0.00	0.50
2015	76.92	0.00	0.00	0.00	199.60	16.70	103.10	162.20	72.60	13.50	11.00	76.51
2016	0.00	0.00	15.30	95.40	153.20	86.70	356.10	77.90	102.80	14.00	0.00	0.50
2017	0.00	0.00	0.00	0.00	199.60	16.70	103.10	207.10	6.40	14.00	0.00	0.50
2018	0.00	69.70	90.10	80.40	23.10	115.80	142.70	183.00	57.00	57.00	9.40	0.00

Table.7: Monthly rainfall (mm) of Mojo station

Year	Jan	Feb	Mar	Apr	May	Jun	Jul	Aug	Sep	Oct	Nov	Dec
1986	0.00	56.20	34.00	59.20	32.70	182.80	66.10	65.10	72.60	3.10	0.00	0.00
1987	0.00	22.80	96.60	75.70	205.30	8.90	154.30	233.60	53.30	14.50	0.00	0.00
1988	20.50	6.50	6.80	29.70	10.70	124.80	255.70	300.70	243.30	62.80	0.00	0.00
1989	0.00	14.90	125.10	84.90	0.20	77.00	175.50	415.30	116.40	22.50	0.00	1.80
1990	0.00	131.10	48.20	54.60	13.80	20.60	291.80	228.90	125.40	0.40	0.00	0.00
1991	0.00	31.10	147.10	4.30	13.80	55.20	329.90	205.00	92.20	0.00	0.00	0.00
1992	41.20	5.40	9.90	48.50	14.00	86.20	182.90	287.00	82.90	27.40	10.70	1.90
1993	2.00	19.50	0.00	83.30	73.00	59.60	286.50	216.60	82.10	5.40	0.00	0.00
1994	0.00	0.00	22.60	39.70	31.40	87.20	251.00	117.50	127.30	0.00	40.10	2.50
1995	0.00	45.60	37.00	73.40	31.40	32.70	185.80	143.70	70.90	2.50	0.00	0.00
1996	30.40	7.60	97.50	72.20	127.00	214.90	221.30	220.90	79.50	0.00	3.00	0.00
1997	30.40	0.00	37.60	16.80	16.10	130.60	216.10	158.60	77.80	55.30	21.00	0.00
1998	32.30	7.60	50.70	46.00	46.00	112.10	161.30	274.80	149.00	154.10	0.00	0.00
1999	0.00	0.00	18.40	0.00	4.20	90.90	541.50	362.00	67.40	87.40	0.00	0.00
2000	0.00	0.00	12.00	10.10	33.20	128.00	285.90	230.80	114.10	12.60	25.40	0.00
2001	0.00	28.50	79.40	22.50	111.00	131.50	184.70	175.60	54.90	0.00	0.00	0.00
2002	0.00	0.00	8.90	13.70	6.50	62.40	193.50	169.20	95.20	0.00	0.00	14.90
2003	40.60	55.90	74.90	84.30	23.20	129.00	393.20	148.60	96.10	0.00	0.00	14.30
2004	15.50	0.00	99.30	114.60	9.80	129.70	393.80	201.20	116.90	99.10	32.40	0.00
2005	0.00	19.10	160.50	149.60	195.40	200.50	320.60	308.70	143.50	14.60	10.90	0.00
2006	1.60	38.50	90.50	61.60	19.20	109.00	344.40	362.70	131.80	24.90	2.60	12.30
2007	54.10	23.70	83.80	49.60	111.00	129.70	222.80	227.90	91.40	7.60	0.00	0.00
2008	1.50	0.00	0.00	61.90	76.70	137.00	431.00	404.40	188.70	89.40	50.80	0.00
2009	39.20	6.00	26.30	62.90	12.70	95.30	213.80	330.30	66.20	214.50	6.50	34.60
2010	0.00	85.20	7.70	151.90	119.50	73.40	254.20	170.40	246.70	0.00	1.40	0.00
2011	0.00	0.00	47.40	54.90	122.00	54.60	193.00	175.60	170.40	0.00	0.00	0.00
2012	0.00	0.00	37.80	43.00	7.60	131.50	524.40	419.70	147.00	0.00	0.00	0.00
2013	0.00	0.00	85.80	32.90	121.30	98.50	420.00	232.30	69.20	36.40	0.00	0.00
2014	0.00	16.80	51.90	2.90	7.60	27.40	260.70	257.20	154.30	96.30	0.00	0.00
2015	0.00	0.00	0.00	0.00	178.10	117.60	143.50	266.20	93.90	8.50	21.00	0.00
2016	12.10	32.90	18.20	240.30	90.00	117.70	545.00	266.20	77.80	96.30	31.50	0.00
2017	0.00	32.90	57.40	28.80	157.00	18.00	254.70	266.40	77.80	0.00	1.00	133.40
2018	0.00	17.00	51.90	10.70	7.60	55.50	331.60	218.60	44.10	0.00	18.00	0.00

Table.8: Monthly rainfall (mm) of Wolencity station

Year	Jan	Feb	Mar	Apr	May	Jun	Jul	Aug	Sep	Oct	Nov	Dec
1986	0.00	169.00	92.70	104.40	16.00	80.90	155.80	95.10	154.10	8.00	0.00	0.00
1987	0.00	37.70	220.40	132.30	272.60	1.00	91.00	165.60	24.70	9.70	0.00	0.00
1988	15.00	17.20	5.60	30.50	6.50	29.80	185.30	206.20	186.90	16.90	0.00	0.00
1989	0.00	189.60	149.50	286.00	0.00	83.40	185.90	244.20	119.20	1.40	0.00	14.00
1990	0.00	322.50	91.70	95.30	14.40	0.00	243.50	190.60	140.90	9.30	0.00	0.00
1991	2.70	90.00	137.00	16.90	7.10	23.80	223.10	184.30	44.40	8.00	0.00	0.00
1992	0.00	57.40	163.40	101.50	0.00	42.50	130.80	356.80	90.70	17.50	3.40	8.10
1993	47.10	50.70	0.00	114.30	31.00	42.20	210.90	139.60	140.80	19.60	0.00	0.00
1994	0.00	2.10	27.40	23.70	26.00	66.30	304.50	185.90	77.50	2.80	36.90	13.40
1995	0.00	57.40	163.40	94.70	12.90	46.10	156.10	310.20	135.50	12.10	0.00	3.50
1996	92.10	0.00	180.00	91.50	168.80	86.10	200.70	150.60	73.60	42.50	0.00	0.00
1997	29.80	0.00	38.20	23.20	44.70	145.70	255.30	131.10	88.60	117.80	51.80	0.00
1998	41.60	40.60	0.00	33.50	47.00	48.10	154.40	336.40	197.20	179.00	0.00	0.00
1999	11.10	0.00	104.10	0.00	0.00	39.10	246.50	232.90	52.00	167.40	3.60	0.00
2000	0.00	0.00	15.50	18.40	47.90	58.40	249.20	249.50	110.90	96.30	30.50	6.10
2001	0.00	13.60	128.00	20.00	65.90	76.50	223.10	184.30	88.60	117.80	10.00	0.00
2002	0.00	0.00	48.90	61.40	10.00	18.70	166.20	231.80	36.00	0.00	0.00	97.70
2003	32.50	32.10	119.60	152.60	0.00	61.20	396.20	321.70	7.50	0.00	0.00	28.30
2004	47.30	81.40	146.90	235.00	0.00	91.80	287.00	295.00	94.00	52.00	0.00	18.20
2005	30.00	24.00	93.00	72.10	132.40	97.50	69.40	123.10	50.60	0.40	2.30	0.00
2006	9.40	32.20	42.90	75.90	17.90	11.80	142.00	144.60	53.80	6.10	0.00	25.60
2007	30.20	28.70	49.70	86.80	29.50	116.00	210.40	273.10	94.30	0.00	18.40	0.00
2008	18.30	0.00	4.00	59.00	53.10	20.60	376.30	271.90	59.30	59.80	49.20	0.00
2009	95.10	0.00	22.00	19.00	15.10	16.20	133.40	123.80	45.50	116.80	0.00	61.30
2010	0.00	87.00	107.70	18.40	74.70	67.60	191.10	175.70	160.00	0.00	50.20	0.00
2011	0.00	0.00	56.00	6.30	67.10	28.00	178.70	175.30	140.40	0.00	13.50	0.00
2012	0.00	0.00	20.00	31.00	18.70	73.40	326.20	253.00	88.70	0.00	0.00	3.50
2013	11.00	1.70	72.20	38.60	46.50	44.60	437.90	144.60	118.50	60.60	16.20	0.00
2014	0.00	2.60	101.40	2.20	34.50	7.20	169.90	207.40	152.40	93.60	26.60	0.00
2015	10.20	0.00	0.00	104.40	166.00	92.50	541.10	836.10	235.70	0.00	0.00	0.00
2016	0.00	0.00	20.00	31.00	18.70	67.60	191.10	175.70	160.00	0.00	50.20	0.00
2017	0.00	0.00	15.50	18.40	47.90	58.40	91.00	165.60	24.70	9.70	0.00	0.00
2018	95.10	0.00	101.40	2.20	34.50	20.60	376.30	271.90	59.30	60.60	13.50	0.00

Table.9: Monthly streamflow (m^3/s) of Hombole station

Year	Jan	Feb	Mar	Apr	May	Jun	Jul	Aug	Sep	Oct	Nov	Dec
1986	10.50	40.60	32.20	83.20	3.20	154.80	159.80	132.50	102.00	5.80	6.50	5.90
1987	0.70	30.20	61.10	85.90	24.60	118.10	230.30	171.30	194.10	54.00	6.30	8.00
1988	21.30	17.70	8.40	34.90	58.90	79.60	216.40	220.10	91.20	45.80	12.40	65.00
1989	0.00	17.00	15.80	79.80	50.20	75.40	249.00	159.20	163.80	2.30	8.00	9.80
1990	0.00	24.00	29.88	25.46	87.18	97.32	189.00	135.80	113.90	0.00	13.70	0.10
1991	0.00	5.00	17.60	13.50	79.60	151.50	185.60	202.50	155.10	46.40	29.10	0.00
1992	0.00	34.20	123.80	31.00	151.20	184.10	224.00	161.50	99.30	13.70	8.00	0.00
1993	14.70	42.00	90.20	62.30	43.10	180.50	224.30	215.90	100.20	0.20	9.00	16.50
1994	10.50	77.30	44.20	107.30	27.20	159.80	261.80	233.30	172.30	0.80	8.50	14.90
1995	10.50	74.30	38.20	106.30	20.20	160.80	257.60	233.30	152.40	0.80	10.50	9.00
1996	0.70	35.20	66.10	86.90	38.60	128.50	298.30	243.60	218.60	54.00	9.30	8.00
1997	21.30	23.70	28.40	89.60	58.90	90.60	349.90	388.30	120.70	45.80	13.40	65.00
1998	0.00	11.00	15.80	81.80	50.20	78.40	324.20	258.00	213.50	2.30	7.00	9.80
1999	0.00	18.00	29.88	24.46	112.38	224.82	217.00	291.90	131.10	0.00	14.70	0.10
2000	0.00	15.00	17.60	16.50	100.00	152.50	234.80	306.20	257.60	46.40	26.10	0.00
2001	0.00	33.20	140.80	33.00	168.00	218.20	378.00	216.40	125.70	13.70	3.00	0.00
2002	14.70	27.00	90.20	58.30	63.10	176.50	256.90	215.90	112.80	0.20	2.00	16.50
2003	10.50	66.30	52.60	94.30	20.20	153.80	271.80	233.30	166.30	0.80	4.50	24.90
2004	24.80	31.30	49.50	143.90	30.10	153.90	238.50	272.60	186.00	76.90	12.00	0.00
2005	45.90	95.60	83.20	181.90	133.70	192.80	246.00	315.20	183.50	108.40	17.40	0.00
2006	0.70	63.20	133.08	90.90	74.60	172.10	356.30	243.60	262.10	54.00	15.30	8.00
2007	51.30	55.10	91.80	94.80	120.10	184.52	261.80	381.20	159.60	24.80	32.00	0.00
2008	0.00	56.00	0.00	61.40	94.30	101.90	277.00	360.90	270.70	88.20	94.40	22.90
2009	21.30	26.70	28.40	89.60	58.90	91.60	349.90	388.30	124.70	45.80	23.40	65.00
2010	2.60	100.80	55.50	129.80	74.40	284.10	313.90	205.80	255.80	1.80	42.70	15.00
2011	14.10	40.10	44.30	39.80	66.10	198.00	180.90	340.80	161.00	0.00	55.30	0.00
2012	0.00	19.00	15.80	89.60	50.20	90.40	324.20	298.00	238.50	2.30	21.00	9.80
2013	4.40	58.00	50.44	113.30	85.00	176.20	230.47	353.20	225.30	58.40	38.30	0.00
2014	1.70	87.40	61.50	39.20	93.60	85.70	219.90	262.40	283.70	35.00	27.70	0.00
2015	0.00	34.00	29.88	55.96	131.88	224.82	237.80	309.90	173.90	0.00	35.70	0.10